UNIVERSITY OF OKLAHOMA

GRADUATE COLLEGE

MICROBIOLOGICALLY INFLUENCED CORROSION OF CARBON STEEL IN SULFIDOGENIC ENVIRONMENTS: THE LINK TO THIOSULFATE REDUCTION AND BIOLOGICAL STABILITY OF ALTERNATIVE FUELS

A DISSERTATION

SUBMITTED TO THE GRADUATE FACULTY

in partial fulfillment of the requirements for the

Degree of

DOCTOR OF PHILOSOPHY

By

RENXING LIANG
Norman, Oklahoma
2015

MICROBIOLOGICALLY INFLUENCED CORROSION OF CARBON STEEL IN SULFIDOGENIC ENVIRONMENTS: THE LINK TO THIOSULFATE REDUCTION AND BIOLOGICAL STABILITY OF ALTERNATIVE FUELS

A DISSERTATION APPROVED FOR THE
DEPARTMENT OF MICROBIOLOGY AND PLANT BIOLOGY

BY

_____
Dr. Joseph M. Suflita, Chair

_____
Dr. Michael J. McInerney

_____
Dr. Paul A. Lawson

_____
Dr. Mark A. Nanny

_____
Dr. Jan Sunner

Acknowledgements

I have many people to acknowledge during my adventurous and enjoyable journey at the University of Oklahoma in the past 5 years. This dissertation will not be accomplished without their intellectual advice, helpful criticism, encouragement and other support in different ways.

First, I would like to thank my major advisor, Dr. Joseph M. Suflita, for giving me the opportunity to work in your lab. You are such a great mentor who taught me a lot on how to do science as a microbiologist. The rigorous training on communication skills, scientific writing and critical thinking will benefit the rest of my future career. I would like to particularly thank Dr. Michael J. McInerney for offering the opportunity to step into a collaborative project. Without your insight into the project and manuscript, I would not be able to have my first publication. My gratitude also goes to my other committee members for their advice and guidance on both research and coursework: Dr. Paul A. Lawson, Dr. Mark A. Nanny and Dr. Jan Sunner. Your expertise in microbial taxonomy, organic chemistry and metabolomics are very helpful in various aspects of my research.

In addition, I would like to particularly thank Dr. Irene Davidova for leading me to the world of anaerobic microbiology at the bench and teaching me the requisite skills to cultivate and isolate anaerobic microorganisms. I also want to extend my gratitude to Dr. Benjamin G. Harvey from Naval Air Warfare Center for providing the terpene fuel and performing fuel analysis by using the GC/MS instrument. Special thanks will also go to Drs. Kathleen Duncan and Sylvie Le Borgne, who taught me the molecular

techniques required for my research. Additional thanks goes to Drs. Egemen Aydin and Vincent Bonifay for their expertise on the metabolite analysis.

I also want to extend my gratitude to the current and former members of Suflita lab (particularly Dr. Deniz Aktas, Dr. Tiffany Lenhart, Dr. Christopher N. Lyles, Chris Marks and Brian H. Harriman) who are always willing to offer help on big research questions and other small issues in the lab. Additionally, I am very thankful for people in Dr. Michael J. McInerney's lab for sharing instrument and chemicals whenever needed. Particular thanks should go to Neil Wofford and Robert S Grizzle for their help on how to grow the thermophilic enrichments and other analytic issues.

Finally, I would like to thank my parents for their endless love and support particularly during my struggling moments in pursuing my degree at University of Oklahoma. I am also very grateful for my two sisters for their understanding and taking care of my parents while I am far away from home for so long.

Table of Contents

List of Tables

List of Figures

Chapter 3

Chapter 4

Abstract

Biocorrosion or microbiologically influenced corrosion (MIC) refers to the mutiple underlying mechanisms wherein microbial activity directly or indirectly enhances the corrosion of metallic and non-metallic materials. Biocorrosion associated with metallic materials (e.g., carbon steel) is notoriously known for causing costly damage in both the upstream and downstream energy infrastructure, often with catastrophic environmental consequences. While numerous mechanisms are known or have been proposed for this long-standing problem, a thorough fundamental understanding of biocorrosion is still lacking and therefore no panacea exists for the diagnosis and treatment of this complicated process. The first two chapters of this dissertation focus on the biocorrosion of carbon steel in upstream operations by the dominant thiosulfate reducing bacteria (TRB) cultivated from hot oil pipelines or from high salinity produced water after the hydraulic fracturing of shale formations. The last two chapters deal with an assessment of the biological stability of second-generation and next-generation biofuels and their impact on corrosion of carbon steel in the downstream fueling infrastructure.

It is well recognized that microorganisms can corrode metallic surfaces under diverse conditions with a combination of different electron donors and acceptors. Historically, the importance of sulfate-reducing bacteria (SRB) in biocorrosion processes has been well documented, but it is entirely possible that other important groups of microorganisms also play crucial roles in catalyzing this activity.
We found that TRB were more numerically abundant than SRB in a “PIG” sample from a hot oil pipeline on Alaska’s North Slope. The thiosulfate-reducing and methanogenic

enrichments cultivated from this sample were dominated by thermophiles from the genus of *Anaerobaculum*. The corrosion assay indicated that sulfidogenesis coupled to the thiosulfate-reducing enrichment was more aggressive in exacerbating the corrosion of carbon steel relative to the methanogenic enrichment. This work highlighted the importance of fermentative, thiosulfate-reducing bacteria in the corrosion of oil pipelines under thermophilic conditions. In contrast, methanogenic processes coupled to either complex organic matter metabolism or the metal itself was far less important in catalyzing the corrosion of carbon steel.

An exploration of the microbial ecology of highly saline produced water systems from a hydraulic fractured shale gas production facility was also carried out. A molecular survey revealed that the microbial community of this produced water system was predominated by halophilic bacteria affiliated with the genus *Halanaerobium*. We further hypothesized that these organisms played important roles in carbon and sulfur cycling in the fractured shale formations and contributed to corrosion through sulfide and acid production. One of the dominant microorganisms (*Halanaerobium* sp., strain DL-01) was isolated and found to degrade guar gum, the major gelling agent in the fracture fluid and produce acetate and sulfide when thiosulfate was served as a terminal electron acceptor. A corrosion scenario in this hydraulically fractured site was tentatively proposed based on the metabolic capacity of *Halanaerobium* sp. DL-01 and the well-known corrosivity of acetate and sulfide in oil and gas industry. This work mainly implicated that sulfide and acetate produced by fermentative, thiosulfate-reducing halophiles in the deep fractured subsurface may contribute to corrosion in the downstream gas pipelines and storage.

Apart from the conventional corrosion problems associated with upstream energy facilities in the oil and gas industry, the increasing global interest in the adoption of alternative fuels raised new issues about the compatibility of emerging biofuels with the existing carbon-steel infrastructure. A protocol was developed to comprehensively assess the biological stability of fuels and applied to the study of second-generation biofuels (camelina-JP5 and FT-F76). That is, the biodegradability of the fuels as well as their potential to exacerbate carbon steel biocorrosion was assessed using three coastal seawaters as starting inocula. The highest sulfate reduction rates were always associated with camelina-JP5, a finding that suggested that this hydroprocessed fuel might be more susceptible to biodegradation relative to other fuels. Metabolite profiling attested to the anaerobic metabolism of n-alkanes and alkylbenzenes in the fuel. The relatively strong linear correlation between sulfate reduction and corrosion (both general and pitting corrosion) suggested that biogenic sulfide production linked to anaerobic metabolism of fuel constitutes can largely account for the increased biocorrosion in marine environments. An important implication of this work was that caution should be exerted with the use of hydroprocessed camelina-JP5 during long term storage due to its relative liability.

While numerous efforts are still underway toward the development of second generation alternative fuels, next generation biofuels such as terpene dimer fuel (TDF) have recently been synthesized. This fuel was designed to meet the demand for a high-density biofuel that might be used in conjunction with petroleum fuels. It was hypothesized that TDF might resist anaerobic biodegradation due to the dimerization and hydrogenation of the parent substrates. Using the same protocol, it was found that

TDF was relatively recalcitrant and had negligible influence on corrosion over an extended incubation period. These results suggest that this synthetic biofuel might be safe with respect to corrosion of carbon steel but may raise environmental concerns due to its relative persistence under anaerobic conditions should it ever be spilled. Given the well-recognized importance of surface inclusions as sites for pit initiation, the relationship between the manganese dissolution from the metal and pitting corrosion in TDF-laden environments was investigated. The low manganese (Mn)/weight loss value differentially associated with coupons exhibiting a greater degree of pitting corrosion substantiated the hypothesis that this ratio is potentially useful as an indicator of this important corrosion process.

Preface

Biocorrosion or microbiologically influenced corrosion (MIC) is a long-standing problem that plagues both upstream and downstream energy infrastructure including the production, distribution, use and storage systems. Biocorrosion of metallic infrastructure (pipelines, storage tanks and ballast tanks, etc.) in hydrocarbon-laden environments can result in enormous economic losses, catastrophic environmental consequences and even death of human beings. Sulfate reducing bacteria (SRB) are typically considered to be the major culprit responsible for biocorroson and thus have been extensively studied over many decades. Several studies have found that non-sulfate-reducing sulfidogenic microorganisms (e.g. thiosulfate-reducing bacteria) are more numerically abundant than SRB in produced water associated with oil and gas production operations. However, the roles of these fermentative, thiosulfate-reducing microorganisms in biocorrosion have been far less studied and thus their contributions to corrosion is often overlooked or underestimated. In this regard, questions remain as to the identity of these non-sulfate-reducing sulfidogenic microorganisms and their function in catalyzing corrosion particularly in environments where SRB are controlled or scarce. On the other hand, new questions arise with respect to the incorporation of emerging alternative fuels into the existing downstream metallic infrastructure. What is the biological stability of new biofuels and their impact on corrosion of the existing carbon-steel fuel infrastructure? This dissertation consists of four chapters and all are aimed to address the above questions as they relate to the biocorroson of carbon steel in sulfidogenic environments. Chapters 1 and 2 highlighted the importance of the overlooked thiosulfate-reducing bacteria in the corrosion of oil pipelines or shale gas

production facilities that are characterized as possessing high temperature or salinity as a dominant ecological factor, respectively. Chapters 3 and 4 were dedicated to assessing the biological stability of various advanced alternative fuels and their potential impact on the corrosion of carbon steel in anaerobic marine environments.

Chapter 1 is a collaborative effort with Dr. Michael J. McInerney's laboratory to interrogate the roles of thermophilic, thiosulfate-reducing bacteria and methanogenic archaea in the biocorrosion of oil pipelines located on the oilfields of Alaska's North Slope. Mr. Robert S. Grizzle initiated the project to characterize the thiosulfate-reducing and methanogenic enrichments and to investigate the physiological roles of the resulting cultures in carbon and sulfur cycling. My efforts to extend this project included: i) verifying the sulfidogenic and methanogenic processes occurring in these two enrichments using yeast extract as an electron donor; ii) determining the roles of these cultures in the biocorrosion of carbon steel using microscopy, profilometry, weight loss and total iron analysis; iii) transferring the methanogenic enrichment with iron granules as a sole electron donor source in order to examine prospects for direct electron extraction from metal surfaces. This work highlighted the importance of fermentative, thiosulfate-reducing bacteria in the corrosion of carbon-steel pipelines under thermophilic conditions. This chapter was written to be consistent in both style and format with the journal, *Frontiers in Microbiology*.

Chapter 2 examines the microbial ecology of produced water that is associated with hydraulic fracturing operations and characterizes the dominant halophilic bacteria involved in the cycling of organic matter and biocorrosion of natural gas pipelines in a shale formation. My primary contribution to this work included: i) working in

consultation with Dr. Irene Davidova to isolate and identify one of the numerically abundant microorganisms in the produced water; ii) investigating the physiological role of the isolate and its potential for catalyzing the biocorrosion of carbon steel; iii) assessing the efficacy of biocides against the pure culture in order to evaluate the efficacy of biocides in hydraulic fracture sites. The microbial community analysis of produced water was conducted in collaboration with the laboratories of Drs. Kathleen E. Duncan and Bradley S. Stevenson. My laboratory colleague, Mr. Christopher R. Marks, performed the microbial enumeration procedure and contributed to the geochemical analysis of the production waters. The integration of both culture-dependent and -independent techniques in this collaborative work provide a better insight and understanding of the microbial ecology of produced water associated with hydraulic fracturing and the roles of the dominant, halophilic microorganisms in sulfidogenesis and biocorrosion of the carbon-steel infrastructure. The corrosion scenario proposed can facilitate the development of strategies for both monitoring and treating biocorrosion issues associated with natural gas recovery operations. Chapter 2 was written in the style of the journal, *Environmental Science and Technology*.

Chapter 3 focuses on assessing the biological stability of second-generation alternative fuels and their impact on corrosion of carbon steel in anaerobic marine environments. My major contribution in this area involved the continuous efforts to develop a protocol (appendix A) to assess both the biodegradation of fuel coupled with a standardized biocorrosion assay. In chapter 3, I evaluated the biological stability of both petroleum and biomass-derived fuels (camelina-JP5 and FT-F76) and their link to the biocorrosion of carbon steel using three different coastal seawaters as starting

inoculum. My primary role in this comprehensive work was designing the experiment, constructing the assay microcosms, conducting a targeted metabolite profiling of the samples using GC/MS and quantifying both generalized and pitting corrosion. Dr. Egemen Aydin of Dr. Jan Sunner's laboratory performed the metabolite analysis using HPLC-q-TOF/MS. The major implications of these work is that the hydroprocessed biofuel, camelina-JP5, was more amenable to biodegradation relative to its petroleum-based counterpart and would likely result in higher risk of corroding the carbon-steel infrastructure. Chapter 3 was also written and formatted for the journal *Environmental Science and Technology*.

Chapter 4 is an extension of the aforementioned protocol to assess the biological stability of next generation terpene-based biofuels. This work was a collaborative effort with Dr. Benjamin G. Harvey of Naval Air Warfare Center, whose laboratory performed the residual fuel analysis at the termination of the experiment. My major contribution to this work was establishing the anaerobic incubations, monitoring sulfate depletion, performing metabolites profiling and evaluating the degree of metal corrosion. The manganese measurement was conducted in the laboratory of Dr. Mark A. Nanny with help from Mr. Shuo Li. This work showed that a candidate next generation terpene dimer fuel was relatively resistant to biodegradation, and as a consequence, the corrosion of carbon steel can essentially be neglected under obligate anaerobic conditions. Additionally, the results of manganese dissolution assays from the metal surfaces of coupons provided some insight and a potential chemical signal differentially associated with pitting corrosion. Chapter 4 was written following the style of the journal *Energy & Fuels*.

Chapter 1: Roles of thermophilic thiosulfate-reducing bacteria and methanogenic archaea in the biocorrosion of oil pipelines

Abstract

Thermophilic sulfide-producing microorganisms from an oil pipeline network were enumerated using different sulfur oxyanions as electron acceptors at 55 ^{o}C. Most-probable number (MPN) analysis showed that thiosulfate-reducing bacteria were the most numerous sulfidogenic microorganisms in pipeline inspection gauge (PIG) scrapings. Thiosulfate-reducing and methanogenic enrichments were obtained from the MPN cultures that were able to use yeast extract as the electron donor. Molecular analysis revealed that both enrichments harbored the same dominant bacterium, which belonged to the genus *Anaerobaculum*. The dominant archaeon in the methanogenic enrichment was affiliated with the genus *Methanothermobacter*. With yeast extract as the electron donor, the general corrosion rate by the thiosulfate-reducing enrichment (8.43 ± 1.40 milli-inch per year, abbreviated as mpy) was about 5.5 times greater than the abiotic control (1.49 ± 0.15 mpy), while the comparable measures for the methanogenic culture were 2.03 ± 0.49 mpy and 0.62 ± 0.07 mpy, respectively. Total iron analysis in the cultures largely accounted for the mass loss of iron measured in the weight loss determinations. Profilometry analysis of polished steel coupons incubated in the presence of the thiosulfate-reducing enrichment revealed 59 pits over an area of 71.16 mm^2, while only 6 pits were evident in the corresponding methanogenic incubations. The results show the importance of thiosulfate-utilizing, sulfide-producing fermentative bacteria such as *Anaerobaculum* sp. in the corrosion of carbon steel, but

also suggest that *Anaerobaculum* sp. are of far less concern when growing syntrophically with methanogens.

Introduction

The United States alone has about 2.5 million miles of pipelines that crisscross the country and transport the majority of energy reserves (Quickel and Beavers, 2011). Corrosion is a major cause of pipeline failures that can lead to economic loss and severe environmental contamination (Kilbane and Lamb, 2005). It is well recognized that the majority of internal corrosion of oil pipelines is associated with microorganisms (Almahamedh et al., 2011). Previous studies using culture-independent approaches demonstrated that various physiological groups of microbes like sulfate-reducing bacteria, fermentative bacteria, metal reducers and methanogens are the frequent and near ubiquitous inhabitants in pipelines transporting hydrocarbon reserves (Neria-González et al., 2006; Duncan et al., 2009; Keasler et al., 2010; Rajasekar et al., 2010;Stevenson et al., 2011). It was hypothesized that the resident microorganisms inside the pipelines contribute to corrosion under the prevailing anaerobic conditions through their metabolic ability to use a wide variety of electron acceptors such as sulfate and thiosulfate (Suflita et al., 2008).

The production of corrosive sulfides by sulfidogenic organisms is an important mechanism of pipeline corrosion (Davidova et al., 2012). Sulfate-reducing bacteria are considered to be the major corrosion culprits and have been most extensively studied (Hamilton, 1985; Beech and Sunner, 2004). However, previous work suggested that strict sulfate-reducing bacteria may be present in lower numbers than other sulfide producers including organisms that reduce thiosulfate (Obuekwe et al., 1983; Obuekwe

and Westlake, 1987; Crolet, 2005; Agrawal et al., 2010). It was proposed that thiosulfate could be generated by the chemical oxidation of H_2S with O_2 (Cline and Richards, 1969). Meanwhile, other studies demonstrated that thiosulfate was produced through electrochemical dissolution of MnS in stainless steel during the initiation of pitting corrosion (Alkire and Lott, 1989; Lott and Alkire, 1989). Indeed, thiosulfate has been detected at concentrations up to 0.5 mM in production facilities (Magot et al. 1997). The biological turnover of thiosulfate can be rapid and potentially a more significant contributor to the sulfide pool when reduced than sulfate alone (Jørgensen, 1990). Therefore, the presence of thiosulfate and its utilization by bacteria can represent a major risk factor for pipeline biocorrosion. In support of this concept, Magot et al. (1997) found that mesophilic, thiosulfate-reducing bacteria from a petroleum pipeline were capable of corroding carbon steel at a rate comparable to the sulfate reducers (Magot et al. 1997).

Previous studies found that sequences related to the genera *Thermoanaerobacter*, *Anaerobaculum* and *Thermacetogenium* were dominant in clone libraries and pyrosequencing assays of Alaska North Slope (ANS) oil facilities that were operated at approximately 50 ^{o}C (Duncan et al., 2009; Gieg et al., 2010; Stevenson et al., 2011). Species within these genera are known to be capable of reducing thiosulfate. Although the above thermophilic thiosulfate-reducers were suspected to be involved in corrosion processes, their direct role in sulfide production and biocorrosion was not clearly demonstrated. Moreover, many of these organisms are typically classified as fermentative bacteria and thus, little attention has been given to their role in sulfidogenesis and biocorrosion. It has been noted that anti-corrosion strategies

involving biocides that target sulfate-reducing bacteria may be ineffective against thiosulfate-reducing bacteria (Crolet, 2005).

Thermophilic methanogens affiliated with the genus *Methanothermobacter* were also detected at the ANS oil facility (Duncan et al., 2009; Stevenson et al., 2011). It was recognized that the syntrophic association of methanogens with fermentative microorganisms may be important for enhancing corrosion. Co-cultures of *Methanothermobacter* strain MG and *Thermococcus* species produced elevated concentrations of fatty acids through yeast extract fermentation, which can increase the corrosion of carbon steel (Davidova et al., 2012). More imptantly, the possibility of direct electron extraction from iron by methanogens has been postulated as an important corrosion mechanism (Dinh et al., 2004; Uchiyama et al., 2010).

Understanding the microbial interactions involved in the cycling of organic substrates and sulfur oxyanions is crucial to the development of strategies to minimize or prevent biocorrosion. We used both cultivation-dependent and -independent techniques to enumerate and identify sulfidogenic and methanogenic microorganisms from a hot ANS petroleum production facility. The potential impact of thiosulfate-reducing bacteria and methanogenic archaea on corrosion of carbon steel was further evaluated.

Materials and Methods

Sampling source and collection

Samples were collected from a segment of pipeline in the ANS oil production complex that delivered production water from a central processing facility to an injection well (Stevenson et al., 2011). The average temperature of the fluid flowing

through this area was ~50°C. Samples of the pipeline inspection gauge (PIG) scrapings, which included solid materials scraped from the inner surface of the pipeline and some liquid, were collected in sterile glass serum bottles. The bottles were sealed with rubber stoppers, capped, and flushed with nitrogen to maintain anaerobic conditions (Stevenson et al., 2011). The sample was then shipped to the University of Oklahoma and stored at room temperature under nitrogen gas and used as an inoculum for MPN determinations.

Media and most-probable number enumerations

A basal marine medium was used to enumerate themophilic sulfide-producing microorganisms capable of using sulfate, sulfite, thiosulfate or polysulfide as electron acceptors (Tanner et al., 2007). The basal marine medium contained the following components (l^{-1}): yeast extract, 0.5 g; NaCl, 20.0 g; $NaHCO_3$, 1.0 g; $CaCl_2 \cdot 2H_2O$, 0.04 g; PIPES [piperazine-N,N'-bis(2-ethanesulfonic acid)], 3.786 g (10 mM); a 0.1% resazurin solution, 1 ml; a 2.5% $Na_2S \bullet 9H_2O$ solution, 20 ml; a modified trace metals solution (Wolin et al., 1963), 10 ml; a modified vitamin solution (Wolin et al., 1963), 0.5 ml; and a marine minerals solution, 10 ml. The marine minerals solution contained (l^{-1}): KCl, 200 g; NH_4Cl, 100 g; $MgSO_4 \cdot 7H_2O$, 40 g; and KH_2PO_4, 20 g. The 2.5% $Na_2S \bullet 9H_2O$ solution was prepared as described previously (McInerney et al., 1979) and added after boiling and gassing the medium. The pH of the medium was adjusted to 7.0 using 0.1 N HCl or 0.1 N NaOH.

Two sets of basal marine media were prepared to determine the dominant sulfide producers using a most-probable number method (McInerney et al., 2007). One set was amended with a mixture of short-chain volatile fatty acids (VFAs) at 200 µM each of

formic, acetic, propionic, butyric, and valeric acids as the electron donors. The second set did not have VFAs added. Yeast extract was added to supply additional growth factors and carbon sources likely produced by an active microbial community. Twenty-percent stock solutions of Na_2SO_4, Na_2SO_3, and $Na_2S_2O_3$, and a 1 M stock solution of polysulfide ($Na_2S_{3.25}$) (Widdel and Pfennig, 1992) were added individually at 6 $ml \cdot l^{-1}$ to the basal marine medium with and without VFAs. Media with and without VFAs, both lacking sulfidogenic electron acceptors, were included as controls. The medium was heated, degassed with 100% N_2, sealed, and brought inside of the anaerobic chamber. The medium was reduced by the addition of the sodium sulfide solution and then dispensed into 16 x 150 mm screw-capped, Hungate tubes, 9 ml per tube. The tubes were sealed with Hungate caps and septa, brought out of the chamber where the gas phase was replaced with an atmosphere of 80% N_2: 20% CO_2, as described previously (Tanner et al., 2007), and then autoclaved. Additions, inoculations, and sampling of sterile anoxic media were done using sterile, degassed syringes and needles.

For each condition, each of three tubes was inoculated with 1 ml of PIG envelope sample. Subsequent 1:10 serial dilutions were made in triplicate in the same medium as the 1:10 dilution until a final dilution of 10^{-6}. All tubes were then incubated at 55°C for sixteen weeks. The MPN tubes were scored positive if sulfide production was at least 20% higher than that of the uninoculated and unamended controls. The MPNs tubes containing polysulfide as the electron acceptor were scored positive when the number of cells visible in multiple microscopic fields at 400X was greater (at least two times) than that in control tubes without electron acceptors. The calculation of the MPN was deduced from the statistical table provided previously (Banwart, 1981).

Characterization of enrichments from MPN cultures

Enrichments for all electron acceptors except polysulfide were established from highest positive MPN dilution tubes. Enrichment media and equipment was the same as that used for the MPN assay, except that rubber stoppers and Balch tubes were used. Two milliliters from a positive MPN tube was transferred into each of three Balch tubes containing 9 ml of the cultivation medium. Controls without VFAs but with an electron acceptor, with VFAs but without an electron acceptor, and lacking both VFAs and a sulfidogenic electron acceptor were prepared in a similar manner. The enrichments were incubated at 55°C for 12 weeks and then transferred to the same fresh medium. After each transfer, samples were taken to measure growth, sulfide production and to obtain DNA for community analysis.

Thiosulfate-reducing and methanogenic enrichments with and without the addition of VFAs were selected for further characterization. Since the enrichment media included yeast extract as well as the VFA solution, the concentration of yeast extract was varied to determine if these enrichments used yeast extract as the electron donor. The thiosulfate-reducing enrichments were grown in medium without VFAs at yeast extract concentrations of 0 $g \cdot l^{-1}$, 1 $g \cdot l^{-1}$, 5 $g \cdot l^{-1}$and 10 $g \cdot l^{-1}$ with an initial thiosulfate concentration of around 15 mM. The methanogenic enrichment was inoculated into media with the same yeast extract concentrations as above but without thiosulfate. The reduction of thiosulfate, accumulation of sulfide, and methane production were monitored with time.

Corrosion assay

The carbon steel (1018) used for this study had a composition of 0.14–0.20% C, 0.6–0.9% Mn, 0.035% maximum S, 0.030% maximum P, and the remainder Fe. It was cut into small round coupons with diameters of 9.53 mm and a thickness of approximately 1 mm. The coupons (original weight: 0.5253±0.0077 g) were initially polished to a 3-5 micron finish to form a smooth level surface. The coupons were then cleaned with deionized water, and sonicated for 15 minutes in distilled water followed by two successive acetone treatments. The coupons were then dried with flush of N_2, placed in sealed serum bottles under N_2 and autoclaved.

The coupons were weighed individually and added to the culture tubes aseptically inside an anaerobic chamber. All incubations were performed in triplicate and incubated at 55 ^{o}C. The protocol for cleaning the coupons at the end of experiment followed the ASTM Standard G1-03(G1-03, 2003) with some modification. The acid cleaning solution (3.5 $g.l^{-1}$ of hexamethylene tetramine in 6M HCl) was prepared to remove accumulated corrosion product from the coupon surface. Ten milliliters of acid cleaning solution were directly added to the cultures with coupons and the cultures were sonicated for 15 minutes. The coupons were removed and rinsed (in order) with deionized water, acetone, and methanol. The cleaned coupons were dried and stored under N_2 prior to analysis.

Corrosion was determined by both weight loss and total iron determinations. Individual coupons were weighed in the glove bag as described above. The corresponding general corrosion rate was calculated from mass loss according to NACE Standard RP0775 (RP, 2005). The total iron (including insoluble iron dissolved from the surfaces of coupon and medium) in the acid cleaning solution was reduced with 10%

hydroxylamine hydrochloride to reduce any ferric iron to its ferrous state (Stookey, 1970) and then diluted with nanopure water to quantify the total ferrous iron by the ferrozine assay (Lovley and Phillips, 1986).

Field emission-scanning electron microscopy (FE-SEM) and profilometry

A set of corrosion product-covered coupons were withdrawn from replicate incubations and dried under N_2. High resolution FE-SEM was performed using a Zeiss NEON 40 EsB (Carl Zeiss, Oberkochen, Germany) scanning electron microscope. Images of the coupon surfaces were obtained using an acceleration voltage of 1 kV and a working distance of 4 mm. Another set of coupons from replicate incubations were cleaned as described above and then scanned with a Nanovea non-contact optical profilometer PS50 (MicroPhotonics, Inc, Irvine, CA) with a 2 μm step size (Harris et al., 2010). The electronically recorded raw data were analyzed using Ultra MountainsMap Topography XT6.0 software (MicroPhotonics, Inc, Irvine, CA). The pits were defined as the regions that were 20 μm below the mean plane and had an equivalent diameter greater than 10 μm. Equivalent diameter is the diameter of an irregular region whose outer circumference equals a circular disk with a diameter of 10 μm.

Analytical techniques

Dissolved sulfide was measured using a colorimetric assay with N,N-dimethyl-p phenylenediamine·HCl, zinc acetate, and concentrated sulfuric acid (Tanner, 1989). Gas-phase H_2S concentrations were measured by injecting 1-ml of the enrichment headspace directly into the assay tube containing the above reagent, which was then shaken vigorously prior to conducting the assay. Sulfate was measured by ion chromatography using a Dionex DX500 ion chromatograph equipped with an AS4A

column (Caldwell et al., 1998). Thiosulfate concentrations were analyzed with a colorimetric assay (Nor and Tabatabai, 1975) and measured spectrophotometrically at 460 nm. Volatile fatty acids and methane were analyzed at the beginning and at the end of the incubations by gas chromatography (GC) (Struchtemeyer et al., 2005).

Community analysis by 16S rRNA gene sequencing

The highest dilution MPN tubes in which all three replicates were scored positive for sulfide production and the resulting enrichments that showed electron acceptor loss and sulfide production above controls were chosen for DNA analyses. Five milliliters of each culture was centrifuged for 15 minutes at 6000 x g. The cell pellet was washed twice in 1 ml of a sterile phosphate-buffered saline (PBS) followed by centrifugation for 3 minutes at 8000 x g. The final pellet was resuspended in 500 µl of sterile PBS solution and used immediately for DNA extraction or frozen at -20 ^{o}C. DNA was extracted from 250-µl samples using the PowerSoil DNA Isolation Kit (MOBIO Laboratories). Due to low cell biomass, two sets of tubes per sample were pooled onto one spin filter in order to achieve a higher DNA concentration. The DNA was then extracted from the spin filter into 75 µl sterile molecular biology-grade water (Eppendorf, Hamburg, Germany) and stored at -20°C until needed.

The bacterial 16S rRNA gene was amplified using the forward bacterial primer GM5F (5′-CCTACGGGAGGCAGCAG-3′) with a GC clamp (Muyzer et al., 1993) and the universal reverse primer D907R (5′-CCGTCAATTCCTTTRAGTTT-3′) (Amann et al., 1992). Archaeal amplification was conducted using the forward primer Arc333 with GC clamp and the reverse primer Arc958R (Struchtemeyer et al., 2005). Thermal cycling of all PCR reactions was performed with a “touchdown” PCR method (Muyzer

et al., 1993). Denaturing gradient gel electrophoresis (DGGE) was then performed using the PCR-amplified bacterial and archaeal 16S rRNA gene products. The protocol described by Muyzer et al. (1993) was modified by using a 6% polyacrylamide gel and a 40-80% denaturing gradient, and running the gel in 1X Tris-acetate-EDTA (TAE) buffer solution for 16 hours at 65 V at a constant 60°C temperature (Muyzer et al., 1993). The DGGE gels were stained with SYBR Safe and photographed under UV light. Bands of interest were excised and suspended in 30 µl of PCR-grade water; 5 µl of the excised DNA solution was used as template DNA for PCR reactions as described above. The 16S rRNA gene PCR products amplified from the excised DGGE bands were then sequenced at the Oklahoma Medical Research Foundation (Oklahoma City, OK) on an ABI 3730 capillary sequencer using the primers mentioned above.

Bacterial 16S rRNA gene clone libraries were prepared from DNA extracted using the PowerSoil DNA Isolation Kit from thiosulfate-using and methanogenic enrichments that had been transferred at least four times. Fragments of nearly full length 16S rRNA gene were generated by PCR amplification using the primers 8F and 1492R (Stackebrandt and Goodfellow, 1991) and cloned into *Escherichia coli* using the TOPO TA Cloning Kit for Sequencing (Invitrogen Corp., Carlsbad, CA). Transformed colonies were picked and transferred to 96-well microtitre plates containing Luria-Bertani broth with 25% (v/v) glycerol and 50 $\mu g \cdot ml^{-1}$ kanamycin, and grown overnight at 37°C. Plasmid DNA was purified from the transformed cells and sequenced using the M13F and M13R vector flanking regions as priming sites on an ABI 3730 capillary sequencer (Microgen: Laboratory for Genomics and Bioinformatics, Oklahoma City, OK).

The consensus bacterial 16S rRNA gene sequences were obtained using Sequencher version 5.1 (Gene Codes, Ann Arbor, MI). The software package mothur v.1.30.2(Schloss et al., 2009) was used to remove vector and chimera sequences, and define operational taxonomic units (OTUs) at a 97% identity level. A sequence representing each OTU was chosen and compared to previously reported 16S rRNA gene sequences using the BLASTN version 2.2.21+ (Zhang et al., 2000). A naïve Bayesian rRNA classifier (Wang et al., 2007) based on a 80% confidence threshold available through the RDP was used to assign phylogenetically consistent taxonomy to each representative sequence. Each representative sequence was rescreened to exclude chimeras using Pintail (Ashelford et al., 2005). Sequences that most closely matched the representative OTU sequence and selected outgroup sequences were aligned with CLUSTALX (version 1.81) (Thompson et al., 1997). Tree construction was performed using the Neighbor-Joining method (Saitou and Nei, 1987) with bootstrap values of 70% or greater used to determine each clade based on 1,000 replicates (Felsenstein, 1985). Each of the four bacterial 16S rRNA gene sequence libraries contained between 16 and 21 sequences, for a total of 74 near full-length sequences (approximately 1480 bp).

Accession numbers

The archaeal 16S rRNA gene sequences were deposited in GenBank under Accession numbers JQ014192-JQ014196. The bacterial sequences were deposited under Accession No. JQ014197-JQ014201 and KF137640.

Results

Cell enumerations and sulfide production

Most-probable number tubes with sulfite and thiosulfate had sulfide concentrations above control values in at least two tubes at all dilutions (up to 10^{-6}) regardless of whether VFAs were present or not (Table S1&S2). With sulfate as the electron acceptor, positive MPN tubes were detected at dilutions up to 10^{-5}. The MPN of the thiosulfate-reducing microorganisms was estimated at greater than 1.1 x10^{6} cells·ml^{-1} for both media with and without VFAs (Table 1). The MPN of sulfide producers using other sulfidogenic electron acceptors was lower than that for thiosulfate reducers (Table 1). The MPN of sulfite-reducing microorganisms was 2.2 x 10^{5} cells·ml^{-1} for both media with and without the VFA amendments. Sulfate-reducing microorganisms were only detected in medium with VFAs and had a MPN of 2.4 x 10^{4} cells·ml^{-1} (Table 1). The MPN of polysulfide-reducing microorganisms was 4.6 x 10^{5} cells·ml^{-1} and 4.3 x 10^{4} cells·ml^{-1}, in medium with and without VFAs, respectively. The MPN data indicated that thiosulfate reducers were the most numerous cultured, sulfide producers in the PIG scrapings from this facility.

Most-probable number tubes with thisosulfate, both with and without the VFAs, produced large amounts of sulfate, up to 7.7± 1.8 to 9.4 ± 0.64 mM in the 10^{-4} to 10^{-6} dilutions (Table S1&S2). Sulfate accumulation in MPN tubes with thiosulfate far exceeded that in controls that lacked an added electron acceptor. The production of both sulfide and sulfate in the thiosulfate-using MPNs provided evidence for the disproportionation of thiosulfate (Jørgensen, 1990), but this activity was lost upon subsequent enrichment and cultivation attempts.

Thiosulfate reduction and methanogenesis with yeast extract as the electron donor

Thiosulfate-reducing MPN cultures with and without VFAs and their respective controls (e.g. cultures amended with VFAs but not thiosulfate as well as those lacking both thiosulfate and VFAs), were transferred into media of the same composition. The total amount of thiosulfate used by enrichments transferred four times was relatively low, 7.9 ± 3.4 and 15.7 ± 2.8 μmoles in enrichments with and without VFAs, respectively. Similarly, only small amounts of sulfide were produced, 17.8 ± 2.1 and 11.2 ± 5.9 in enrichments with and without thiosulfate, respectively. The low levels of thiosulfate use and sulfide production suggested that the enrichments were electron donor deficient. To gain a better understanding of carbon cycling in these enrichments, VFA use and methane production were measured at the end of a four-week incubation period (Table 2). Little to no change in the total amount of butyrate (≤ 0.2 ± 0.02 μmoles) and valerate (≤ 0.3 ± 0.03 μmoles) were noted. Enrichments with VFAs and thiosulfate, with thiosulfate and without VFAs, and without either VFAs or thiosulfate produced substantial amounts of acetate, 12.1 ± 2.2, 8.1 ± 4.8, and 9.0 ± 3.0 μmoles, respectively (Table 2). All of the enrichments produced between 3 to 4 μmoles of propionate. In addition, low levels of isobutyrate, 2-methylbutyrate, and isovalerate were detected in our assays. The production of branch-chained fatty acids suggests the syntrophic cooperation in methanogenic degradation of amino acids. Total VFA levels remained unchanged in uninoculated controls (data not shown). Large amounts of methane were produced in enrichments that lacked thiosulfate addition (Table 2). The production of acetate, propionate, and branched-chain fatty acids suggested that the small amount of yeast extract present in the medium was being utilized as an electron donor to support thiosulfate reduction or ultimately methane production. Yeast extract

likely mimics the organic compounds exchanged by members of the anaerobic community. To test this possibility, the amount of yeast extract in the medium was varied. Figure S1A&B shows that thiosulfate reduction and the concomitant production of sulfide was dependent on the amount of yeast extract amended to the cultures. The amount of methane produced was also proportional to the amount of yeast extract present (Figure S1C). Very little methane was produced in the absence of yeast extract. The data from Figure S1 confirmed that yeast extract was an electron donor to support biological thiosulfate reduction and methane production in the enrichment cultures.

Molecular analyses of thiosulfate-reducing and methanogenic enrichments

Denaturing gradient gel electrophoresis profiles for archaea were generated from the initial MPN cultures and enrichments that had been transferred two and four times (Figure S2, showing the fourth transfer). The intensity of the archaeal DGGE bands detected in thiosulfate-reducing cultures decreased with increasing transfers. By the fourth transfer, archaeal sequences were not detected in thiosulfate-reducing enrichments. Denaturing gradient gel electrophoresis band sequences obtained from MPN (JQ014192) and second transfer enrichments (JQ014194) were both closely affiliated with *Methanothermobacter thermautotrophicus* type-strain Delta H (Figure 1). By the fourth transfer, one dominant archaeal band was evident in enrichments with and without a VFA amendment that lacked a sulfidogenic electron acceptor (Figure S2). The sequence (JQ014196) was classified to the genus *Methanothermobacter* with 100% confidence and shared 100% sequence identity to the sequence of *Methanothermobacter crinale* strain HMD (GenBank Accession No. HQ828065) (Figure 1). The presence of the *Methanothermobacter* related sequence is consistent

with the methane production from metabolism of yeast extract in the absence of a sulfidogenic electron acceptor. A second DGGE band was sequenced from the initial MPN cultures (JQ014193) and after the second transfer (JQ014195). These two sequences fell into the same 97% OTU and classified in the genus *Thermococcus* at 100% confidence. The most similar isolate 16S rRNA sequence to JQ014193 and JQ014195 is that of the type strain of *Thermococcus sibiricus* MM739 (AJ238992) (Figure 1).

Denaturing gradient gel electrophoresis analysis indicated that cultures with thiosulfate had relatively high bacterial diversity based on the number of bands in the profiles, which decreased with increasing transfers (Figure S3, showing the fourth transfer). A group of highly visible and similar bands were seen in all of the enrichments with each transfer, indicating the presence of a small but dominant group of bacteria present in these cultures regardless of electron donor or acceptor conditions of the medium. Although the bands showed high resolution and intensity, the physical separation between them was too small to allow for accurate excision and direct sequencing. In this case, bacterial 16S rRNA gene sequence libraries (total number of sequences: 74) were generated from the enrichments that had been transferred four times. Three OTUs (at 97% similarity) were obtained from the four enrichment conditions. Phylogenetic analysis separated the sequences into three clades at the order level: *Synergistales, Thermoanaerobacterales, and Unclassified/OP9* (Figure 2). Of the 74 sequences from these enrichments, 72 of them were classified into the same 97% OTU (JQ014197) within the phylum *Synergistetes* affiliated with the genus *Anaerobaculum* at 100% sequence identity. The *Anaerobaculum*-related sequences formed the majority of clones obtained from each of the four enrichment conditions.

The presence of a common bacterial sequence in all four enrichment conditions is consistent with the DGGE analysis, which detected some closely adjacent bands at the bottom of each lane (Figure S3), beginning with the MPN dilutions (data not shown). Enrichments with thiosulfate and lacking VFAs had one OTU (JQ014200) that grouped within the phylum *Firmicutes* in the family *Thermoanaerobacteraceae* at 100% confidence (Figure 2). This OTU (JQ014200) showed a 99.6% sequence identity to the cultured isolate *Thermacetogenium phaeum* PBT (GenBank Accession No. AB020336). A third OTU (KF137640), from enrichments without thiosulfate but containing VFAs showed highest similarity to unclassified uncultured clones and those identified as affiliated with Candidate Division OP9.

Iron corrosion by the thiosulfate-reducing enrichments

In petroleum systems, complex forms of organic matter analogous to yeast extract are ubiquitous in oil formations and production facilities. Such organic matter likely originates from the maturation of kerogen, the degradation of complex hydrocarbons, extracellular polymeric substances in biofilm matrices, cellular material and combinations thereof (Duncan et al., 2009). In order to simulate water-soluble organic matter in oil field systems, yeast extract concentration was used as the electron donor to evaluate the prospective role of thiosulfate-reducing and the methane-producing enrichments in the biocorrosion of carbon steel.

Thiosulfate-reducing enrichments with carbon steel coupons turned the medium completely black after 3 days, most likely due to the precipitation of iron sulfides. The accumulation of up to 2.5 ± 0.12 mM dissolved sulfide was detected over a 14-day incubation period in the presence of coupons (Figure 3A), which was comparable to the

amount of sulfide produced by the same enrichments without coupons. Meanwhile, very thick, fluffy corrosion products formed on the surfaces of the coupons and much of the deposits flaked off into the medium. Figure S4A shows the FE-SEM image of a coupon immersed in the medium after 14 days. The rod-shaped cells, morphologically similar to *Anaerobaculum* species, can be seen underneath the precipitates. As can be seen in Figure 3B, the general corrosion rate as determined by weight loss (8.43 ± 1.40 mpy) is much higher than that in autoclaved (1.49 ± 0.15 mpy) and substrate-unamended controls (3.83 ± 1.18 mpy). The total iron analysis followed the same trend, indicating that total iron analysis can be used as a complementary approach to assess general corrosion. Meanwhile, high-resolution, three-dimensional profilometric scanning images demonstrated that the damage caused on the surface of the coupon in the active culture is more pronounced than in the autoclaved controls (Figure S5A&B). Unlike the relatively smooth steel surface in the control, severe pitting was evident on the coupon surface in the presence of active thiosulfate-reducing bacteria. The pit counting analysis showed 59 pits with sizes of more than 10 μm in diameter and 20 μm in depth, whereas no pits of this size was detected in the sterile control. Twenty-nine pits in coupons exposed to active thiosulfate-reducing bacteria were greater than 20 μm in diameter and depth.

Biocorrosion by methanogenic enrichment cultures

The highest amount of methane (52.52 ± 0.56 μmols) was produced when methanogenic enrichments were grown a medium containing yeast extract and a coupon (Figure 4A). Meanwhile, only negligible methane production (1.68 ± 0.19 μmols) was detected in controls without yeast extract or a coupon. The FE-SEM confirmed biofilm

formation by the methanogenic enrichment (Figure S4B, the arrows indicate the cells inside the biofilm matrix). In Figure 4B, it can be seen that the metabolic capability of the methanogenic enrichment resulted in more iron loss than in the autoclaved control (with *P* value of 0.04). However, the general corrosion rate (2.03 ± 0.49 mpy) caused by the methanogenic enrichment was approximately 4 times less than thiosulfate-reducing enrichment (8.43 ± 1.40 mpy). Surface profilometry analysis revealed that the methanogenic enrichment created more pitting corrosion to the coupon surface (Figure S5C&D) relative to the sterile control, but far fewer pits were observed (6) than the thiosulfate-reducing enrichment (59).

As seen in Figure 4A, 9.27 ± 1.68 µmoles of methane were produced after 18 days of incubation in a medium that lacked yeast extract but did have a coupon. Intriguingly, the corrosion noted in the absence of yeast extract was slightly higher than that in the autoclaved control (Figure 4B). The above observations prompted us to investigate corrosion by the methanogenic enrichment with iron as the sole source of electrons. Methane production was observed when the methanogenic enrichment was repetitively transferred in a medium with iron granules as the sole source of electrons. After 6 successive transfers, the corrosive activity of the methanogenic enrichment was quantified. The methanogenic enrichment produced methane with the coupon alone, but more methane was produced when yeast extract was also available in the medium (Figure 4C). This suggests that the fermentative organisms in the consortium survived the repeated transfers. Cell morphologies similar to *Anaerobaculum* species (the large rod indicated by the bottom arrow in Figure S4D) and *Methanothermobacter* species (the small rod indicated by the upper arrow in Figure S4D) (Cheng et al., 2011) were

both observed on the coupon surface. However, cells attached to the surface were morphologically most similar to *Methanothermobacter* (Cheng et al., 2011) when the iron served as the sole source of electrons. Contrary to the previous observation with the methanogenic enrichment grown with yeast extract (Figure 4B), the methanogenic enrichment repetitively transferred with only iron granules caused indistinguishable corrosion (with *P* value of 0.24) compared to the autoclaved control (Figure 4D). The corrosion observed in Figure 4B could be explained by carry-over of yeast extract or other nutrients with the inoculum. Similar to the methanogenic enrichment grown on yeast extract, more corrosion was observed when the methanogenic enrichment maintained in medium with iron granules was grown in a medium with yeast extract than with the coupon alone (Figure 4D), confirming that the fermentative organisms in the methanogenic enrichment still survived after 6 transfers with iron, and that they enhanced corrosion when yeast extract was available.

Discussion

Most-probable number studies of oil pipeline PIG samples confirmed that microorganisms that use thiosulfate, sulfite, or polysulfide as electron acceptors were numerically more dominant than those that use sulfate as an electron acceptor (Table 1). Thiosulfate-users were at least 100-fold more numerous than sulfate-reducing bacteria. Our findings are consistent with studies of corrosion at a Canadian oil facility where about 30% of the isolated sulfidogenic organisms were strict sulfite reducers, 50% used only thiosulfate and elemental sulfur as electron acceptors, and only 20% were strict sulfate-reducing bacteria (Obuekwe et al., 1983;Obuekwe and Westlake, 1987). Nielsen (1991) also showed that biofilm formation and hydrogen sulfide production

increased by a factor of about two in enrichments supplemented with either sulfite or thiosulfate as the electron acceptor compared to sulfate-reducing enrichments (Nielsen, 1991). A more recent study of an Indian oil field found that MPN of thiosulfate-reducing bacteria were 4- to 8-fold higher than sulfate-reducing bacteria (Agrawal et al., 2010). Although the number of sulfate-reducing bacteria found in the Indian oil field sites and the ANS were similar (10^5 cells·ml^{-1}), the MPN of thiosulfate-reducing bacteria was higher in our study. The overall conclusion from the above analysis reinforces the importance of non-sulfate-reducing, sulfidogenic microorganisms and the utilization of sulfur oxyanions other than sulfate in the biocorrosion of petroleum facilities. We detected evidence of thiosulfate disproportionation in our MPN cultures inoculated with PIG fluids. Disproportionation of inorganic sulfur molecules has not been widely studied in oil production facilities and may have significant implications for the biogeochemical cycling of sulfur in many environments (Jørgensen, 1990;Park et al., 2011). Although thiosulfate disproportionation activity was lost upon transfer, microorganisms with this metabolic capacity should also be acknowledged as potential contributors to pipeline biocorrosion problems.

Molecular analysis was employed to link the physiochemical properties of the enrichment cultures to specific microbial interactions. Sequences related to *Anaerobaculum* sp. were identified in all four of the enrichments after four transfers. This finding is consistent with the detection by DGGE analysis of a common band in all of the enrichments. Members of the genus *Anaerobaculum* belong to the family *Synergistaceae* and are fermentative organisms that produce acetate, CO_2, and H_2 as their major metabolic end products (Menes and Muxí, 2002;Maune and Tanner, 2012).

Anaerobaculum sp. utilize a wide range of organic substrates including glucose, various organic acids, peptides, and complex organic substrates such as yeast extract (Menes and Muxí, 2002;Maune and Tanner, 2012). *Anaerobaculum* sp. are also capable of reducing thiosulfate, elemental sulfur, and cystine, but not sulfate or sulfite, to hydrogen sulfide (Rees et al., 1997;Menes and Muxí, 2002;Maune and Tanner, 2012). The bacterial clone libraries, due to the number of sequences examined, identified only dominant members of the enrichments and were not intended to fully sample the diversity. In addition, a number of other thermophilic, fermentative, thiosulfate-reducing bacteria belonging to the genera *Thermotoga* (Fardeau et al., 1997), *Thermoanaerobacter* (Fardeau et al., 2000) and *Garciella* (Miranda-Tello et al., 2003) have been isolated from high temperature petroleum reservoirs and processing facilities worldwide. We also detected sequences related to *Thermoanaerobacter* sp. in some of our enrichments. The cultivation-dependent and cultivation-independent approaches employed in this work and by others (Fardeau et al., 1997;Magot et al., 1997;Fardeau et al., 2000;Orphan et al., 2000;Miranda-Tello et al., 2003;Duncan et al., 2009;Stevenson et al., 2011) collectively show the ubiquity and the importance of fermentative, thiosulfate-reducing bacteria within oil fields. However, a large majority of studies related to corrosion have traditionally focused on sulfate-reducing bacteria and their accepted role as the primary sulfidogenic organisms in petroleum environments. The potential of thermophilic, fermentative sulfidogenic microorganisms to catalyze biocorrosion processes has been underappreciated. In this regard, it is imperative to evaluate the role of these organisms in biocorrosion of carbon steel in order to provide further guidance for better monitoring and preventing corrosion in the energy sector.

Anaerobic corrosion of iron leads to the mass loss of the iron surface and the release of ferrous iron into the aqueous phase (De Windt et al., 2003). The measurement of iron mass loss is a long established routine method and thus has been most frequently employed to determine corrosion (Enning et al., 2012). Although few studies are available (De Windt et al., 2003) attempting to measure the total iron dissolved from metal surfaces, we also performed total iron analysis to assess the corrosive potential of thermophilic, thiosulfate-reducing bacterial enrichments. We generally found that such procedures can be used as a good approach to quantify corrosion. The data clearly show that the corrosion caused by communities containing thiosulfate-reducing bacteria was more pronounced than the abiotic controls. The higher number of pits formed by thiosulfate-reducing bacteria show that they cause severe biocorrosion and indicate that these organisms are involved in pitting corrosion. It has been suggested that the accumulation of VFAs, particularly acetate (Callbeck et al., 2013), and hydrogen sulfide changes the microenvironment at the metal-liquid surface and initiates pitting corrosion (Campaignolle et al., 1996;Miranda et al., 2006). However, it was unclear whether our thiosulfate-reducing bacteria enrichment caused corrosion by the above mechanism. By using electrochemical measurements, Magot et al. demonstrated that mesophilic thiosulfate-reducing bacteria isolated from a corroding offshore Congo oil well induced severe pitting (Magot et al. 1997), with corrosion penetration rates of up to 4 mm per year. They concluded that the fermentative organisms were the causative agents for the failure of pipelines in Elf Congo, which experienced severe bacterial pitting corrosion within a year after replacement. Another study revealed that the dominant group of thiosulfate-reducing bacteria were

Enterobacteriaceae, which was responsible for severe localized corrosion of carbon steel in a marine system (Bermont-Bouis et al., 2007). It should be noted that thiosulfate reduction is a common feature of most sulfate-reducing bacteria, and these organisms were implicated as the principal cause of biocorrosion in the presence of thiosulfate (Miranda et al., 2006).

An archaeal co-culture of *Thermococcus* sp. and *Methanothermobacter* sp. isolated from the ANS caused corrosion when incubated in a medium with both yeast extract and elemental iron (Davidova et al., 2012). The presence of a hydrogen-consuming methanogen increased production of VFAs by *Thermococcus* sp. compared to *Thermococcus* sp. growing alone. It is likely that the accumulation of VFAs was an important factor in corrosion. It is reasonable to expect that the *Anaerobaculum* sp. and *Methanothermobacter* sp. present in our enrichments act in a similar manner to impact biocorrosion of carbon steel. Indeed, we demonstrated that the methanogenic enrichment produced methane and a similar suite of VFAs as was found with the *Thermococcus* sp.-*Methanothermobacter* sp. coculture through the fermentation of complex organic matter such as yeast extract. The methanogenic enrichment with *Anaerobaculum* sp. and *Methanothermobacter* sp. formed a biofilm on the surface of the coupon and corroded the coupons, but to a lesser extent than the thiosulfate-reducing enrichment. Hydrogenotrophic methanogens are commonly isolated from petroleum formations and are known to make up a significant portion of the indigenous microbial communities in such systems (Cheng et al., 2011;Mayumi et al., 2011;Nakamura et al., 2012). Sequences related to *M. crinale* and *M. thermautotrophicus* have been identified in the ANS facility and other petroleum

environments (Orphan et al., 2000;Pham et al., 2008;Duncan et al., 2009;Gieg et al., 2010). Clone library analysis of the same PIG sample showed that 75% of the detected archaeal OTUs were affiliated to *Methanothermobacter thermautotrophicus* (Stevenson et al., 2011). Hydrogenotrophic methanogens allow a complex anaerobic food chain to develop in petroleum environments by serving as a biological electron acceptor. By virtue of their ability to form syntrophic partnerships with fermentative microorganisms, hydrogenothrophic methanogens can accelerate corrosion probably by enhancing acid production by fermentative microorganisms.

Our work utilized both culture-dependent and culture-independent methods to implicate the importance of thiosulfate-reducing bacteria and methanogenic microorganisms in the biocorrosion of a hot petroleum production facility. A fermentative, thiosulfate-reducing enrichment was more corrosive than a methanogenic enrichment. The information gathered argues for the crucial role played by non-sulfate-reducing, sulfidogenic organisms and methanogens in biocorrosion of pipelines under thermophilic conditions. Thus, traditional approaches to detect and prevent microbially induced corrosion should be reconsidered to place a greater emphasis on the numerically dominant, fermentative thiosulfate-reducing microorganisms in sulfur cycling and biocorrosion in the energy production systems.

Acknowledgements

Financial and logistical support from the industrial sponsors of the OU Biocorrosion Center is gratefully acknowledged. The work was also supported in part by a grant (AwardN0001408WX20857) from the Office of Naval Research. We also appreciate

the technical assistance of Neil Wofford and the microscopy advice generously offered by Dr. Iwona Beech.

References

Agrawal, A., Vanbroekhoven, K., and Lal, B. (2010). Diversity of culturable sulfidogenic bacteria in two oil–water separation tanks in the north-eastern oil fields of India. *Anaerobe* 16**,** 12-18.

Alkire, R.C., and Lott, S.E. (1989). The role of inclusions on initiation of crevice corrosion of stainless steel II. Theoretical studies. *J. Electrochem. Soc.*136**,** 3256-3262.

Almahamedh, H.H., Williamson, C.H., Spear, J.R., Mishra, B.H., and Olson, D.L. (2011). Identification of microorganisms and their effects on corrosion of carbon steels pipelines. paper no. 11231. Corrosion/2011. NACE international, Houston, Texas.

Amann, R., Stromley, J., Devereux, R., Key, R., and Stahl, D. (1992). Molecular and microscopic identification of sulfate-reducing bacteria in multispecies biofilms. *Appl. Environ. Microbiol.* 58**,** 614-623.

Ashelford, K.E., Chuzhanova, N.A., Fry, J.C., Jones, A.J., and Weightman, A.J. (2005). At least 1 in 20 16S rRNA sequence records currently held in public repositories is estimated to contain substantial anomalies. *Appl. Environ. Microbiol.* 71**,** 7724-7736.

Banwart, G.J.P. (1981). *Basic food microbiology,.* AVI Publishing Co., Westport, Conn.

Beech, I.B., and Sunner, J. (2004). Biocorrosion: towards understanding interactions between biofilms and metals. *Curr. Opin. Biotech.* 15**,** 181-186.

Bermont-Bouis, D., Janvier, M., Grimont, P., Dupont, I., and Vallaeys, T. (2007). Both sulfate-reducing bacteria and Enterobacteriaceae take part in marine biocorrosion of carbon steel. *J. Appl. Microbio.l* 102**,** 161-168.

Caldwell, M.E., Garrett, R.M., Prince, R.C., and Suflita, J.M. (1998). Anaerobic biodegradation of long-chain n-alkanes under sulfate-reducing conditions. *Environ. Sci. Technol.* 32**,** 2191-2195.

Callbeck, C.M., Agrawal, A., and Voordouw, G. (2013). Acetate production from oil under sulfate-reducing conditions in bioreactors injected with sulfate and nitrate. *Appl. Environ. Microbiol.*

Campaignolle, X., Crolet, J.L., Dabosi, F., and Caumette, P. (1996). The role of thiosulfate on the microbially induced pitting of carbon steel. paper no.10256. Corrosion/1996. NACE international, Denver, Colorado.

Cheng, L., Dai, L., Li, X., Zhang, H., and Lu, Y. (2011). Isolation and characterization of *Methanothermobacter crinale* sp. nov., a novel hydrogenotrophic methanogen from the Shengli oil field. *Appl. Environ. Microbiol.* 77**,** 5212-5219.

Cline, J.D., and Richards, F.A. (1969). Oxygenation of hydrogen sulfide in seawater at constant salinity, temperature and pH. *Environ. Sci. Technol.* 3**,** 838-843.

Crolet, J.L. (2005). Microbial corrosion in the oil industry: a corrosionist's view. *Petroleum microbiology. ASM Press, Washington, DC***,** 143-169.

Davidova, I.A., Duncan, K.E., Perez-Ibarra, B.M., and Suflita, J.M. (2012). Involvement of thermophilic archaea in the biocorrosion of oil pipelines. *Environ. Microbiol.* 14**,** 1762-1771.

De Windt, W., Boon, N., Siciliano, S.D., and Verstraete, W. (2003). Cell density related H_2 consumption in relation to anoxic Fe(0) corrosion and precipitation of corrosion products by Shewanella oneidensis MR-1. *Environ. Microbiol.* 5**,** 1192-1202.

Dinh, H.T., Kuever, J., Mußmann, M., Hassel, A.W., Stratmann, M., and Widdel, F. (2004). Iron corrosion by novel anaerobic microorganisms. *Nature* 427**,** 829-832.

Duncan, K.E., Gieg, L.M., Parisi, V.A., Tanner, R.S., Tringe, S.G., Bristow, J., and Suflita, J.M. (2009). Biocorrosive Thermophilic Microbial Communities in Alaskan Worth Slope Oil Facilities. *Environ. Sci. Technol.* 43**,** 7977-7984.

Enning, D., Venzlaff, H., Garrelfs, J., Dinh, H.T., Meyer, V., Mayrhofer, K., Hassel, A.W., Stratmann, M., and Widdel, F. (2012). Marine sulfate-reducing bacteria cause serious corrosion of iron under electroconductive biogenic mineral crust. *Environ. Microbiol.* 14**,** 1772-1787.

Fardeau, M.L., Magot, M., Patel, B., Thomas, P., Garcia, J.L., and Ollivier, B. (2000). *Thermoanaerobacter subterraneus* sp. nov., a novel thermophile isolated from oilfield water. *Int. J. Syst. Evol. Micrbiol.* 50**,** 2141-2149.

Fardeau, M.L., Ollivier, B., Patel, B., Magot, M., Thomas, P., Rimbault, A., Rocchiccioli, F., and Garcia, J.L. (1997). *Thermotoga hypogea* sp. nov., a xylanolytic, thermophilic bacterium from an oil-producing well. *Int. J. Syst. Bacteriol.* 47**,** 1013-1019.

Felsenstein, J. (1985). Confidence limits on phylogenies: an approach using the bootstrap. *Evolution***,** 783-791.

G1-03, A. (2003). Standard practice for preparing, cleaning, and evaluating corrosion test specimens.

Gieg, L.M., Davidova, I.A., Duncan, K.E., and Suflita, J.M. (2010). Methanogenesis, sulfate reduction and crude oil biodegradation in hot Alaskan oilfields. *Enviro. Microbiol.* 12**,** 3074-3086.

Hamilton, W. (1985). Sulphate-reducing bacteria and anaerobic corrosion. *Ann. Rev. Microbiol.* 39**,** 195-217.

Harris, J.B., Webb, R.B., and Jenneman, G.B. (2010). Evaluating Corrosion Inhibitors as a Means to Control MIC in Produced Water. Corrosion/2010. NACE international, San Antonio, Texas.

Jørgensen, B.B. (1990). A thiosulfate shunt in the sulfur cycle of marine sediments. *Science (New York, NY)* 249**,** 152.

Keasler, V., Bennett, B., Bromage, B., Franco, R.J., Lefevre, D., Shafer, J., and Moninuola, B. (2010). Bacterial characterization and biocide qualification for full wellstream crude oil pipelines. Corrosion/2010. Paper no.10250. NACE international, San Antonio, Texas.

Kilbane, I., and Lamb, B. (Year). Quantifying the contribution of various bacterial groups to microbiologically influenced corrosion. Paper no. 05629. Corrosion/2005. NACE international, Houston, Texas.

Lott, S.E., and Alkire, R.C. (1989). The role of inclusions on initiation of crevice corrosion of stainless steel I. Experimental studies. *J. Electrochem. Soc.* 136**,** 973-979.

Lovley, D.R., and Phillips, E.J.P. (1986). Organic matter mineralization with reduction of ferric iron in anaerobic sediments. *Appl. Environ. Microbiol.* 51**,** 683-689.

Magot, M., Ravot, G., Campaignolle, X., Ollivier, B., Patel, B.K.C., Fardeau, M.L., Thomas, P., Crolet, J.L., and Garcia, J.L. (1997). *Dethiosulfovibrio peptidovorans* gen. nov., sp. nov., a new anaerobic, slightly halophilic, thiosulfate-reducing bacterium from corroding offshore oil wells. *Int. J. Syst. Bacteriol.* 47**,** 818-824.

Maune, M.W., and Tanner, R.S. (2012). Description of *Anaerobaculum hydrogeniformans* sp. nov., an anaerobe that produces hydrogen from glucose, and emended description of the genus *Anaerobaculum*. *Int. J. Syst. Evol. Microbiol.* 62**,** 832-838.

Mayumi, D., Mochimaru, H., Yoshioka, H., Sakata, S., Maeda, H., Miyagawa, Y., Ikarashi, M., Takeuchi, M., and Kamagata, Y. (2011). Evidence for syntrophic acetate oxidation coupled to hydrogenotrophic methanogenesis in the

high-temperature petroleum reservoir of Yabase oil field (Japan). *Environ. Microbiol.* 13**,** 1995-2006.

Mcinerney, M., Voordouw, G., Jenneman, G., Sublette, K., Hurst, C., Crawford, R., Garland, J., Lipson, D., Mills, A., and Stetzenbach, L. (2007). Oil field microbiology. *Manual of environmental microbiology***,** 898-911.

Mcinerney, M.J., Bryant, M.P., and Pfennig, N. (1979). Anaerobic bacterium that degrades fatty acids in syntrophic association with methanogens. *Arch. Microbiol.* 122**,** 129-135.

Menes, R.J., and Muxí, L. (2002). *Anaerobaculum mobile* sp. nov., a novel anaerobic, moderately thermophilic, peptide-fermenting bacterium that uses crotonate as an electron acceptor, and emended description of the genus Anaerobaculum. *Int. J. Syst. Evol. Microbiol.* 52**,** 157-164.

Miranda-Tello, E., Fardeau, M.L., Sepúlveda, J., Fernández, L., Cayol, J.L., Thomas, P., and Ollivier, B. (2003). *Garciella nitratireducens* gen. nov., sp. nov., an anaerobic, thermophilic, nitrate-and thiosulfate-reducing bacterium isolated from an oilfield separator in the Gulf of Mexico. *Int. J. Syst. Evol. Microbiol.* 53**,** 1509-1514.

Miranda, E., Bethencourt, M., Botana, F., Cano, M., Sánchez-Amaya, J., Corzo, A., De Lomas, J.G., Fardeau, M.L., and Ollivier, B. (2006). Biocorrosion of carbon steel alloys by an hydrogenotrophic sulfate-reducing bacterium *Desulfovibrio capillatus* isolated from a Mexican oil field separator. *Corros. Sci.* 48**,** 2417-2431.

Muyzer, G., De Waal, E.C., and Uitterlinden, A.G. (1993). Profiling of complex microbial populations by denaturing gradient gel electrophoresis analysis of polymerase chain reaction-amplified genes coding for 16S rRNA. *Appl. Environ. Microbiol.* 59**,** 695-700.

Nakamura, K., Takahashi, A., Mori, C., Tamaki, H., Mochimaru, H., Nakamura, K., Takamizawa, K., and Kamagata, Y. (2012). *Methanothermobacter tenebrarum* sp. nov., a hydrogenotrophic thermophilic methanogen isolated from gas-associated formation water of a natural gas field in Japan. *Int J Syst Evol Micrbiol*.

Neria-González, I., Wang, E.T., Ramírez, F., Romero, J.M., and Hernández-Rodríguez, C. (2006). Characterization of bacterial community associated to biofilms of corroded oil pipelines from the southeast of Mexico. *Anaerobe* 12**,** 122-133.

Nielsen, P.H. (1991). Sulfur sources for hydrogen sulfide production in biofilms from sewer systems. *Water Sci. Technol.* 23**,** 1265-1274.

Nor, Y., and Tabatabai, M. (1975). Colorimetric determination of microgram quantities of thiosulfate and tetrathionate. *Analytical Letters* 8**,** 537-547.

Obuekwe, C., and Westlake, D. (1987). Occurrence of bacteria in Pembina crude oil pipeline system and their potential role in corrosion process. *Appl. Microbiol. Biot.* 26**,** 389-393.

Obuekwe, C., Westlake, D., and Cook, F. (1983). Corrosion of Pembina crude oil pipeline. *Appl. Microbiol. Biot.* 17**,** 173-177.

Orphan, V., Taylor, L., Hafenbradl, D., and Delong, E. (2000). Culture-dependent and culture-independent characterization of microbial assemblages associated with high-temperature petroleum reservoirs. *Appl. Environ. Microbiol.* 66**,** 700-711.

Park, H.S., Chatterjee, I., Dong, X., Wang, S.-H., Sensen, C.W., Caffrey, S.M., Jack, T.R., Boivin, J., and Voordouw, G. (2011). Effect of sodium bisulfite injection on the microbial community composition in a brackish-water-transporting pipeline. *Appl. Environ. Microbiol.* 77**,** 6908-6917.

Pham, V.D., Hnatow, L.L., Zhang, S., Fallon, R.D., Jackson, S.C., Tomb, J.F., Delong, E.F., and Keeler, S.J. (2008). Characterizing microbial diversity in production water from an Alaskan mesothermic petroleum reservoir with two independent molecular methods. *Environ. Microbiol.* 11**,** 176-187.

Quickel, G., and Beavers, J. (2011). Pipeline Failure Results from Lightning Strike: Act of Mother Nature? *J. Fail. Anal.Prev.* 11**,** 227-232.

Rajasekar, A., Anandkumar, B., Maruthamuthu, S., Ting, Y.P., and Rahman, P.K.S.M. (2010). Characterization of corrosive bacterial consortia isolated from petroleum-product-transporting pipelines. *Appl. Microbiol. Biot.* 85**,** 1175-1188.

Rees, G.N., Patel, B.K.C., Grassia, G.S., and Sheehy, A.J. (1997). *Anaerobaculum thermoterrenum* gen. nov., sp. nov., a novel, thermophilic bacterium which ferments citrate. *Int. J. Syst. Bacteriol.* 47**,** 150-154.

Rp0775 NACE Standard. (2005). Preparation, installation, analysis, and interpretation of corrosion coupons in oilfield operations. Houston, Texas, *USA.*

Saitou, N., and Nei, M. (1987). The neighbor-joining method: a new method for reconstructing phylogenetic trees. *Mol. Biol. Evol.* 4**,** 406-425.

Schloss, P.D., Westcott, S.L., Ryabin, T., Hall, J.R., Hartmann, M., Hollister, E.B., Lesniewski, R.A., Oakley, B.B., Parks, D.H., and Robinson, C.J. (2009). Introducing mothur: open-source, platform-independent, community-supported software for describing and comparing microbial communities. *Appl. Environ, Microbiol.* 75**,** 7537-7541.

Stackebrandt, E., and Goodfellow, M. (1991). *Nucleic acid techniques in bacterial systematics.* John Wiley & Son Ltd.

Stevenson, B.S., Drilling, H.S., Lawson, P.A., Duncan, K.E., Parisi, V.A., and Suflita, J.M. (2011). Microbial communities in bulk fluids and biofilms of an oil facility have similar composition but different structure. *Environ. Microbiol.* 13**,** 1078-1090.

Stookey, L.L. (1970). Ferrozine---a new spectrophotometric reagent for iron. *Anal. Chem.* 42**,** 779-781.

Struchtemeyer, C.G., Elshahed, M.S., Duncan, K.E., and Mcinerney, M.J. (2005). Evidence for aceticlastic methanogenesis in the presence of sulfate in a gas condensate-contaminated aquifer. *Appl. Environ. Microbiol.* 71**,** 5348-5353.

Suflita, J.M., Phelps, T.J., and Little, B. (2008). Carbon dioxide corrosion and acetate: a hypothesis on the influence of microorganisms. *Corrosion* 64**,** 854-859.

Tanner, R.S. (1989). Monitoring sulfate-reducing bacteria: comparison of enumeration media. *J. Microbiol. Meth.* 10**,** 83-90.

Tanner, R.S., Hurst, C., Crawford, R., Garland, J., Lipson, D., Mills, A., and Stetzenbach, L. (2007). Cultivation of bacteria and fungi. *Manual of environmental microbiology***,** 69-78.

Uchiyama, T., Ito, K., Mori, K., Tsurumaru, H., and Harayama, S. (2010). Iron-corroding methanogen isolated from a crude-oil storage tank. *Appl. Environ. Microbiol.* 76**,** 1783-1788.

Wang, Q., Garrity, G.M., Tiedje, J.M., and Cole, J.R. (2007). Naive Bayesian classifier for rapid assignment of rRNA sequences into the new bacterial taxonomy. *Appl. Environ. Microbiol.* 73**,** 5261-5267.

Widdel, F., and Pfennig, N. (1992). The genus *Desulfuromonas* and other gram-negative sulfur-reducing eubacteria. *The prokaryotes* 4**,** 3379-3389.

Wolin, E., Wolin, M.J., and Wolfe, R. (1963). Formation of methane by bacterial extracts. *J. Biol. Chem.* 238**,** 2882-2886.

Zhang, Z., Schwartz, S., Wagner, L., and Miller, W. (2000). A greedy algorithm for aligning DNA sequences. *J. Computa. Biol.*7**,** 203-214.

Table 1 Most-probable numbers of sulfide producers in media with and without volatile fatty acids (VFA) and with different electron acceptors.

Electron Acceptor	VFA presence	MPN (cell • ml^{-1})	Two-sided 95% confidence interval (cell • ml^{-1})	
			Lower	Upper
Sulfate	+	2.4×10^4	5.8×10^3	9.9×10^4
	-	BDL[a]	BDL	BDL
Sulfite	+	2.2×10^5	1.0×10^5	4.5×10^5
	-	2.2×10^5	1.0×10^5	4.5×10^5
Thiosulfate	+	$>1.1 \times 10^6$	NA[b]	NA
	-	$>1.1 \times 10^6$	NA	NA
Polysulfide	+	4.6×10^5	2.2×10^5	9.7×10^5
	-	4.3×10^4	1.6×10^4	1.1×10^5

[a] BDL(below detection limit; <100 cells• ml^{-1}l) indicates none of the tubes were scored as positive;
[b]NA, not applicable because all MPN tubes were positive for sulfide production with thiosulfate as electron acceptor.

Table 2 Net production of methane and volatile fatty acids by enrichments transferred four times in medium (containing 0.05% yeast extract) with and without thiosulfate and volatile fatty acids.

Additions	Methane[a] (µmoles)	Acetate (µmoles)	Propionate (µmoles)	Isobutyrate (µmoles)	2-methyl-butyrate (µmoles)	Valerate (µmoles)	Isovalerate (µmoles)
SO_3^{2-} + VFA	0.11±0.02 [a]	12.1±2.25	3.5±0.5	0.6±0.1	0.9±0.13	0.1±0.4	1.2±0.2
SO_3^{2-}	0.09±0.04	8.1±4.8	3.0±1.7	0.5±0.3	0.9±0.1	BDL[b]	1.1±0.2
VFA	14.6±1.6	9.0±3.0	4.1±1.3	0.6±0.2	0.6±0.3	0.3±0.03	0.9±0.5
None	26.60±3.8	2.0±2.6	4.0±1.2	0.7±0.2	0.8±0.1	BDL	1.16±0.2

[a] Values for methane and VFAs corrected for initial levels at the time of inoculation.

[b]BDL (Below Detection Limit) indicates a concentration less than 0.05 mM, the detection limit of the gas chromatograph.

Table S 1 Mean endpoint sulfide and sulfate concentrations in most probable numbers tubes with different electron acceptors and volatile fatty acids as the electron donor [a].

Dilution	Electron acceptor added							
	Sulfate			Sulfite		Thiosulfate		
	Sulfide (mM)	Sulfate (mM)	Growth	Sulfide (mM)	Growth	Sulfide (mM)	Sulfate (mM)	Growth
10^{-2}	3.42	0.22	+	3.69	+	5.35	3.90	+
10^{-3}	3.03	1.16	+	3.72	+	6.02	2.99	+
10^{-4}	2.59	2.90	+	3.30	+	3.96	7.67	+
10^{-5}	1.54	5.21	-	2.24	+	4.34	7.74	+
10^{-6}	ND[b]	ND	-	3.00	+	3.39	9.42	+
Uninoculated	1.14	5.78	-	1.05	-	0.89	2.27	-

[a] Sulfide concentrations were corrected for background sulfide concentrations due to the use of sodium sulfide as the reductant. Positive (+) growth score indicates that at least two of three tubes at that dilution had sulfide concentrations that were at least 20% higher than sulfide in the uninoculated control of the same condition.

[b]ND, not detected. When sulfate was the electron acceptor, none of the tubes at dilutions 10^{-5} or higher had sulfide concentrations that were 20% higher than sulfide concentrations in the uninoculated control.

Table S 2 Mean endpoint sulfide and sulfate concentrations in most probable numbers tubes with different electron acceptors and without volatile fatty acids[a].

Dilution	Electron acceptor added							
	Sulfate			Sulfite		Thiosulfate		
	Sulfide (mM)	Sulfate (mM)	Growth	Sulfide (mM)	Growth	Sulfide (mM)	Sulfate (mM)	Growth
10^{-2}	2.40	2.83	-	3.12	+	5.30	3.74	+
10^{-3}	2.50	3.05	-	3.02	+	5.85	4.87	+
10^{-4}	2.10	4.17	-	3.43	+	5.55	5.63	+
10^{-5}	1.40	4.62	-	2.02	+	3.48	8.06	+
10^{-6}	ND[b]	ND	-	2.78	+	3.23	9.19	+
Uninoculated	2.21	6.23	-	1.62	-	1.55	1.81	-

[a] Sulfide concentrations were corrected for background sulfide concentrations due to the use of sodium sulfide as the reductant. Positive (+) growth score indicates that at least two of three tubes at that dilution had sulfide concentrations that were at least 20% higher than sulfide in the uninoculated control of the same condition.

[b]ND, not detected. When sulfate was the electron acceptor, none of the tubes at dilutions 10^{-5} or higher had sulfide concentrations that were 20% higher than sulfide concentrations in the uninoculated control.

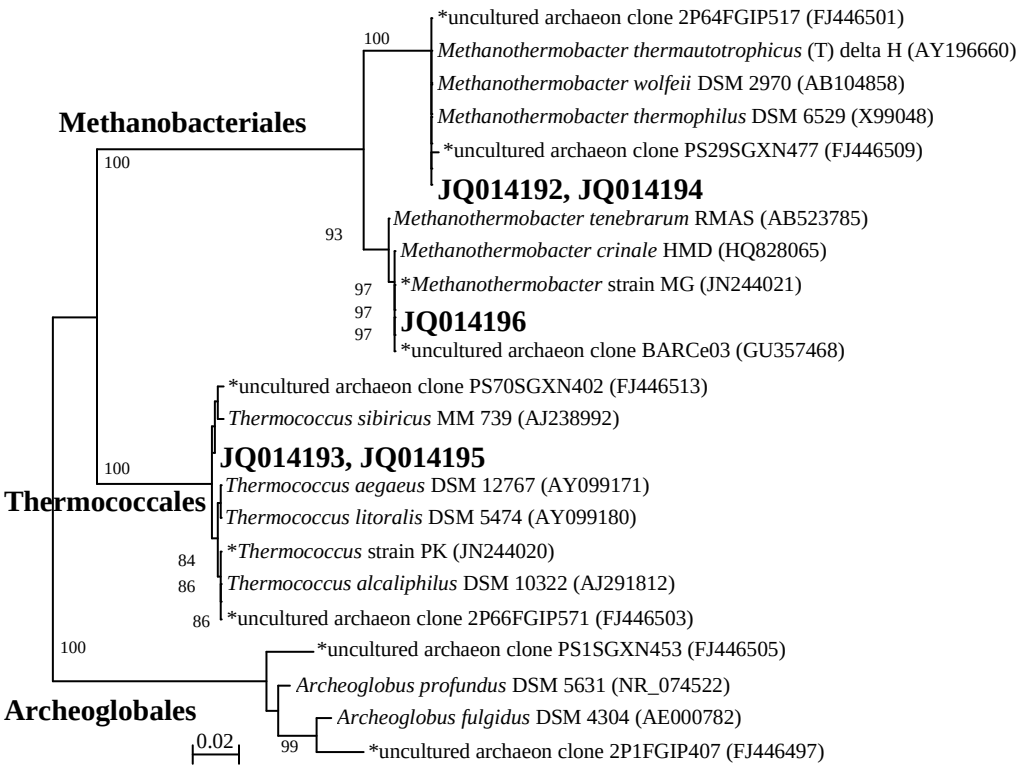

Figure 1 Phylogenetic relationships of archaeal 16S rRNA gene sequences obtained from the excised DGGE bands from enrichments and MPN cultures. The tree is constructed from approximately 350 bp 16S rRNA gene sequences using the neighbor-joining algorithm. One thousand bootstrap replications were performed; only values greater than 70% are shown. The accession numbers shown in bold are of representative sequences from the current study and labels beginning with an * are from samples, enrichments, or isolates taken from the same field (4-5, 10, 20, 50). Bar: 0.02 nucleotide substitutions per nucleotide.

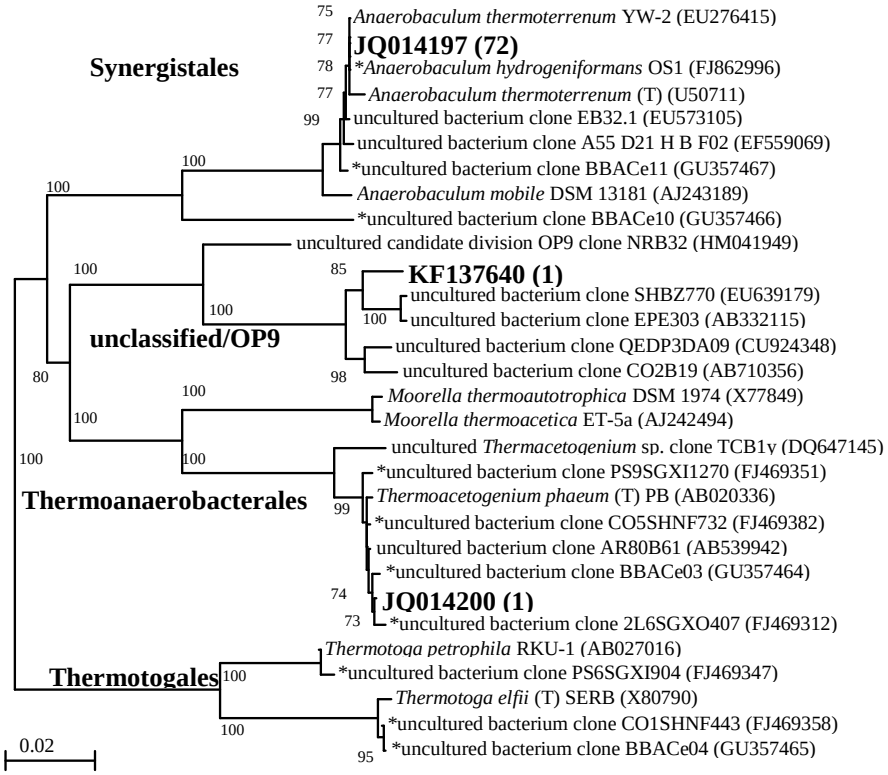

Figure 2 Phylogenetic relationships of bacterial 16S rRNA gene sequences obtained from enrichments by the 4th transfer. The tree is constructed from approximately 1300 bp 16S rRNA gene sequences using the neighbor-joining algorithm. One thousand bootstrap replications were performed; only values greater than 70% are shown. The accession numbers shown in bold are of representative sequences from the current study; the number in parentheses following bold accession numbers is the total number of sequences obtained for each OTU (97% similarity). Labels beginning with an * are from samples, enrichments, or isolates taken from the same field (4-5, 10, 20, 50). Bar: 0.02 nucleotide substitutions per nucleotide.

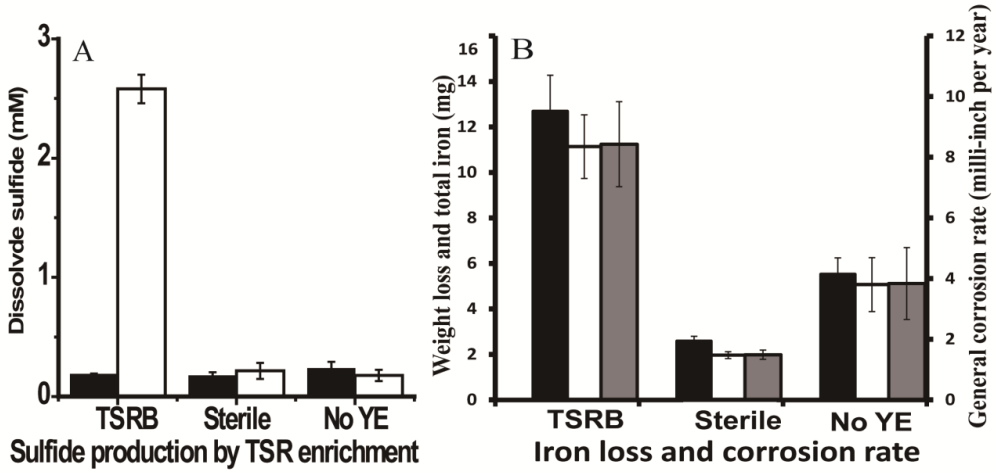

Figure 3 Sulfide production and corrosive activities of thiosulfate-reducing enrichments. (A) Dissolved sulfide accumulation in the medium after 14 days incubation. The black bars represent the dissolved sulfide at zero time, and the clear bars represent dissolved sulfide at the end point of experiment; (B) Weight loss and total iron released from coupon in the cultures after 14 days incubation. The black bars represent corrosion determined by total iron analysis; the clear bars indicate corrosion as determined by weight loss; and the grey bars are general corrosion rates calculated based on the weight loss data. The medium contained 1 g/l yeast extract. Abbreviations: TSRB, thiosulfate-reducing enrichment; Sterile, controls with autoclaved inocula; and No YE, inoculated controls without YE.

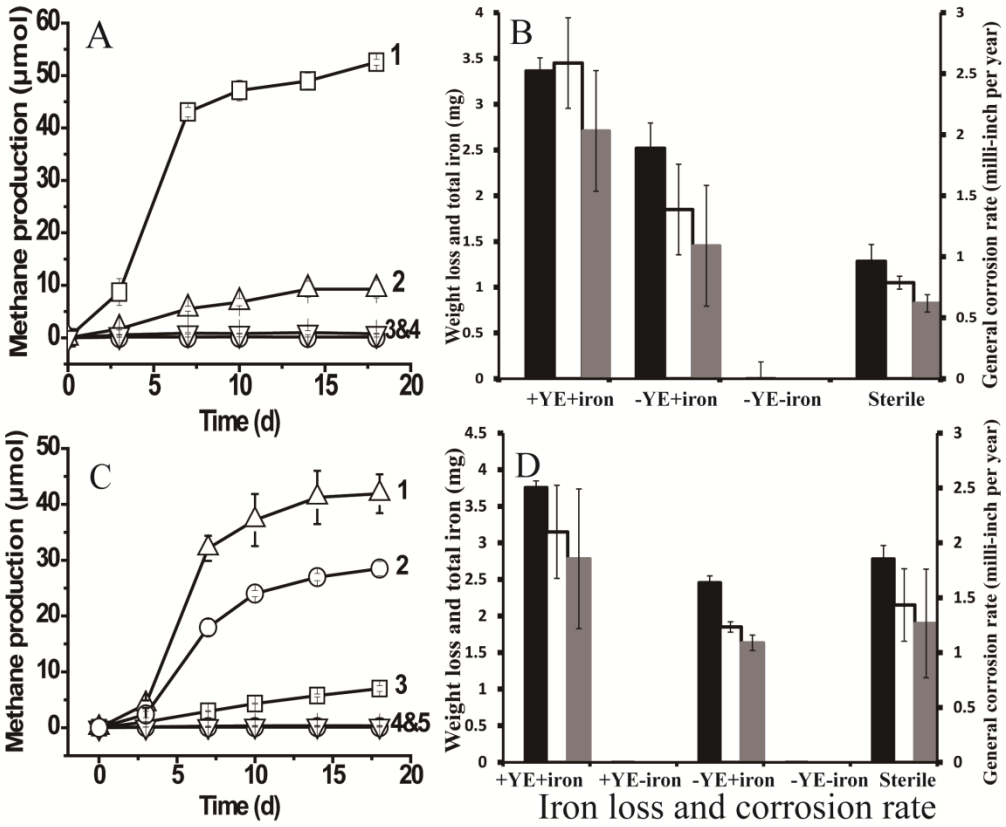

Figure 4 Methane production and corrosive activities of the methanogenic enrichment. (A) Methane production by methanogenic cultures grown with yeast extract under various conditions: Line 1, active inocula with yeast extract (YE) and a carbon-steel coupon in the medium; Line 2, active inocula with only the coupon in the medium; Line 3, active inocula without YE or the coupon; and Line 4, autoclaved inocula with YE and coupon. (B) Weight loss and total iron released from the coupon in methanogenic enrichments previously grown with YE only. (C) Methane production by methanogenic cultures after 6 successive transfers with iron as the sole source of electrons in the medium: Line 1 active inocula with YE and a coupon in the medium; Line 2, active inocula with only YE in the medium; Line 3, active inocula with only a coupon in the medium; and Line 4 and Line 5 (overlapping data) refer to the negative controls, active inocula without YE or the coupon and autoclaved inocula with YE and a coupon, respectively. (D) Weight loss and total iron released from coupon in the cultures of methanogenic enrichment after 6 transfers with iron granules. The black bars in Figs. B&D indicate the corrosion determined by total iron analysis; the clear bars in Figs. B&D represent the corrosion determined by weight loss; and the grey bars in Figs. B&D are general corrosion rate calculated based on the weight loss data. +YE+iron: with both YE and coupon in the medium; Sterile: autoclaved inocula with both YE and coupon in the medium;-YE+iron: with only the coupon in the medium;-YE-iron: without YE or the coupon in the medium; +YE-iron: with only YE in the medium. The methane production (µmols) was calculated based on a 15-ml headspace.

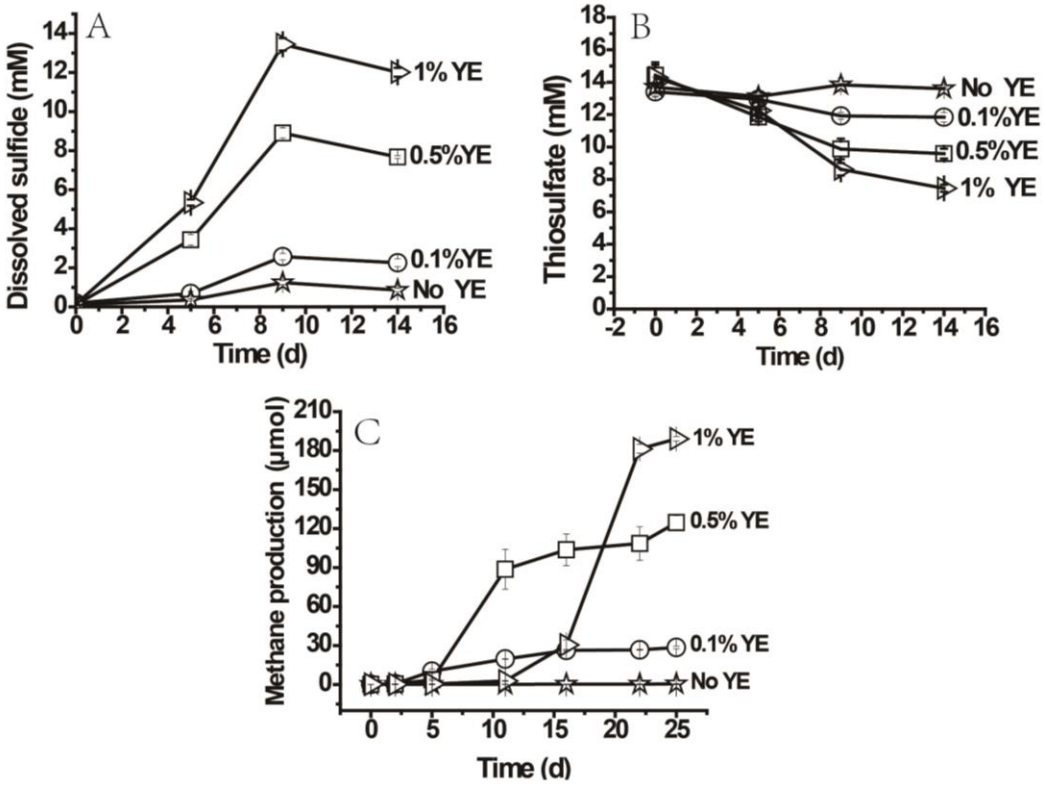

Figure S1 Sulfide production and thiosulfate reduction by thiosulfate-reducing enrichments and methane production by methanogenic enrichments with different concentrations of yeast extract. (A) Sulfide production by the thiosulfate-reducing enrichments; (B) Thiosulfate reduction by the thiosulfate-reducing enrichments; (C) Methane production by the methanogenic enrichment. The percent concentration of yeast extract (YE) added to the medium is shown next to each plot. The methane production (µmols) was calculated based on a 15-ml headspace.

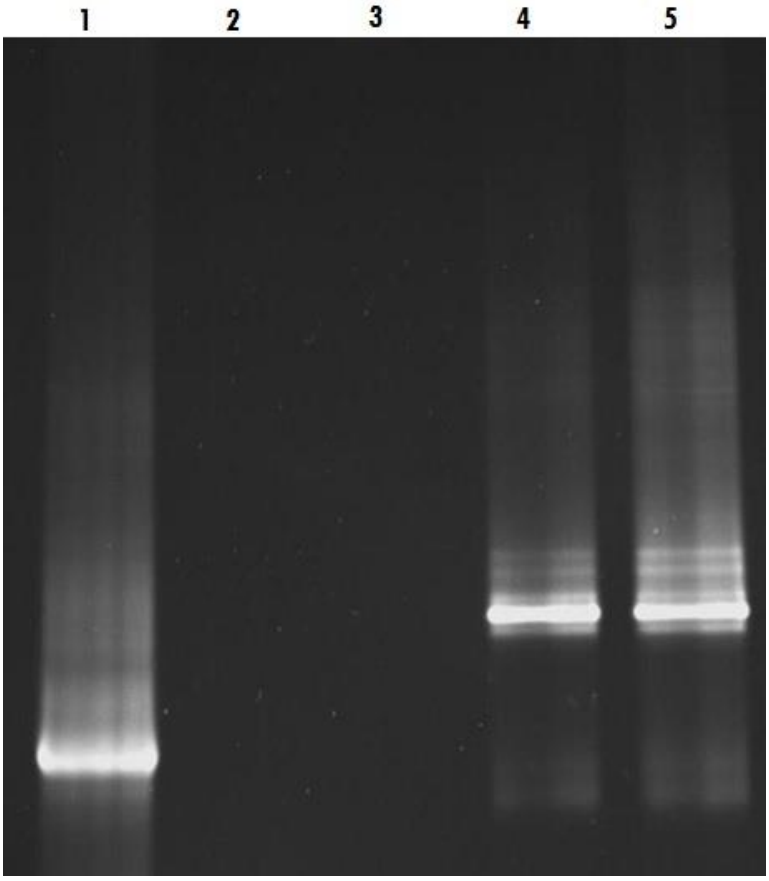

Figure S2 Archaeal DGGE profile from enrichments transferred four times with or without VFAs and with or without thiosulfate added as electron acceptor. Lanes 1-5 represent to the following conditions: 1, *Methanocaldococcus jannaschii* DNA as positive control; 2, VFAs and Thiosulfate; 3, Thiosulfate and no VFAs; 4, VFAs without an electron acceptor; and 5, no VFAs and no electron acceptor.

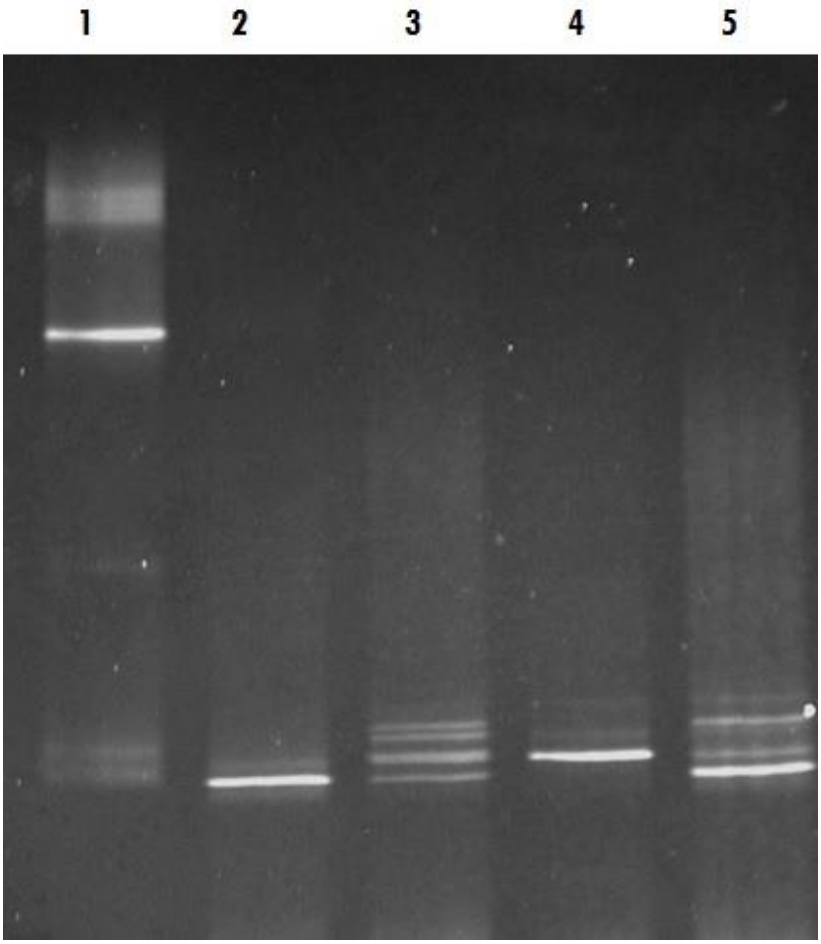

Figure S3 Bacterial DGGE profile from enrichments transferred four times with or without VFAs and with or without thiosulfate added as electron acceptor. Lanes 1-5 represent to the following conditions: 1, *Bacillus licheniformis* as positive control; 2, VFAs+Thiosulfate; 3, No VFAs+thiosulfate; 4, VFAs+ no electron acceptors; 5, No VFAs+ no electron acceptors.

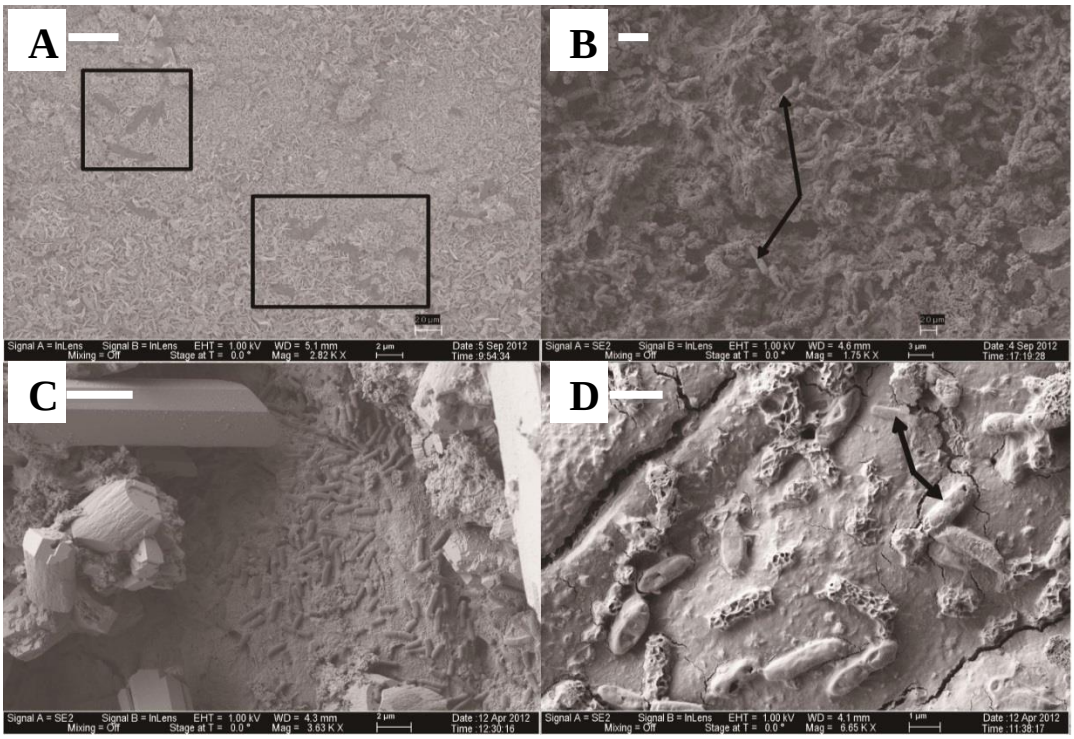

Figure S4 Field-emission, scanning electron micrographs of corroding surfaces and cells colonization. (A) Cells of the thiosulfate-reducing enrichment embedded in the fluffy corrosion products; (B) Biofilm development by methanogenic enrichment grown in medium with yeast extract (YE); (C) Methanogenic enrichment grown with steel coupon as the sole source of electrons; (D) Methanogenic enrichment (after 6 successive transfers with iron granules) grown on YE. The rectangles in (A) and arrows in (B) and (D) indicate the cells attached on the surfaces. The scale bars next to the labels for (A), (B) and (C) are 2 µm whereas that for (D) is 1 µm.

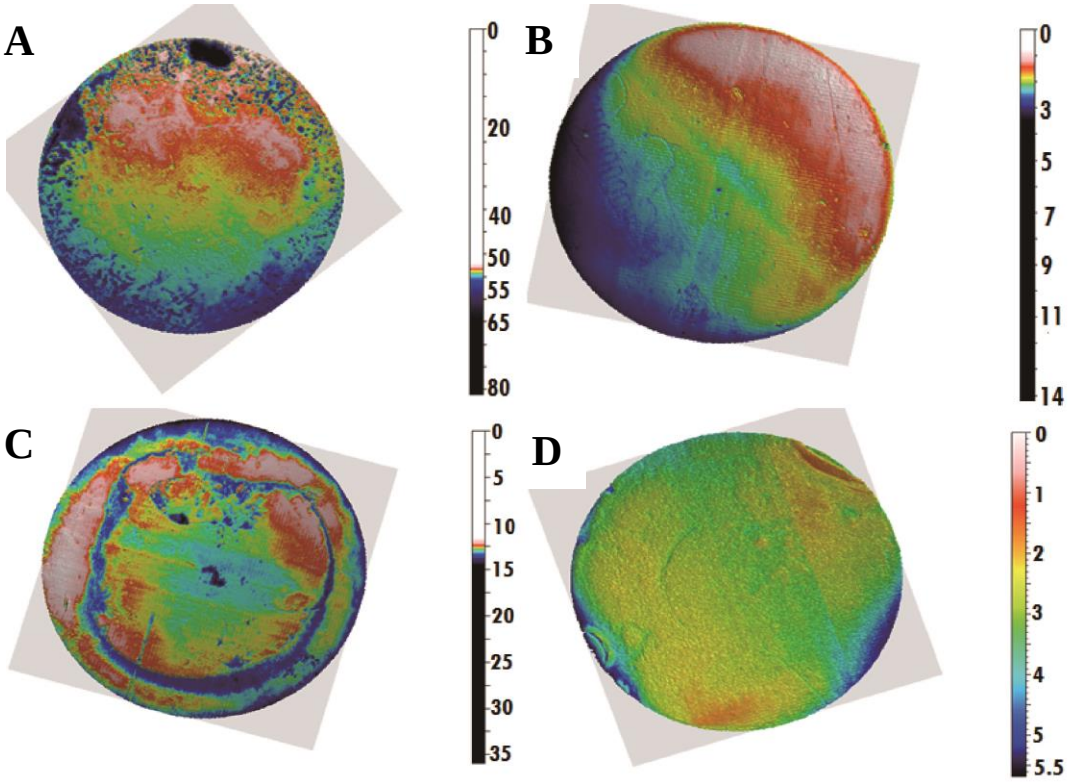

Figure S5 Topological characterization of coupons by three-dimensional profilometry analysis. (A) Active inoculate of a thiosulfate-reducing enrichment; (B) Autoclaved thiosulfate-reducing enrichment inocula control; (C) Active methanogenic enrichment grown with yeast extract; (D) Autoclaved methanogenic enrichment control. The false colors correspond to the various depths of the measured points on the surface and the units for the scale bars are µm. The total surface area of the coupons is 71.16 mm^2 with a diameter of 9.53 mm.

Chapter 2: Metabolic capability of a predominant *Halanaerobium* sp. in hydraulically fractured gas wells and its implication in pipeline corrosion

Abstract

Microbial activity associated with produced water from hydraulic fracturing can lead to gas souring and corrosion of carbon-steel equipment. While the microbial community structure of such waters has been well documented, the ecology of the prevalent microorganisms and their perspective role in corrosion remain underexplored. A halophilic bacterium (*Halanaerobium* sp. strain DL-01) was isolated from produced water dominated by sulfidogenic bacteria within the Order Halanaerobiales. The isolate could degrade guar gum, a polysaccharide polymer used in fracture fluids, to produce acetate and sulfide when thiosulfate was available. Unexpectedly, the degree of carbon-steel coupon dissolution in nonsterile incubations was less than that detected in the sterile controls. Our findings suggest that acidogenic and sulfidogenic halophiles in fractured shale formations can produce corrosive endproducts during polysaccharide metabolism. While these metabolic products were not corrosive under laboratory conditions, they could be transported from the sites of their production to downstream infrastructure and exacerbate corrosion of pipeline and storage tanks in the field.

Introduction

It is estimated that the percentage of total natural gas supplies from geological shale formations will increase from approximately 20% (2010) to 50% by 2025 in the United States.[1] Such remarkable growth of shale gas production is largely attributed to the advancement of hydraulic fracturing technologies.[2] Hydraulic fracturing involves the process of injecting large volumes of water, proppant and a myriad of chemical additives into the deep subsurface with high pressure to liberate natural gas from shale formations.[3] Microbial activity (e.g. biogenic sulfide production) associated with produced water can lead to gas souring and biocorrosion of production facilities [1]. Since the catastrophic failures of gas pipelines and storage tanks caused by corrosion are dangerous and expensive, biocides are typically employed in the fracturing fluid to control deleterious microbial activities.[4-6]

Despite treatments of the fracturing fluid with biocides and the extreme physicochemical conditions in the fractured deep subsurface, a stream of recent studies has revealed that similar predominant microorganisms were associated with produced water from various hydraulically fractured shale formations in the United States.[1, 7-11] Typically, the microbial community was mostly composed of halophiles including acid-producing bacteria and multiple lineages of sulfidogenic microorganisms.[1, 7, 10-12] Most of the dominant halophilic species were affiliated with the genus *Halanaerobium*, which can sometimes account for over 99% of the microflora in produced water.[7, 10] The genus *Halanaerobium* is well known for fermentation of carbohydrate and sulfide production through thiosulfate reduction.[13, 14] Therefore, *Halanaerobium* is clearly an important

genus that might play vital roles in the biodegradation of organic matter and production of sulfide in the fractured shale formations.

Numerous organic chemical additives are typically found in hydraulic fracturing fluids [15] and could serve as electron donors to support microbial growth and sulfidogenic processes.[9, 16] Among them, guar gum is a principal component of fracturing fluids and is commonly used as a thickening agent in the oil and gas industry.[15, 17] As a high-molecular weight polysaccharide composed of galactose and mannose, guar gum has been found to be readily degradable by anaerobic bacteria from the human colon.[18, 19] However, the biodegradation of guar gum by the dominant anaerobic microorganisms in the fractured shale formation remains unknown. Recently, activated sludge and microbial mats were proposed as efficient biological treatments to aerobically degrade guar gum in flowback wastewater from hydraulic fracturing.[17, 20] Additionally, other studies have indicated that concentrations of dissolved organic carbon in produced water decreased rapidly via abiotic or biotic processes in the subsurface.[7, 9] In this regard, we hypothesized that the dominant *Halanaerobium* species in the produced water can partially contribute to the decomposition of guar gum and the production of acetate and sulfide in the fractured deep subsurface.

Better understanding of the *in situ* metabolic activity of the prevalent *Halanaerobium* in complex subterranean environments may help in the control of these acid-producing and sulfidogenic organisms and further mitigate biocorrosion problems. However, culture-independent molecular approaches only provide phylogenetic information and genomic potential of the associated microbial community.[21] These molecular techniques such as high-throughput sequencing typically cannot distinguish

between DNA from live organisms and dead cells,[7] potentially leading to biased conclusions on the *in situ* metabolic activity of indigenous microorganisms. In contrast, cultivation-based approaches can provide complementary insight on the physiology and possible interactions among the live, cultivable microbes. The efficacy of biocides against the indigenous microorganisms can also be critically evaluated against isolates or enrichment cultures to provide guidance on field treatment. Therefore, the integration of both culture-dependent and -independent techniques will help to gain a better understanding of the fate of organic matter in the fractured deep subsurface and the role of associated metabolites such as organic acids and sulfide in the corrosion of carbon-steel pipelines.

The objective of this study was to examine the microbial ecology of produced water associated with hydraulic fracturing and the potential roles of the dominant microorganisms in corrosion of gas pipelines. We characterized the geochemistry and microbial assemblages in produced water from a hydraulically fractured site in the Barnett Shale (Texas, USA). One of the predominant organisms (*Halanaerobium* sp. strain DL-01) was subsequently isolated and its role in the biodegradation of guar gum and corrosion of carbon steel was further examined under both fermentative and thiosulfate-reducing conditions. Moreover, the efficacy of biocides against strain DL-01 was critically evaluated to potentially decrease the prevalence of *Halanaerobium* and thereby mitigate deleterious biocorrosion processes in shale gas production facilities.

Experimental Section

Site Description and Samples Collection. Samples of produced water were collected from a shale gas production facility in the Barnett Shale near Arlington, Texas, USA in

July and September 2012, respectively. The schematic of the sampling site is represented in Figure 1. The upstream comingled produced water (UCPW) near the gas-water separator (Figure 1) was collected in a 1L polypropylene bottle closed without a headspace (Nalgene, Rochester, NY, USA). Downstream water from the receiver (DRW) along the gas pipeline (Figure 1) was obtained in the similar manner. The samples for geochemical analyses and cultivation were stored at 4 ^{o}C before use. For microbial community characterization, 250-300 mL samples were filtered in the field using Nalgene analytical filter funnels containing nitrocellulose filters (sterile, 0.45µm, Nalgene Fisher Scientific, Pittsburgh, PA, USA). The filters were placed into sterile 50 mL centrifuge tubes and preserved with 1 mL of DNAzol (DNAzol DN127, Molecular Research Center, Inc., Cincinnati, OH, USA). The tubes containing the filters were placed on ice until returned to the laboratory (within 5 hours) and then transferred to a freezer (-85 ^{o}C) until DNA extraction.

Microbial Enumeration. A most probable number (MPN) procedure was used to enumerate sulfate-reducing (SRB), acid-producing (APB) and thiosulfate-reducing bacteria (TRB). For SRB and APB, commercially produced media (C&S Labs, Tulsa, OK, USA) were directly compared with media prepared in the lab upon return of samples. All MPN media formulations were adjusted to pH 7.0 and salinities of 5% and 10% (w/v) NaCl, based on available commercial medium salinities routinely employed at this site. The enumeration of SRB was conducted using RST-API medium.[22] The media for APB and TRB enumeration were prepared as previously described.[23, 24] The original aqueous sample (1 mL) was inoculated into 9 mL of media in Balch tubes with a sterile syringe flushed with N_2. Serial dilutions (10-fold) were made by transferring 1

mL of each dilution to separate Balch tubes containing 9 ml of fresh media. MPN tubes were prepared in triplicate and incubated at 37 ^{o}C for 4 weeks. The number of each group of bacteria was enumerated with the statistical table described previously. [25]

Microbial Community Characterization. Filters preserved in the field were thawed and DNA was extracted using the Promega Maxwell ®16 Tissue LEV Total RNA purification kit as described previously [26] with the following modification. The filter was successively rinsed first with RNA dilution buffer after brief vortexing, then RNA lysis buffer, and finally nuclease-free water. All liquid resulting from the rinsing steps was pooled, vortexed briefly and then dispensed into two Maxwell cartridges. DNA eluted by the Maxwell protocol was quantified by fluorometry (Qubit® dsDNA HS Assay, Life Technologies).

The pooled 16S rRNA gene library was prepared (Illumina TruSeq LT kit) with primers S-D-Arch-0519-a-S-15 and S-D-Bact-0785-b-A-18 [27] modified to include a 16bp M13 sequence to allow for the addition of a 12bp barcode [28, 29] unique to each library. The libraries were sequenced on the Illumina MiSeq platform using V2 PE250 chemistry. Paired reads were joined and then demultiplexed in QIIME (Quantitative Insights Into Microbial Ecology) software package [30]. Chimeras were removed and Operational Taxonomic Units (OTUs) were assigned at 97 % similarity using USEARCH 6.1.544.[31] Taxonomy was assigned using the RDP (Ribosomal Database Project) naive Bayesian classifier [32] against the SILVA SSU (small subunit) database (Release 111).[33] Raw sequences were submitted to the NCBI sequence read archive (SRA) database (Accession number: SRX1046644).

Enrichment and Isolation. Samples of upstream, comingled water (UCPW) and downstream water from the receiver (DRW) (10 mL) were inoculated into 160 mL serum bottles containing 50 ml of reduced marine mineral medium [34] adjusted to 4% and 10% salinity. To test potential predominant electron donors in the fractured subterranean systems, the incubations received the following compounds as sources of energy and carbon: 1) gas condensate (1 µL); 2) 20 psi gas mixture of methane, ethane, butane and propane (1:1:1:1); 3) 20 psi H_2:CO_2 (20:80); 4) a mixture of pyruvate (10 mM) and lactate (10 mM); 5) elemental iron (as granules). Sterile and substrate-free controls were prepared. All enrichments were kept at 31 ^oC and monitored for growth by following sulfate consumption and microscopic cell counts. Positive incubations showing active growth were transferred and enrichments obtained in 10% NaCl medium were used for isolations.

Initial isolations were performed by using serial 10-fold dilutions in the same basal medium,[34] containing 10% NaCl and glucose (20 mM) as a growth substrate at 37 ^oC. After several subsequent dilutions, pre-purified cultures were used to inoculate anaerobic culturing bottles containing the same glucose-based medium solidified with 2% agar. After 7 days of incubation, isolated colonies were picked from the culture bottles while inside an anaerobic glove chamber. An isolate obtained in this manner and designated strain DL-1 was maintained in sulfate-free, reduced marine mineral medium containing 10% NaCl, glucose (20 mM) and yeast extract (0.001%). The isolation of a pure culture was confirmed by denaturing gradient gel electrophoresis and by microscopy. Growth was tested with the following electron donors: galactose (20 mM), mannose (20 mM), guar gum (0.5% w/v), and cellulose (0. 2% w/v cut filter paper).

Thiosulfate (10 mM) and sulfate (20 mM) were tested as electron acceptors. Growth was monitored as changes in optical density at 600 nm (where possible), protein production and by sulfide production (see Analytic techniques).

Sequencing and Phylogenetic Analysis. Cells were grown in marine mineral medium (10% NaCl) with 0.5% guar gum at 37 °C as described above. Stationary phase cells (15 mL) were collected by centrifugation at 8000×g for 15 min at room temperature. Cell pellets were further treated with 20 μg/mL proteinase K (Promega) for 15 min at room temperature. Genomic DNA was extracted with Maxwell 16 Tissue LEV total RNA purification kit as previously described.[26] The 16S rRNA gene of strain DL-01 was amplified using PCR Supermix (Invitrogen, Carlsbad, CA) with universal primers fD1 and rP2 described previously.[35] The PCR products were treated with ExoSAP-IT (USB Corporation) and sequenced at the Oklahoma Medical Research Foundation DNA Core Facility (Oklahoma City, OK). The quality of the obtained sequence was verified and assembled with the program suite Sequencher version 5.1 (Gene Codes Corp., Ann Arbor, MI). The assembled sequence (length=1362 bp) was aligned with other closely related type strain sequences retrieved from the NCBI Genbank. The phylogenetic analysis was performed using MEGA 6.0 using the neighbor-joining method [36] and bootstrap analysis with 1000 replicates. The GenBank/EMBL/DDBJ accession number for the 16S rRNA gene sequence of strain DL-01 is KR612329.

Analytical Techniques. The anions sulfate and chloride were analyzed by ion chromatogram as described previously. [37] Sulfate was determined on samples pretreated to remove halides using Dionex OnGuardII Ag/Na cartridges (Thermo Fisher Scientific, Sunnyvale, CA) as described by the manufacturer. The pH was measured in the field

with pH strips (color pHast indicator strips pH 5–10; EM Science, Gibbstown, NJ, made in Germany). The concentration of thiosulfate was quantified using an iodometric CHEMetrics thiosulfate titration kit (CHEMetrics, Inc., Calverton, VA, USA). Dissolved ferrous iron and sulfide were measured by the ferrozine assay [38] and methylene blue method [22] as previously described. Protein was determined using the Thermo Scientific™ Pierce™ BCA™ Protein Assay (Thermo Scientific, Pittsburgh, PA, USA) according to manufacturer's instructions. The fermentation products like formate, acetate, pyruvate and lactate were measured by high performance liquid chromatography (HPLC, Dionex model IC-3000, Sunnyvale, CA) as previously described.[39] The wavelength of the UV absorbance detector was set at 210 nm and the mobile phase was 60% (vol/vol) KH_2PO_4 (25 mM, pH 2.5) and 40% acetonitrile. The pump was operated at a flow rate of 1 mL/min. In addition, portions of the samples were diluted in 30 mM oxalic acid in order to measure ethanol by gas chromatography with flame ionization detection (GC-FID) under the operating conditions described in Davidova et al..[40]

Corrosion Assay. The carbon steel (1018) used in this study was composed of 0.14–0.2% C, 0.6–0.9% Mn, 0.035% maximum S, 0.03% maximum P, and the remainder was Fe. Round carbon-steel coupons (9.53 mm in diameter by 1 mm in thickness) were initially polished to a 3-5 micron finish surface. The coupons were cleaned in an ultrasonic bath sequentially with water and acetone as previously described.[41] The polished, cleaned coupons were dried under a stream of N_2 gas and kept in a sealed serum bottle under N_2 before autoclaving.

The same marine mineral medium [34] was prepared as described above and then 20 ml was transferred to a 70 mL serum bottle containing a pre-weighed coupon in an anaerobic chamber. Guar gum was added as a growth substrate at two different concentrations (1 g/L and 5 g/L) to reflect the variance in concentration in fracturing fluid. Cells of strain DL-01 (2 mL) in early stationary growth phase were inoculated and incubated at 37 ^{o}C. The corrosion experiment was performed in triplicate. The culture was periodically sampled to determine sulfide and acetate concentrations. Biofilm characterization was performed using field-emission scanning electron microscopy (FE-SEM) as previously described.[41] Coupons were cleaned at the conclusion of the experiment to remove the corrosion product following the ASTM standard protocol.[42] The weight loss method and total iron analysis were employed to determine the corrosion rate as reported previously.[41] After weight loss was determined, the surface of coupons was scanned with a Nanovea non-contact optical profilometer PS50 (MicroPhotonics, Inc, Irvine, CA) to measure pitting damage [41]. Pits were defined as regions that were 5 μm below the mean plane and had an equivalent diameter greater than 10 μm.

Efficacy of Biocides against Strain DL-01. The efficacy of common biocides used in the oil and gas industry was determined against *Halanaerobium* sp. strain DL-01 under fermentative and thiosulfate-reducing conditions. The biocides tested included glutaraldehyde, tetrakis (hydroxymethyl) phosphonium sulfate (THPS) and benzyl dodecyl dimethyl ammonium chloride (a representative quaternary ammonium compound, abbreviated as QAC). Glucose (20 mM) was used as a substrate and strain DL-01 was grown in 10% NaCl marine mineral medium [34] at 37 ^{o}C. The assay was

performed in Balch tubes containing 9 ml medium and 1 ml cells of strain DL-01. The inoculated media were exposed to different dosages of biocides (final concentrations varying from 1 mg/L to 500 mg/L depending on the minimum inhibitory concentration of each biocide) under fermentative conditions (no electron acceptor) and thiosulfate-reducing conditions (10 mM thiosulfate). The corresponding sterile controls were inoculated with heat-killed cells of strain DL-01 and served as the basis for determining the efficacy of biocides. Optical density (600 nm wavelength) was measured over time to monitor the microbial growth. Additionally, acetate and sulfide were measured at the conclusion of the experiment as further evidence of microbial activity.

Results

Geochemistry and Microbial Enumerations. The geochemistry of the produced water in the upstream (UCPW) and downstream (DRW) samples is summarized in Table 1. The pH in all samples was between 6.5 and 7.0. The content of Cl^- in the UCPW (4.7-12%) was much higher than the DRW sample (1.7-2.0%). Notably, dissolved ferrous iron (Fe^{2+}) in DRW (11.76 mM) was much higher than UCPW (0.73 mM) probably due to the corrosion that occurred in the downstream pipeline (Figure 1). In addition to sulfate and sulfide, a low level of thiosulfate was detected in the DRW (0.17±0.01 mM). These data suggest that sulfate and thiosulfate could be potential electron acceptors for sulfide production. Interestingly, the concentration of acetate in the DRW (170 mM) was much higher than UCPW sample (0.5 mM). The number of cultivable acid producing bacteria in UCPW was $5x10^3$ cells/mL when grown in medium containing 10% NaCl (Table S1), which was close to the salinity of the original sample (11.7%

NaCl). However, only minimal growth of thiosulfate and sulfate-reducing bacteria was observed. No growth was detected in all tubes in DRW sample.

Microbial Community Characterization. No quantifiable or amplifiable DNA could be extracted from DRW samples. In contrast, an appreciable amount of DNA was obtained from UCPW sampled in both July and September, 2012. The microbial assemblages associated with the UCPW samples were characterized by high-throughput sequencing of PCR-amplified 16S rRNA gene libraries. Sequences affiliated with the order Halanaerobiales were numerically dominant (64.4-70.7%) in both UCPW samples (Figures 2 and S1). Representative sequences from these OTUs were primarily affiliated with the genera *Orenia* and *Halanaerobium* (Figure 2). Interestingly, the relative abundance of OTUs most closely related to the genus *Halanaerobium* increased to become the most dominant taxon (from 17% to ~33%) in the later produced water, whereas the genus *Orenia* decreased from 39% to ~17% (Figure 2). In addition, sequences affiliated with the Order Desulfovibrionales only accounted for ~5 % of the total bacterial community (Figure S1).

Isolation and Characterization. Microbial growth was initially observed with the UCPW inoculum when either pyruvate or lactate served as a substrate. Subsequent transfers revealed that the enrichment was also capable of growth with glucose as a carbon and energy source. Repeated transfer of the enrichment culture and eventual isolation of individual colonies on the same glucose-based medium solidified with 2% agar ultimately was used to obtain a pure culture. The colonies were round, smooth and opaque. Cells of strain DL-01 were short rods and usually appeared in pairs or assembled in string-like chains (Figure S2). Isolate DL-01 could grow under a broad

range of salinities ranging from 2%-15% NaCl, and could ferment glucose, galactose, mannose and the polysaccharide, guar gum. Thiosulfate was found to be a suitable electron acceptor when strain DL-01 was grown with various carbohydrates including guar gum. Phylogenetic analysis based on 16S rRNA gene sequences indicated that strain DL-01 was likely a member of the genus *Halanaerobium* and most closely related to the type strain of *Halanaerobium kushneri* (Figure 3). Notably, the 16S rRNA gene sequence of strain DL-01 places it within OTU-3 (Figure S3), suggesting that the dominant *Halanerobium* phylotype was isolated from UCPW.

Acetate and Sulfide Production by *Halanaerobium* sp. Strain DL-01. Strain DL-01 was capable of growth with guar gum as the sole carbon and energy source under both fermentative and thiosulfate-reducing conditions. Under thiosulfate-reducing conditions, 7.1±0.3 mM dissolved sulfide (subtracted from the unamended background) accumulated in the medium after 27 days (Figure 4A). In contrast, no significant sulfide production was detected in the sterile control and the control without guar gum. Acetate production (as shown in Figure 4B; 11.8 ± 0.8 mM) accumulated over a 27 day incubation under fermentative conditions. When thiosulfate was provided as an electron acceptor, however, twice the amount of acetate was produced during the same time period (Figure 4B). In addition, small amounts of formate (0.2-0.9mM) and ethanol (1.1-3.4 mM) were also detected.

Corrosive Activity of *Halanerobium* sp. Strain DL-01. The sulfide and acetate produced by strain DL-01 might contribute to the corrosion of carbon-steel. To determine the corrosivity of strain DL-01, a carbon-steel coupon was added to the medium in growth experiments. The trend for sulfide and acetate production was

consistent with the data in the absence of a carbon-steel coupon (Figure S4). However, much less dissolved sulfide was measured, probably due to the precipitation of iron sulfide. Examination of the coupons by FE-SEM demonstrated that obvious biofilm was formed on the metal surfaces under either fermentative (Figure S5A) or thiosulfate reducing conditions (Figure S5B). Surprisingly, the corrosion determined by weight loss and total iron analysis was much less than in the abiotic controls (Figure 5) under both conditions. For example, the weight loss in the incubations with the microbial activity is around 4 times less than that in the sterile controls in the presence of thiosulfate (Figure 5). Similarly, the weight loss in the absence of thiosulfate was around half of the abiotic control. The low corrosion rate (less than 1 milli-inch per year, mpy) suggested that strain DL-01 was not corrosive under the defined laboratory conditions. Profilometry of the coupons revealed no obvious pitting corrosion under both fermentative and thiosulfate reducing conditions (Figure S6&S7). Corrosion experiments with a lower concentration of guar gum (0.1%) were subsequently conducted to better reflect the content of guar gum in the fracturing fluid used in this site. Also in this case, the corrosion associated with microbial activity was less than in sterile controls (Figure S8).

Efficacy of Biocides against Strain DL-01. The efficacy of biocides against strain DL-01was assessed on the basis of sulfide and acetate production (Figure S11&S12) and growth relative to sterile controls. A relatively low dosage of QAC (13.5 mg/L) was sufficient to completely inhibit acetate and sulfide production under both thiosulfate-reducing (Figure S9B) and fermentative conditions (Figure S9A). The efficacy of glutaraldehyde against strain DL-01 was much higher in the presence of thiosulfate (100 mg/L, Figure S10A&B) than in its absence (500 mg/L, Figure S9B). In contrast, THPS

(81 mg/L) completely inhibited microbial growth and thus, acetate production when no thiosulfate was present (Figure S10D). However, up to 406 mg/L THPS showed no inhibition on sulfide and acetate production when thiosulfate was present (Figure S10C&D). Accordingly, the minimum inhibitory concentrations (the lowest dosage to completely inhibit microbial growth and activity) of the three biocides are summarized in Figure 6. The minimum inhibition concentration of QAC (13.5 mg/L) was much lower than that of glutaraldehyde (500 mg/L in the absence of thiosulfate) and THPS (no inhibition up to 406 mg/L in the presence of thiosulfate).

Discussion

Microbial activities associated with hydraulically fractured shale formations are of great concern to the oil and gas industry due to the potential for corrosion of pipelines, separators and storage tanks.[11] We characterized the geochemistry and microbial community of produced water from a shale gas production facility in part of the Barnett Shale system. Typically, low levels of acetate (up to ~0.9 mM) are detected in produced waters from hydraulically fractured sites.[43] In contrast, we detected an extremely high concentration of acetate (170 mM) in DRW (Figure 1). While acetate can be introduced through hydraulic fracturing,[44] microbial activity might play a substantial role in the production of acetate. Regardless of the sources of acetate, its accumulation in produced water can potentially exacerbate corrosion of carbon-steel equipment.[45, 46] In addition, sulfidogenic activity might also contribute to the observed corrosion of carbon-steel in the downstream pipeline (DRW) where sulfide (0.25 mM) and sulfate (0.74-1.93 mM) were detected. Although the rapid rate of microbial metabolism makes measurement of thiosulfate quite challenging,[47] thiosulfate

(0.17±0.01 mM) was detected in the DRW produced water when measured in the field using a thiosulfate titration kit. Moreover, a recent study found that the major fraction of the total sulfur in produced water was present as non-sulfate compounds and thereby the importance of sulfidogenic potential of non-sulfate-reducing microorganisms was implied in the fractured subsurface.[10] In fact, fermentative, thiosulfate-reducing bacteria have been demonstrated to be important in catalyzing corrosion of carbon steel in oil production facilities.[41, 48]

Molecular characterization of the microbial assemblages in each sample revealed that the most abundant taxa in the upstream produced water were members of the Order Halanaerobiales, which is consistent with previous studies on the microbial ecology of produced water from shale gas extraction.[1, 7-12] Earlier studies have shown that members of the genus *Halanaerobium* increased dramatically over time in the produced water from the Marcellus and Barnett shale formations in the United States.[1, 7, 10] Despite the limited sampling time points in this study (July and September, 2012), the relative abundance of *Halanaerobium* increased from 17% to ~33% in the later produced water sample (Figure 2). Although sulfate-reducing bacteria within Deltaproteobacteria were not typically detected in previous studies,[7, 10] members of the Order Desulfovibrionales were present in low relative abundance (~5%; Figure S3). The genera *Desulfohalobium* [49, 50] and *Desulfovermiculus* [51] were reported to be halophilic sulfate reducers, suggesting that sulfate reduction might also contribute to sulfidogenesis in subterranean systems with high salinity. Sequences affiliated with Epsilonproteobacteria (~3%) were detected in the produced water sampled in September. The majority of the OTUs within the Epsilonproteobacteria were affiliated

with the genus *Sulfurospirillum* (Figure 2), a group of metabolically versatile bacteria previously shown to reduce sulfur and thiosulfate.[52] The presence of multiple lineages of sulfidogenic organisms and sulfur species ($S_2O_3^{2-}$, SO_4^{2-} and HS^-) suggested that active sulfur cycle involving thiosulfate might be occurring in the deep subterranean shale formations after hydraulic fracturing.

The ubiquity and abundance of members of the genus *Halanaerobium* found in high salinity production water suggests that they could play crucial roles in the cycling of carbon and sulfur in these environments.[7, 12] Cultivation of the abundant microbes in produced water is important to understand the physiology of these taxa and their potential role in corrosion. A numerically dominant organism was isolated from the produced water in this study and identified as *Halanaerobium* sp. DL-01. This isolate was highly similar to the most abundant OTU from the genus *Halanaerobium* within the microbial assemblage of upstream produced water (Figure S3). Further phylogenetic analysis revealed that strain DL-01 was most closely related to *Halanaerobium kushneri* isolated from high saline produced water from an oil reservoir in Central Oklahoma.[53] *Halanaerobium congolense* [14] and *Halanaerobium salsugo* [53] have also been isolated from oil fields, alluding to the ecological importance of the genus *Halanaerobium* in high saline produced water in oil and gas production facilities.

Many species of *Halanaerobium* are capable of fermenting carbohydrates to acetate and other organic acids.[13, 14] We found that strain DL-01 could produce acetate through the fermentation of guar gum, the major gelling agent in the fracturing fluid to increase viscosity.[17] Most importantly, strain DL-01 was able to generate sulfide from thiosulfate reduction, an important physiological feature shared by several other species

of the genus of *Halanaerobium*.[13] Of the numerous chemical additives introduced into the shale formation during hydraulic fracturing, the organic constituents in the fracturing fluid, such as hydrocarbon distillates and carbohydrate polymers (e.g. guar gum) [7], could conceivably serve as electron donors to stimulate potentially deleterious microbial processes such as acetate and sulfide production. The fate of the organic matter in fracturing fluids injected into the deep subsurface is poorly understood, but a recent metagenomic study of produced water from shale gas extraction revealed a relatively high abundance of functional genes associated with metabolism of mono- and polysaccharides.[21] Furthermore, other studies have found that the concentration of dissolved organic matter in produced water decreased over time due to abiotic or biotic processes occurring in the deep subsurface.[7, 43] Until the study described here, the numerically dominant *Halanaerobium* spp. in produced water had not been shown to biodegrade organic matter (e.g. guar gum) in the high saline water and contribute to the production of acetate and sulfide.

The production of acetate and sulfide by strain DL-01 (Figure 4) prompted us to further examine its potential role in the corrosion of carbon steel. Although comparable acetate and sulfide were produced by strain DL-01 (Figure S4) when a carbon-steel coupon was present, the corrosion was less than abiotic control (Figure 5&S8) when strain DL-01 was grown with guar gum as a substrate. It should be noted that guar gum was previously found to efficiently inhibit corrosion of carbon steel in sulfuric acid solutions due to its adsorption on the metal surfaces.[54, 55] However, our data are not in accordance with the inhibition theory because the corrosion in the incubations with guar gum was not significantly different (*t* test, p=0.08) from the guar gum-unamended

controls (Figure S9). Although microbial colonization was observed on the metal surfaces under both fermentative and thiosulfate reducing conditions (Figure S5), the developed layers could be protective and thus hinder further corrosion reactions.[56] Nevertheless, the unexpected low corrosion rate associated with metabolic activity of strain DL-01was intriguing and the underlying mechanisms should be further investigated.

While the inhibitory mechanism of microorganisms in corrosion is not fully understood,[57] the corrosiveness of sulfide and acetate are well-known in the oil and gas industry.[41] Therefore, the collective findings led us to propose a possible corrosion scenario (Figure S11) in the hydraulically fractured site in Barnett Shale. Fracturing fluids containing biodegradable polysaccharide polymers like guar gum (0.1-0.5%) get injected deep into shale formations.[17] The abundant members of the genus *Halanaerobium* decomposed the guar gum, producing acetate and sulfide (if thiosulfate is available). Eventually, the produced acetate and sulfide could be returned in the produced water and transported to downstream pipeline networks (Figure S11). Acetate (170 mM) and sulfide (0.25mM) in saline production waters could act synergistically [58] to corrode the downstream production facilities such as pipelines and storage tanks.

To mitigate the potential corrosion caused by the abundant members of the genus *Halanaerobium*, the efficacy of three biocides was evaluated against *Halanaerobium* sp. DL-01. A relatively high dosage of glutaraldehyde (500 mg/L) was required to completely inhibit strain DL-01. This concentration was much higher than the minimum inhibitory concentrations for *Desulfovibrio alaskensis* strain G20 (12.5 mg/L) and a sulfate-reducing enrichment culture (100 mg/L) obtained from fracturing

fluid.[5] Interestingly, exposure of *Pseudomonas fluorescens* to produced water can cause an increased resistance to glutaraldehyde.[59] It is unclear, however, whether the enhanced tolerance against glutaraldehyde in strain DL-01 was triggered by a similar mechanism. The presence of thiosulfate did increase the resistance of *Halanaerobium* DL-01 to THPS (no inhibition up to 406 mg/L). The ineffectiveness of THPS might be attributed to potential interaction between THPS and thiosulfate.[60] Notably, QAC was found to be more efficient than glutaraldehyde and THPS (Figure 6) under both thiosulfate-reducing and fermentative growth conditions. Therefore, the preferential utilization of QAC might be considered to decrease the microbial activity of the dominant *Halanaerobium* in high salinity produced water. In addition, future work is needed to assess the synergistic effect of multiple biocides [6] against strain DL-01 and the underlying mechanisms for the potential resistance to glutaraldehyde and THPS in high saline brines.[59]

It is generally believed that problematic microorganisms are directly associated with severe corroding sites when assessing risks of biocorrosion in the oil and gas industry. The research presented here however, implies that the presence of sulfidogenic microorganisms might not necessarily exacerbate corrosion in the locations where they were detected. We found that the selected microorganisms (e.g. *Halanaerobium* sp. DL-01) in the produced water after hydraulic fracturing could play an important role in the biodegradation of organic carbon such as guar gum to produce acetate and sulfide. While no increase in corrosion was observed when *Halanaerobium* sp. DL-01 formed biofilms on the surface of carbon steel, the produced acetate and sulfide could be transported downstream with the returning water (Figure S11). Therefore, the microbial

production of sulfide and acetate might greatly contribute to corrosion of carbon-steel pipelines and other equipment in distal, downstream locations (Figure S11). The findings on the efficacy of biocides against strain DL-01 should ultimately help select suitable biocides to decrease the prevalence of *Halanaerobium* spp. in the shale formation and thereby mitigate detrimental biocorriosion processes during hydraulic fracturing operations.[5]

Acknowledgements

The financial and logistical support from the industrial sponsors of the OU Biocorrosion Center was greatly appreciated. We are also grateful to Neil Wofford for his generous technical assistance.

References

(1) Davis, J. P.; Struchtemeyer, C. G.; Elshahed, M. S., Bacterial communities associated with production facilities of two newly drilled thermogenic natural gas wells in the Barnett Shale (Texas, USA). *Microb. Ecol.* **2012,** *64*, (4), 942-954.

(2) Vengosh, A.; Jackson, R. B.; Warner, N.; Darrah, T. H.; Kondash, A., A critical review of the risks to water resources from unconventional shale gas development and hydraulic fracturing in the United States. *Environ. Sci. Technol.* **2014,** *48*, (15), 8334-8348.

(3) Gregory, K. B.; Vidic, R. D.; Dzombak, D. A., Water management challenges associated with the production of shale gas by hydraulic fracturing. *Elements* **2011,** *7*, (3), 181-186.

(4) Gaspar, J.; Mathieu, J.; Yang, Y.; Tomson, R.; Leyris, J. D.; Gregory, K. B.; Alvarez, P. J., Microbial Dynamics and Control in Shale Gas Production. *Environ. Sci. Technol. Lett.* **2014,** *1*, (12), 465-473.

(5) Struchtemeyer, C. G.; Morrison, M. D.; Elshahed, M. S., A critical assessment of the efficacy of biocides used during the hydraulic fracturing process in shale natural gas wells. *Int. Biodeterior. Biodegr.***2012,** *71*, 15-21.

(6) Kahrilas, G. A.; Blotevogel, J.; Stewart, P. S.; Borch, T., Biocides in hydraulic fracturing fluids: A critical review of their usage, mobility, degradation, and toxicity. *Environ. Sci. Technol.* **2014,** *49*, (1), 16-32.

(7) Cluff, M. A.; Hartsock, A.; MacRae, J. D.; Carter, K.; Mouser, P. J., Temporal changes in microbial ecology and geochemistry in produced water from hydraulically fractured marcellus shale gas wells. *Environ. Sci. Technol.* **2014,** *48*, (11), 6508-6517.

(8) Wuchter, C.; Banning, E.; Mincer, T. J.; Drenzek, N. J.; Coolen, M. J., Microbial diversity and methanogenic activity of Antrim Shale formation waters from recently fractured wells. *Front. Microbiol.* **2013,** *4*.

(9) Strong, L. C.; Gould, T.; Kasinkas, L.; Sadowsky, M. J.; Aksan, A.; Wackett, L. P., Biodegradation in waters from hydraulic fracturing: chemistry, microbiology, and engineering. *J. Environ. Eng.* **2013,** *140*, (5).

(10) Murali Mohan, A.; Hartsock, A.; Bibby, K. J.; Hammack, R. W.; Vidic, R. D.; Gregory, K. B., Microbial community changes in hydraulic fracturing fluids and produced water from shale gas extraction. *Environ. Sci. Technol.***2013,** *47*, (22), 13141-13150.

(11) Struchtemeyer, C. G.; Elshahed, M. S., Bacterial communities associated with hydraulic fracturing fluids in thermogenic natural gas wells in North Central Texas, USA. *FEMS Microbiol. Ecol.* **2012,** *81*, (1), 13-25.

(12) Murali Mohan, A.; Hartsock, A.; Hammack, R. W.; Vidic, R. D.; Gregory, K. B., Microbial communities in flowback water impoundments from hydraulic fracturing for recovery of shale gas. *FEMS Microbiol. Ecol.* **2013,** *86*, (3), 567-580.

(13) Ravot, G.; Casalot, L.; Ollivier, B.; Loison, G.; Magot, M., rdlA, a new gene encoding a rhodanese-like protein in *Halanaerobium congolense* and other thiosulfate-reducing anaerobes. *Res. Microbiol.* **2005,** *156*, (10), 1031-1038.

(14) Ravot, G.; Magot, M.; Ollivier, B.; Patel, B.; Ageron, E.; Grimont, P.; Thomas, P.; Garcia, J. L., Haloanaerobium congolense sp. nov., an anaerobic, moderately halophilic, thiosulfate-and sulfur-reducing bacterium from an African oil field. *FEMS Microbiol. lett.* **1997,** *147*, (1), 81-88.

(15) Stringfellow, W. T.; Domen, J. K.; Camarillo, M. K.; Sandelin, W. L.; Borglin, S., Physical, chemical, and biological characteristics of compounds used in hydraulic fracturing. *J. Hazard. Mater* **2014,** *275*, 37-54.

(16) Youssef, N.; Elshahed, M. S.; McInerney, M. J., Microbial processes in oil fields: culprits, problems, and opportunities. *Adv. Appl. Microbiol.* **2009,** *66*, 141-251.

(17) Lester, Y.; Yacob, T.; Morrissey, I.; Linden, K. G., Can We Treat Hydraulic Fracturing Flowback with a Conventional Biological Process? The Case of Guar Gum. *Environ. Sci. Technol. Lett.* **2013,** *1*, (1), 133-136.

(18) Balascio, J. R.; PALMER, J. K.; SALYERS, A. A., Degradation of guar gum by enzymes produced by a bacterium from the human colon. *J. Food. Biochem.* **1981,** *5*, (4), 271-282.

(19) Salyers, A.; West, S.; Vercellotti, J.; Wilkins, T., Fermentation of mucins and plant polysaccharides by anaerobic bacteria from the human colon. *Appl. Environ. Microbiol.* **1977,** *34*, (5), 529-533.

(20) Akyon, B.; Stachler, E.; Wei, N.; Bibby, K., Microbial mats as a biological treatment approach for saline wastewaters: the case of produced water from hydraulic fracturing. *Environ. Sci. Technol.* **2015,** *49*, (10), 6172-6180.

(21) Mohan, A. M.; Bibby, K. J.; Lipus, D.; Hammack, R. W.; Gregory, K. B., The functional potential of microbial communities in hydraulic fracturing source water and produced water from natural gas extraction characterized by metagenomic sequencing. *PloS one* **2014,** *9*, (10), e107682.

(22) Tanner, R. S., Monitoring sulfate-reducing bacteria: comparison of enumeration media. *J. Microbiol. Methods.* **1989,** *10*, (2), 83-90.

(23) TM0194, NACE standard, Field Monitoring of bacterial growth in oil and gas systems. *Houston, TX: NACE* **2004**.

(24) Tanner, R. S.; Hurst, C.; Crawford, R.; Garland, J.; Lipson, D.; Mills, A.; Stetzenbach, L., Cultivation of bacteria and fungi. *Manual of environmental microbiology* **2007**, (Ed. 3), 69-78.

(25) Banwart, G. J. P. *Basic food microbiology*,. AVI Publishing Co., Westport, Conn., 1981; p 37-40.

(26) Oldham, A. L.; Drilling, H. S.; Stamps, B. W.; Stevenson, B. S.; Duncan, K. E., Automated DNA extraction platforms offer solutions to challenges of assessing microbial biofouling in oil production facilities. *AMB Express* **2012,** *2*, (1), 1-11.

(27) Klindworth, A.; Pruesse, E.; Schweer, T.; Peplies, J.; Quast, C.; Horn, M.; Glöckner, F. O., Evaluation of general 16S ribosomal RNA gene PCR primers for classical and next-generation sequencing-based diversity studies. *Nucleic. Acids. Res.* **2012**, gks808.

28. Hamady, M.; Walker, J. J.; Harris, J. K.; Gold, N. J.; Knight, R., Error-correcting barcoded primers for pyrosequencing hundreds of samples in multiplex. *Nat. Methods.* **2008,** *5*, (3), 235-237.

(29) Wawrik, B.; Mendivelso, M.; Parisi, V. A.; Suflita, J. M.; Davidova, I. A.; Marks, C. R.; Van Nostrand, J. D.; Liang, Y.; Zhou, J.; Huizinga, B. J., Field and laboratory studies on the bioconversion of coal to methane in the San Juan Basin. *FEMS Microbiol. Ecol.* **2012,** *81*, (1), 26-42.

(30) Caporaso, J. G.; Kuczynski, J.; Stombaugh, J.; Bittinger, K.; Bushman, F. D.; Costello, E. K.; Fierer, N.; Pena, A. G.; Goodrich, J. K.; Gordon, J. I., QIIME allows analysis of high-throughput community sequencing data. *Nat. Methods.* **2010,** *7*, (5), 335-336.

(31) Edgar, R. C., Search and clustering orders of magnitude faster than BLAST. *Bioinformatics* **2010,** *26*, (19), 2460-2461.

(32) Wang, Q.; Garrity, G. M.; Tiedje, J. M.; Cole, J. R., Naive Bayesian classifier for rapid assignment of rRNA sequences into the new bacterial taxonomy. *Appl. Environ. Microbiol.* **2007,** *73*, (16), 5261-5267.

(33) Yilmaz, P.; Parfrey, L. W.; Yarza, P.; Gerken, J.; Pruesse, E.; Quast, C.; Schweer, T.; Peplies, J.; Ludwig, W.; Glöckner, F. O., The SILVA and "All-species Living Tree Project (LTP)" taxonomic frameworks. *Nucleic. Acids. Res.* **2013**, gkt1209.

(34) Widdel, F.; Bak, F., Gram-negative mesophilic sulfate-reducing bacteria. In *The prokaryotes*, Springer: 1992; pp 3352-3378.

(35) Weisburg, W. G.; Barns, S. M.; Pelletier, D. A.; Lane, D. J., 16S ribosomal DNA amplification for phylogenetic study. *J. Bacteriol.* **1991,** *173*, (2), 697-703.

(36) Tamura, K.; Stecher, G.; Peterson, D.; Filipski, A.; Kumar, S., MEGA6: molecular evolutionary genetics analysis version 6.0. *Mol. Biol. Evol.* **2013,** *30*, (12), 2725-2729.

(37) Lyles, C. N.; Aktas, D. F.; Duncan, K. E.; Callaghan, A. V.; Stevenson, B. S.; Suflita, J. M., Impact of organosulfur content on diesel fuel stability and implications for carbon steel corrosion. *Environ. Sci. Technol.* **2013,** *47*, (11), 6052-6062.

(38) Stookey, L. L., Ferrozine---a new spectrophotometric reagent for iron. *Anal. Chem.* **1970,** *42*, (7), 779-781.

(39) Lyles, C. N.; Le, H. M.; Beasley, W. H.; McInerney, M. J.; Suflita, J. M., Anaerobic hydrocarbon and fatty acid metabolism by syntrophic bacteria and their impact on carbon steel corrosion. *Front. Microbiol.* **2014,** *5*.

(40) Davidova, I. A.; Duncan, K. E.; Perez-Ibarra, B. M.; Suflita, J. M., Involvement of thermophilic archaea in the biocorrosion of oil pipelines. *Environ. Microbiol.* **2012,** *14*, (7), 1762-1771.

(41) Liang, R.; Grizzle, R. S.; Duncan, K. E.; McInerney, M. J.; Suflita, J. M., Roles of thermophilic thiosulfate-reducing bacteria and methanogenic archaea in the biocorrosion of oil pipelines. *Front. Microbiol.* **2014,** *5*.

(42) ASTM G1-03, A., Standard practice for preparing, cleaning, and evaluating corrosion test specimens. **2003**.

(43) Orem, W.; Tatu, C.; Varonka, M.; Lerch, H.; Bates, A.; Engle, M.; Crosby, L.; McIntosh, J., Organic substances in produced and formation water from unconventional natural gas extraction in coal and shale. *Int. J. Coal. Geol.* **2014,** *126*, 20-31.

(44) Sydansk, R. D., Hydraulic fracturing process using a polymer gel. In Google Patents: 1988.

(45) Suflita, J. M.; Phelps, T. J.; Little, B., Carbon dioxide corrosion and acetate: a hypothesis on the influence of microorganisms. *Corrosion* **2008,** *64*, (11), 854-859.

(46) Azambuja, D.; Muller, I., The influence of acetate concentration on the dissolution of iron in aqueous solutions. *Corros. Sci.* **1994,** *36*, (11), 1835-1845.

(47) Jørgensen, B. B., A thiosulfate shunt in the sulfur cycle of marine sediments. *Science* **1990,** *249*, (4965), 152-154.

(48) Magot, M.; Ravot, G.; Campaignolle, X.; Ollivier, B.; Patel, B. K.; Fardeau, M.-L.; Thomas, P.; Crolet, J.-L.; Garcia, J.-L., *Dethiosulfovibrio peptidovorans* gen. nov., sp. nov., a new anaerobic, slightly halophilic, thiosulfate-reducing bacterium from corroding offshore oil wells. *Int. J. Syst. Evol. Microbiol.* **1997,** *47*, (3), 818-824.

(49) Ollivier, B.; Hatchikian, C.; Prensier, G.; Guezennec, J.; Garcia, J.-L., Desulfohalobium retbaense gen. nov., sp. nov., a halophilic sulfate-reducing bacterium from sediments of a hypersaline lake in Senegal. *Int. J. Syst. Evol. Microbiol.* **1991,** *41*, (1), 74-81.

(50) Jakobsen, T. F.; Kjeldsen, K. U.; Ingvorsen, K., *Desulfohalobium utahense* sp. nov., a moderately halophilic, sulfate-reducing bacterium isolated from Great Salt Lake. *Int. J. Syst. Evol. Microbiol.* **2006,** *56*, (9), 2063-2069.

(51) Belyakova, E.; Rozanova, E.; Borzenkov, I.; Tourova, T.; Pusheva, M.; Lysenko, A.; Kolganova, T., The new facultatively chemolithoautotrophic, moderately

halophilic, sulfate-reducing bacterium *Desulfovermiculus halophilus* gen. nov., sp. nov., isolated from an oil field. *Microbiology* **2006,** *75*, (2), 161-171.

(52) Kodama, Y.; Watanabe, K., *Sulfurospirillum cavolei* sp. nov., a facultatively anaerobic sulfur-reducing bacterium isolated from an underground crude oil storage cavity. *Int. J. Syst. Evol. Microbiol.* **2007,** *57*, (4), 827-831.

(53) Bhupathiraju, V. K.; McInerney, M. J.; Woese, C. R.; Tanner, R. S., Haloanaerobium kushneri sp. nov., an obligately halophilic, anaerobic bacterium from an oil brine. *Int. J. Syst. Evol. Microbiol.* **1999,** *49*, (3), 953-960.

(54) Umoren, S.; Ogbobe, O.; Igwe, I.; Ebenso, E., Inhibition of mild steel corrosion in acidic medium using synthetic and naturally occurring polymers and synergistic halide additives. *Corros. Sci.* **2008,** *50*, (7), 1998-2006.

(55) Abdallah, M., Guar gum as corrosion inhibitor for carbon steel in sulfuric acid solutions. *Portugaliae Electrochimica Acta* **2004,** *22*, (2), 161-175.

56. Zuo, R., Biofilms: strategies for metal corrosion inhibition employing microorganisms. *: Appl. Microbiol. Biotechnol.* **2007,** *76*, (6), 1245-1253.

(57) Kip, N.; van Veen, J. A., The dual role of microbes in corrosion. *The ISME journal* **2014**.

(58) Singer, M.; Brown, B.; Camacho, A.; Nesic, S., Combined effect of CO_2, H_2S and acetic acid on bottom of the line corrosion. Paper No. 07661, *NACE International* **2007**.

59. Vikram, A.; Lipus, D.; Bibby, K., Produced Water Exposure Alters Bacterial Response to Biocides. *Environ. Sci. Technol.* **2014,** *48*, (21), 13001-13009.

60. Williams, T. M.; McGinley, H. R. *Deactivation of industrial water treatment biocides*, Paper No.10049 , NACE International **2010**.

Table 1 Geochemical characteristics of produced water from upstream (UCPW) and downstream (DRW) of a shale gas production facility in Barnett Shale formations.

Samples	Sampling time	pH	Sulfate (mM)	Fe^{2+} (mM)	Sulfide (mM)	Thiosulfate (mM)	Salinity (Cl^- g/L)	Acetate (mM)
Upstream (UPCW)	July 2012	7.0	0.74	1.73	0.04	BDL[a]	117	NR[b]
	September 2012	6.8	1.84	0.73	BDL	BDL	46.8	0.5
Downstream (DRW)	July 2012	6.5	0.79	NR	0.25	BDL	19.7	NR
	September 2012	7.0	1.93	11.76	BDL	0.17	16.9	170

[a]BDL, below detection level (5 ppm); [b]NR, data not recorded.

Table S1 Most probable number of of acid-producing bacteria, sulfate-reducing bacteria and thiosulfate-reducing bacteria in the upstream (UPCW) and downstream (DRW) samples

Bacterial groups	Salinity	Medium	UPCW	DRW
Sulfate-reducing bacteria	5% NaCl	C&S Labs	<1	0[a]
	10% NaCl	C&S Labs	0	0
Acid-producing bacteria	5% NaCl	C&S Labs	4	0
	10% NaCl	C&S Labs	$5x10^3$	0
Thiosulfate-reducing bacteria	5% NaCl	RST-TRB	2	0
	10% NaCl	RST-TRB	2	0

[a] indicates that no microbial activity was observed in any of the MPN tubes

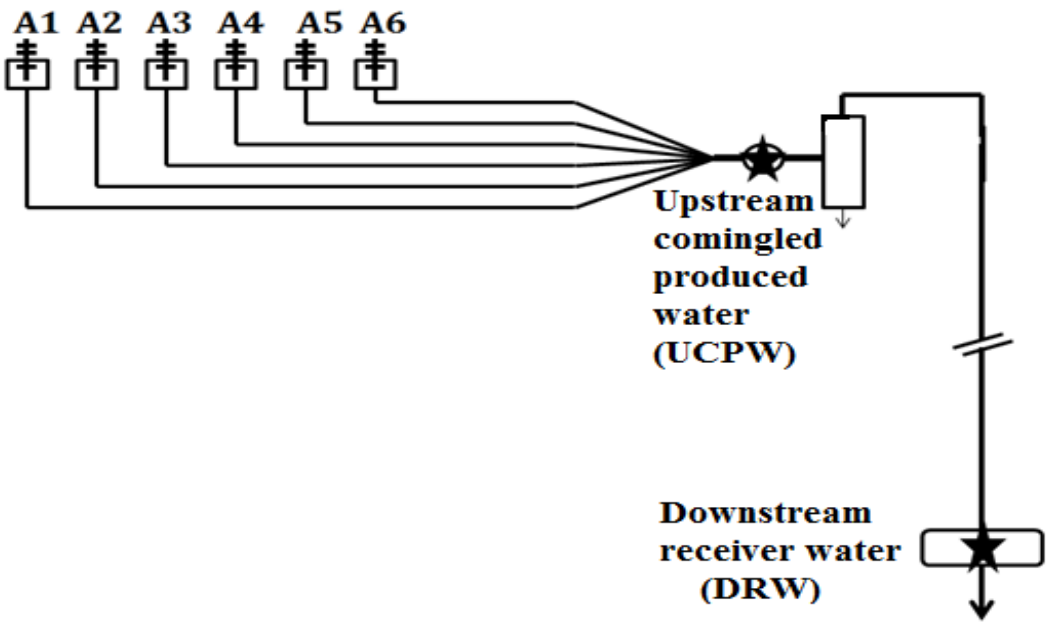

Figure 1 Schematic diagram of the shale gas production facility in Barnett Shale. Six wells (A1-A6) were drilled in this site and the stars indicated the locations where upstream (UCPW) and downstream (DRW) samples were collected. The distance between the two locations is around 1 kilometer. Severe corrosion was detected in the downstream pipeline where replacement was mandated for maintenance.

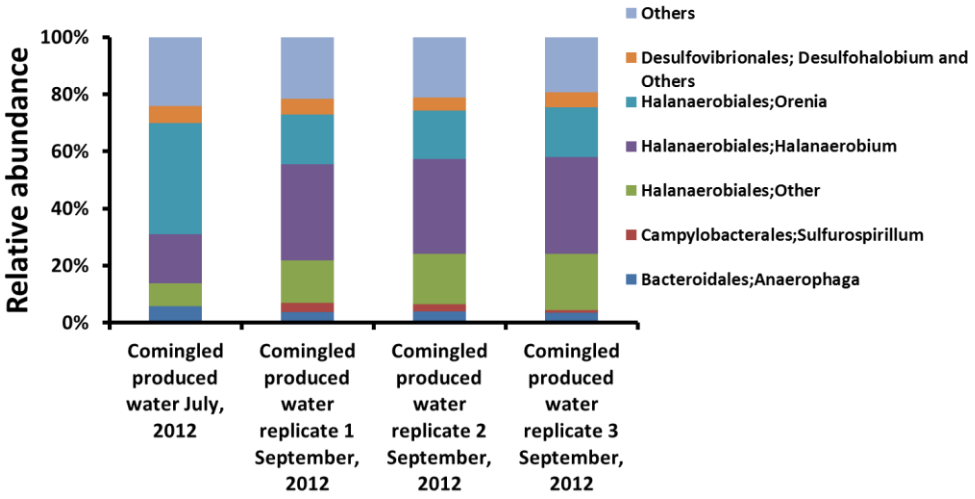

Figure 2 Relative abundance of major taxa (Genus level classification) in upstream comingled produced water. Three biological replicates (1, 2 and 3) were included in the later produced water collected in September, 2012.

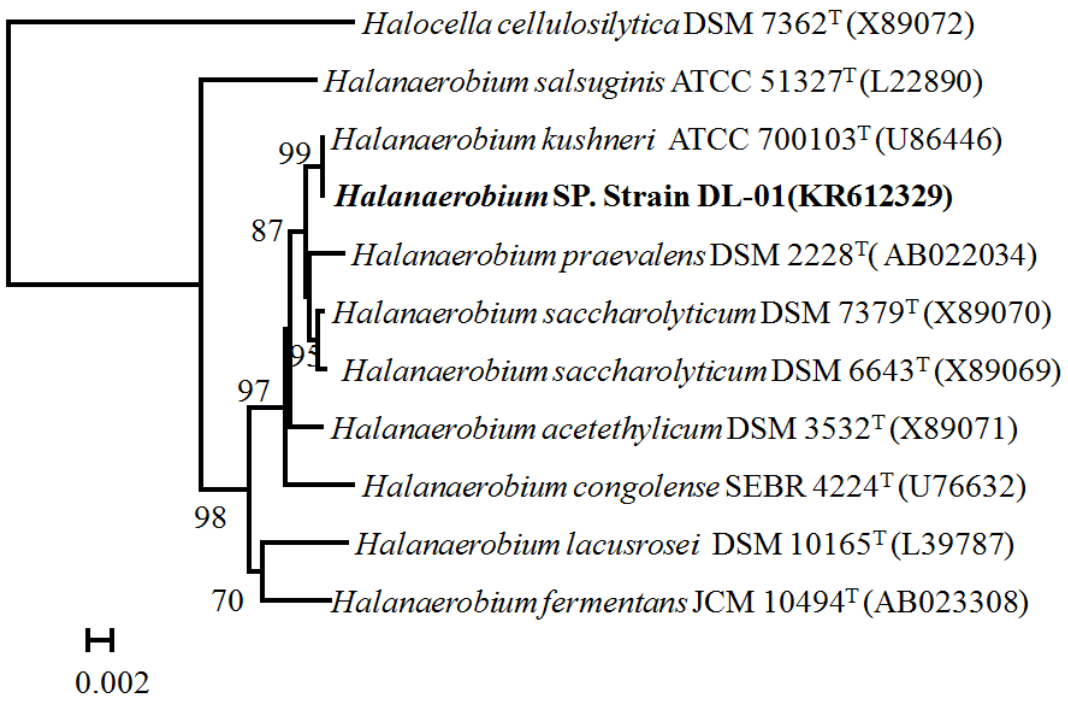

Figure 3 Phylogenetic relationship of *Halanaerobium* sp. strain DL-01(in bold) to other species within the genus *Halanaerobium*. The accession of each strain is indicated in the parenthesis. The tree was constructed based on approximately 1362 bp 16S rRNA gene sequences.1000 bootstrap replications were performed and only those greater than 70% are shown. Bar indicated 0.002 nucleotide substitutions per nucleotide position.

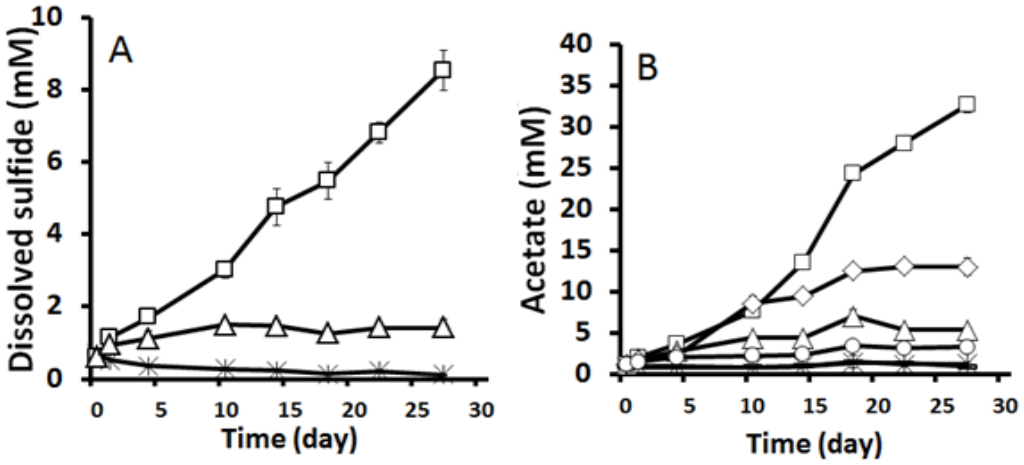

Figure 4 Sulfide (A) and acetate (B) production by strain DL-01 when grown on 0.5% guar gum under fermentative and thiosulfate-reducing conditions. Legends: □, 0.5% guar gum+thiosulfate; Δ,no guar gum+thiosulfate; ✳, sterile (0.5% guar gum+thiosulfate); ◇, 0.5% guar gum+no thiosulfate;○, no guar gum+no thiosulfate; -, (overlapping data with ✳), sterile (0.5% guar gum+ no thiosulfate). Sterile indicates that cells of DL-01 were heat killed by autoclaving.

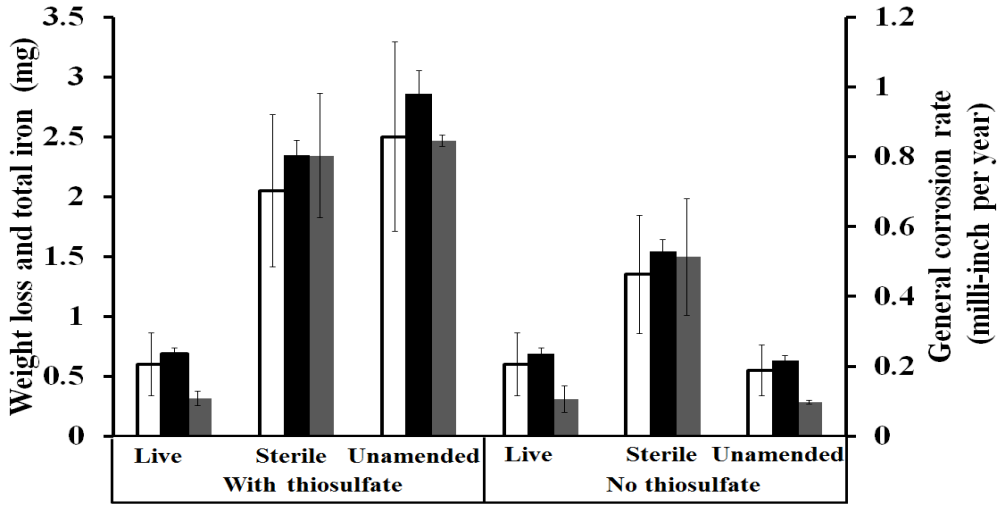

Figure 5 Weight loss and total iron analysis for DL-01 grown on guar gum (0.5%) with a carbon-steel coupon in the medium under fermentative and thiosulfate-reducing conditions. The clear bars represent the corrosion determined by weight loss and black bars indicate the general corrosion rate calculated according to the corresponding weight loss data; whereas the grey bars represent the corrosion determined by total iron analysis. Live: Cells of DL-01 were grown with guar gum as a substrate; Sterile: Cells of DL-01 were heat-killed by autoclaving; Unamended: no guar gum was amended.

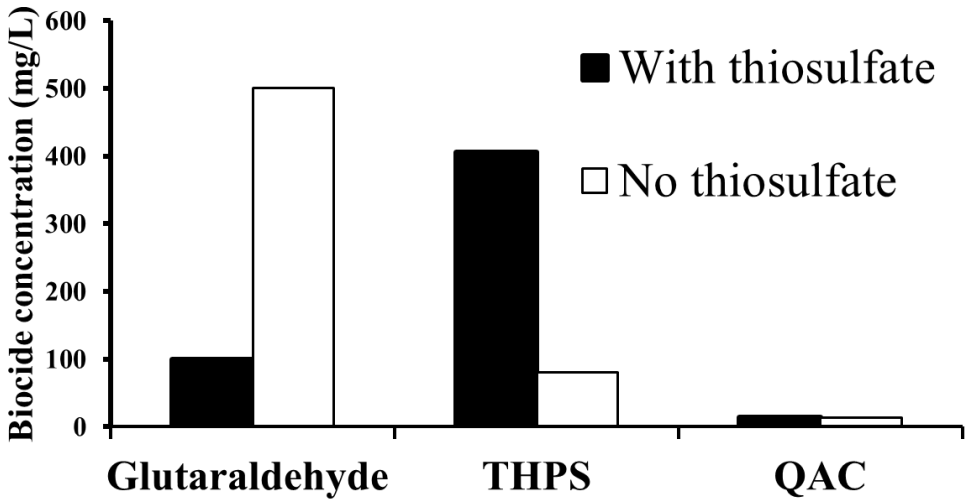

Figure 6 Minimum inhibitory concentrations of biocides against *Halanaerobium* DL-01 based on microbial growth, sulfide and acetate production relative to sterile controls, which the cells of DL-01 were heat-killed by autoclaving. Black and clear bars indicate the conditions with and without thiosulfate, respectively.

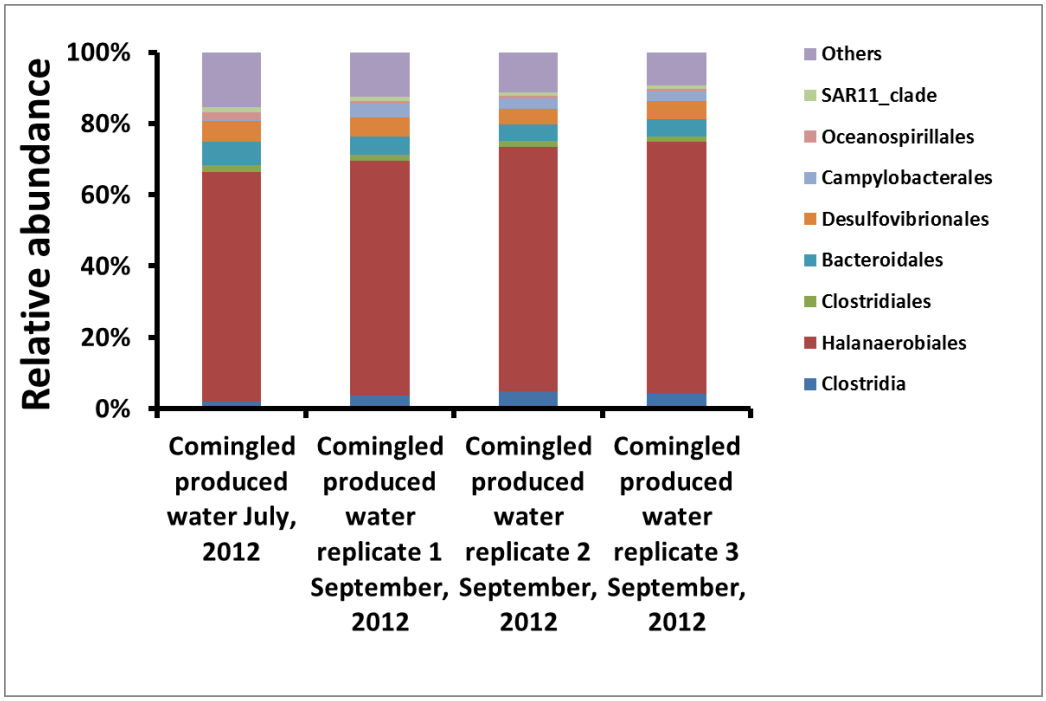

Figure S1 Relative abundance of major taxa (Order level) in upstream comingled production water. Three biological replicates (1, 2 and 3) were included in the later produced water collected in September, 2012.

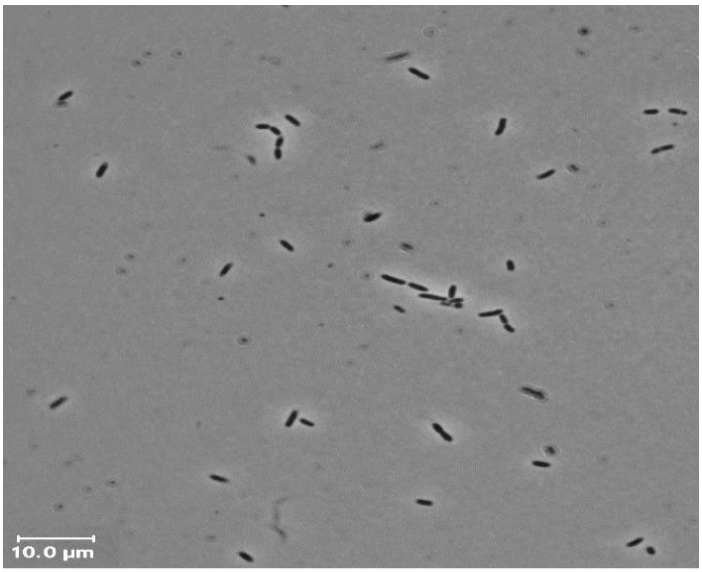

Figure S2 Cell morphology of *Halanaerobium* sp. DL-01. The image was taken under a Phase-contrast microscopy. Scar bar, 10 µm.

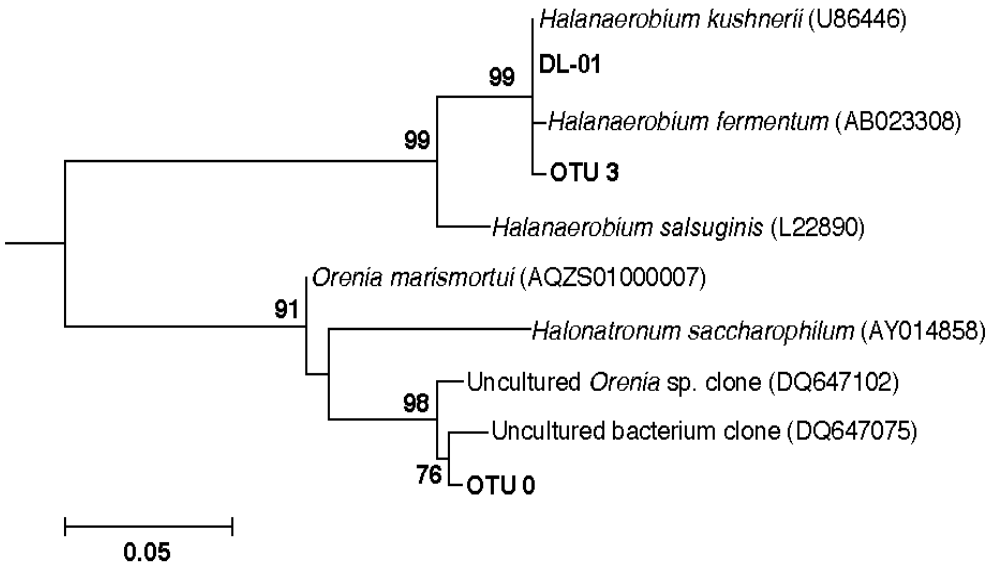

Figure S3 Phylogenetic relationship of *Halanaerobium* sp. DL-01 (in Bold) to other related species and the most related OTU (OTU 3 in bold) from the comingled produce water where DL-01 was originally isolated. The accession numbers are indicated in the parenthesis. Note: only a fragment (~300 bp) of 16S rRNA gene was used to construct the phylogenetic tree due to the limited sequence length from Illumina- based sequencing.

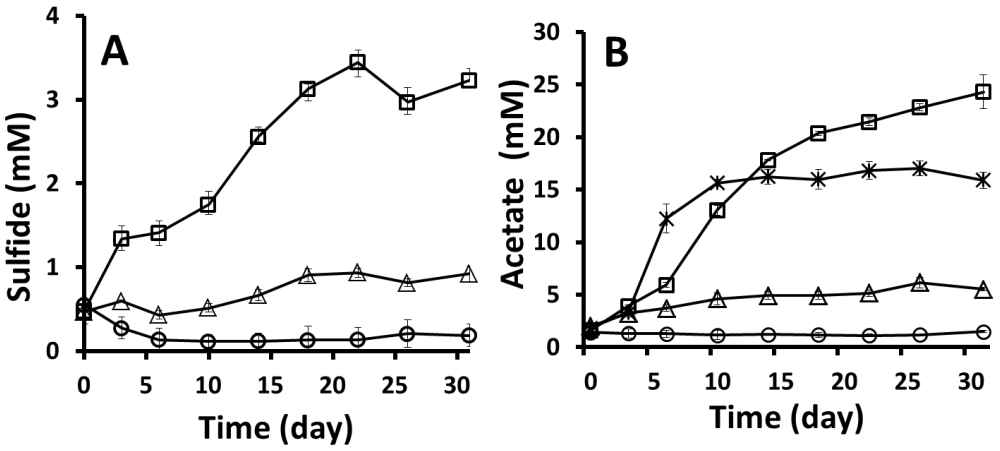

Figure S4 Sulfide (A) and acetate (B) production by *Halanaerobium* grown on guar gum (0.5%) in the presence of a carbon-steel coupon. Legends: □, 0.5% guar gum+thiosulfate; ✳, 0.5% guar gum+no thiosulfate Δ, no guar gum+thiosulfate; ○, sterile (0.5% guar gum+thiosulfate). Sterile indicates that cells of DL-01 were heat killed by autoclaving.

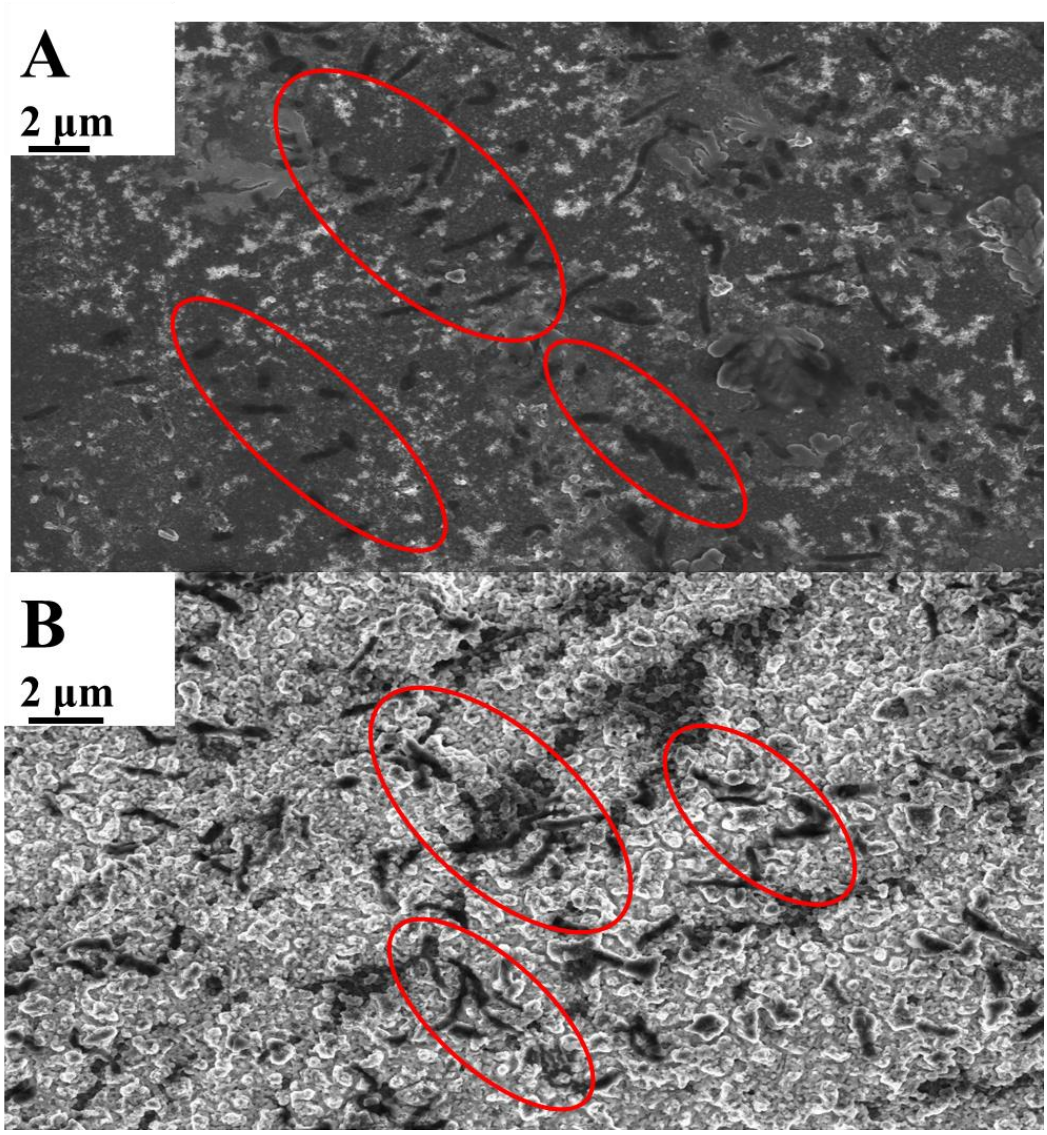

Figure S5 Biofilm characterization of carbon-steel coupons under fermentative (A) and thiosulfate-reducing conditions (B).The areas with obvious colonization by cells are highlighted in red ovals in A and B.

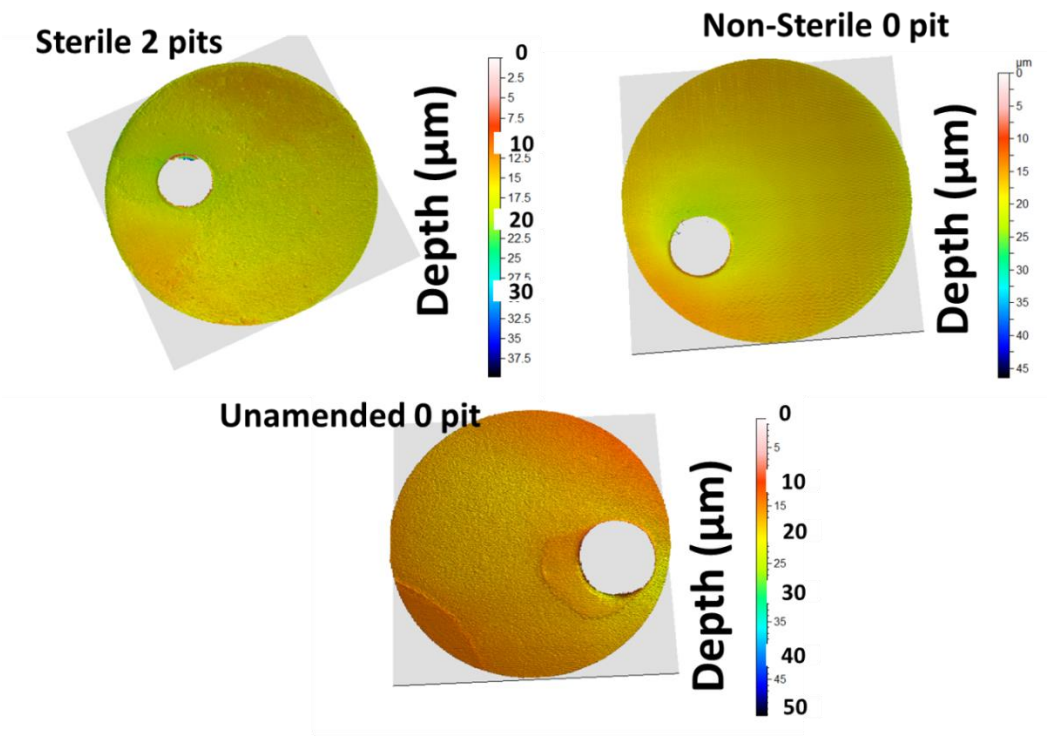

Figure S6 Profilometry images of carbon-steel (1018) coupons exposed to media when DL-01 grown on guar gum (0.5%) under thiosulfate-reducing conditions. Pits were defined as: 5 µm below mean plane and greater than 10 µm in equivalent diameter. Non-sterile: Live cells of DL-01 were grown with guar gum as a substrate; Sterile: Cells of DL-01 were heat-killed by autoclaving; Unamended: no guar gum was amended.

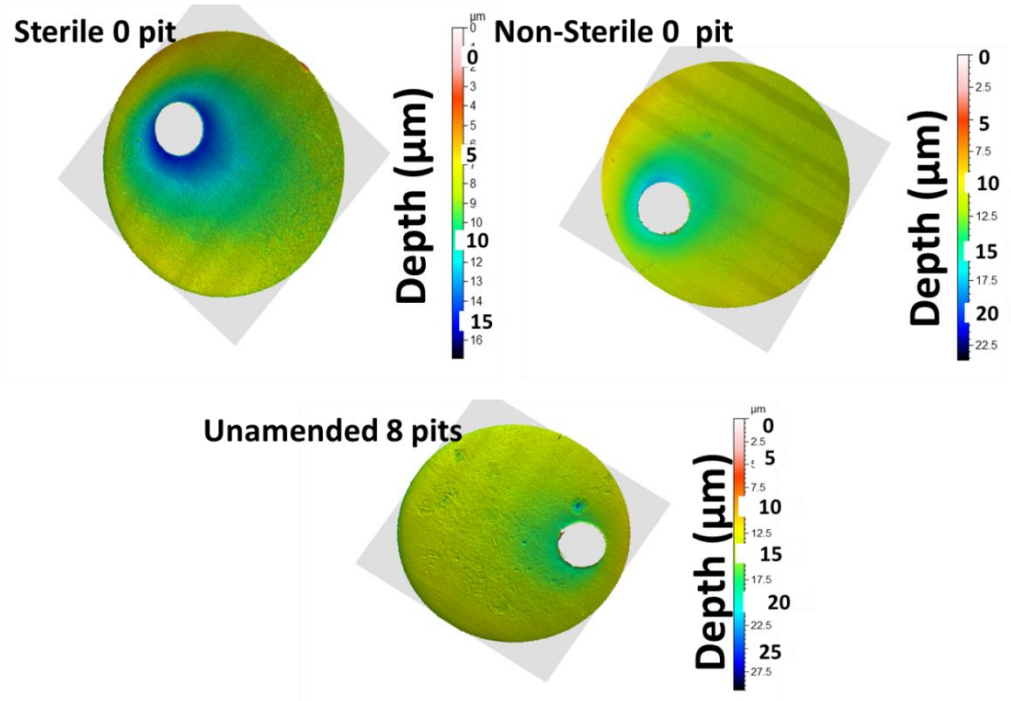

Figure S7 Profilometry images of carbon-steel (1018) coupons exposed to media when DL-01 grown on guar gum (0.5%) under fermentative conditions with no thiosulfate. Pits were defined as: 5 µm below mean plane and greater than 10 µm in equivalent diameter. Non-sterile: Live cells of DL-01 were grown with guar gum as a substrate; Sterile: Cells of DL-01 were heat-killed by autoclaving; Unamended: no guar gum was amended.

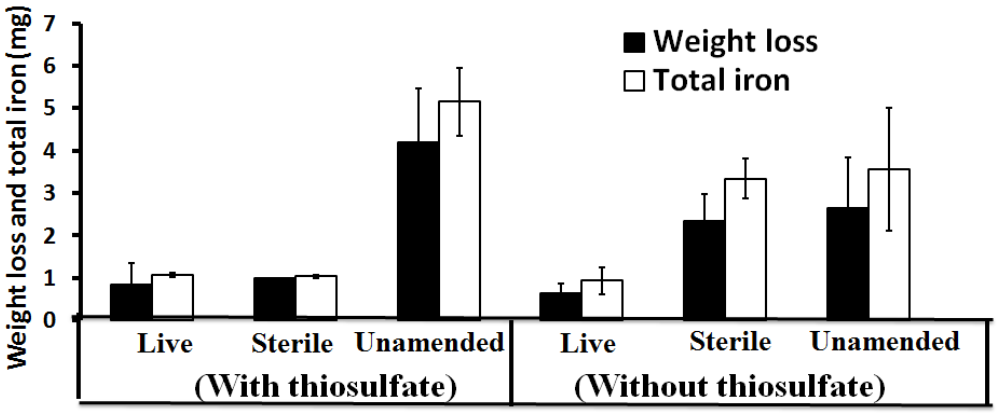

Figure S8 Weight loss and total iron analysis for DL-01 grown on guar gum (0.1%) with a carbon-steel coupon in the medium under fermentative and thiosulfate-reducing conditions. The black bars represent the corrosion determined by weight loss whereas the clear bars represent the corrosion determined by total iron analysis.

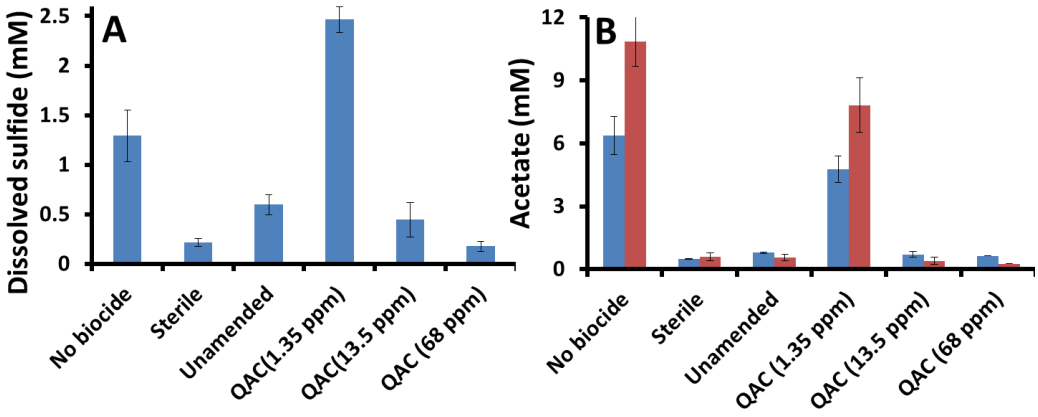

Figure S9 Efficacy of QAC on sulfide (A) and acetate (B) production by *Halanerobium* sp. DL-01. Blue bars indicate sulfide (A) or acetate (B) production under thiosulfate reducing conditions and red ones (B) refer to acetate production under fermentative conditions without thiosulfate. Note: ppm equals to mg/L in the text.

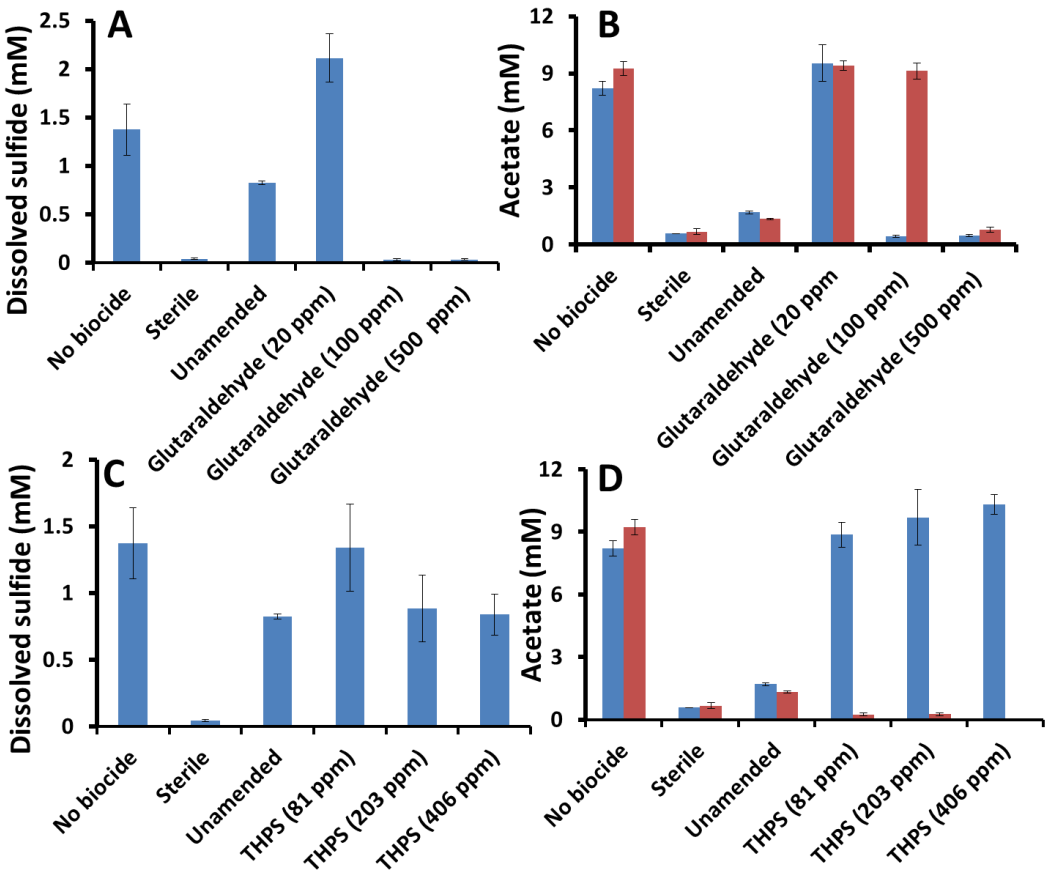

Figure S10 Efficacy of glutaraldehyde and THPS on sulfide (A & C) and acetate (B&D) production by *Halanerobium* sp. DL-01. Blue bars indicate sulfide (A & C) or acetate (B&D) production under thiosulfate reducing conditions and red ones (B&D) refer to acetate production under fermentative conditions without thiosulfate. Note: ppm equals to mg/L in the text.

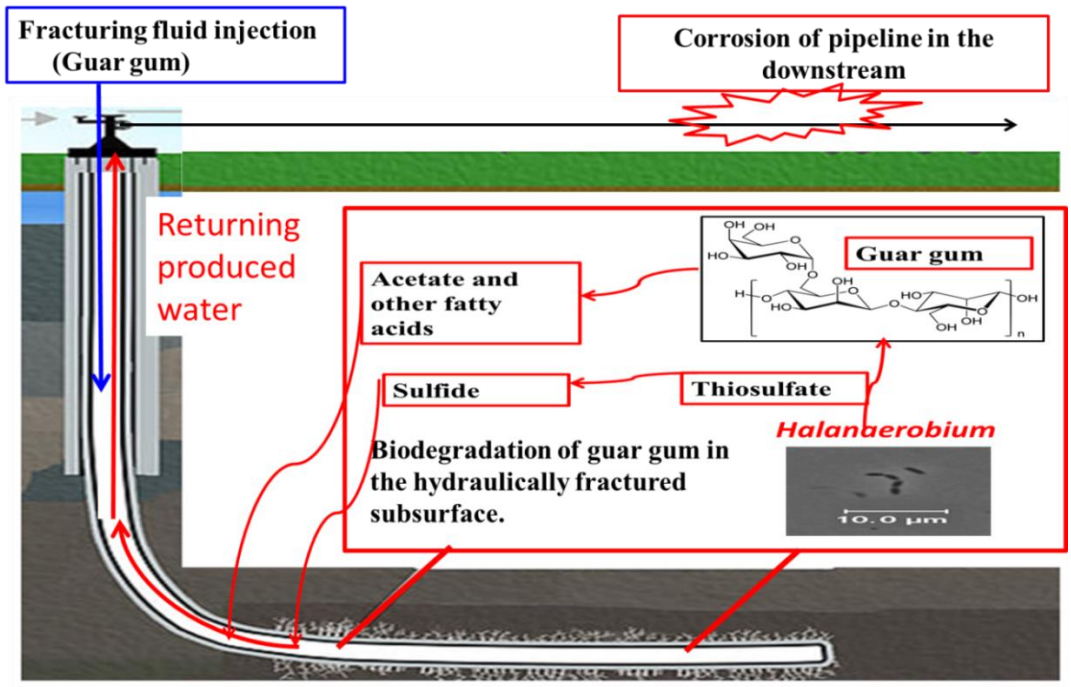

Figure S11 A proposed corrosion scenario in a hydraulically fractured site in Barnett Shale. Note: the schematic of the well was modified from http://www2.epa.gov/hfstudy.

Chapter 3: Anaerobic biodegradation of alternative fuels and associated biocorrosion of carbon steel in marine environments

Abstract

There is a global interest in adopting advanced biofuels to help secure energy supplies, reduce dependence on dwindling fossil reserves and decrease greenhouse gas emissions. Fuels that biodegrade too easily can exacerbate through-wall pitting corrosion of pipelines and tanks and result in unintentional environmental releases. Conversely, fuels that resist decay are unlikely to stimulate corrosion, but might lead to other environmental problems should they be accidentally released in the environment. Thus, it is imperative to determine if alternative biofuels are really compatible with the existing energy infrastructure. We tested the biological stability and potential to exacerbate carbon steel corrosion of two emerging biofuels, camelina-JP5 and Fisher-Tropsch-F76, alone and in combination with their petroleum-based counterparts (the military fuels JP5 and F76), using three coastal seawaters as inocula. A carbon-steel coupon was placed in incubation mixtures containing the fuel of choice and an inoculum consisting of seawater only, a seawater and sediment slurry or a seawater amended with a hydrocarbon-degrading sulfate-reducing positive control bacterium. Sulfate reduction rates were higher (8.7±0.2 - 23.4±0.6 μM/day) when the positive control bacterium was included in the fuel-amended seawater incubations, relative to the fuel-unamended controls (3.7±0.4 - 11.5±3.3 μM/day). The inclusion of sediment in the incubations accelerated sulfate reduction rates, but the pattern of fuel decay was comparable with different inocula. The highest rates of sulfate reduction were found in incubations amended with camelina-JP5 (57.2±2.2 - 80.8±8.1 μM/day) or its blend with

petro-JP5 (76.7±2.4 μM/day). The elevated sulfate depletion rates relative to negative controls suggested that fuel constituents were being biodegraded. Indeed, the detection of a suite of metabolites only in the fuel-amended incubations confirmed that alkylated benzene hydrocarbons were metabolized via known anaerobic mechanisms. Most importantly, general (r^2=0.73) and pitting (r^2=0.69) corrosion were positively correlated with sulfate loss in the incubations. Thus, the anaerobic biodegradation of labile fuel components coupled with sulfate respiration greatly contributed to the biocorrosion of carbon steel. While all fuels were susceptible to anaerobic metabolism, special attention should be given to camelina-JP5 biofuel. It was significantly less stable (i.e. more amenable to biodegradation) relative to other fuel options and its widespread use would likely exacerbate infrastructure biocorrosion. We recommend that this biofuel be used with caution and that whenever possible extended storage periods should be avoided.

Introduction

Over the ensuing decades, world energy demand will likely increase to meet the needs of a burgeoning human population.[1] Tremendous progress has been made toward the sustainable production of alternative fuels from renewable resources to address concerns over finite petroleum reserves and the emission of greenhouse gases.[2] As the largest energy-consuming entity in the United States, the Department of Defense has spearheaded the effort to incorporate alternative fuels to reduce the dependence on petroleum fuels and boost green energy development.[3] For example, it is estimated that 50% of the total energy consumption for US Navy will be coming from alternative sources by 2020.[4] The fast-growing, alternative fuels market will hopefully become cost-competitive to supplement conventional petroleum-based reserves.[5]

Numerous challenges are associated with adopting alternative fuels to augment or replace petroleum-derived fuels [6]. Typically, fungible biofuels require various tests to ensure that they have physicochemical properties comparable to their petroleum-based counterparts.[6-8] However, even though fuel performance might meet both explicit and implicit requirements[9], the biological stability of the emerging alternative fuels [10, 11] and their compatibility with the existing carbon-steel infrastructure [12] should not be overlooked. Fuel biodeterioration and biocorrosion of the carbon-steel infrastructure can lead to serious economic and environmental problems.[13] It is noteworthy that naval fuels are often exposed to sulfate-rich seawater in compensated fuel ballast systems where anaerobic conditions will eventually develop.[14, 15] Recent studies have demonstrated that sulfate-reducing bacteria can metabolize hydrocarbons in conventional petroleum fuels and thereby exacerbate the biocorrosion of carbon steel under anaerobic conditions.[14, 16] Therefore, the biological stability of emerging alternative fuels and their potential to impact the biocorrosion of carbon steel should be critically assessed before they enter into existing fuel containment and distribution systems. [10]

Typically, the chemical composition of biomass-derived alternative fuels is slightly or significantly different from their petroleum counterparts [17] due to different feedstock [2] and processing technologies.[18] Such differences might impact the biological stability of alternative fuels and their potential to corrode the fuel transportation and storage infrastructure.[10] For example, the first generation biodiesel is primarily composed of fatty acid methyl esters (FAMEs).[19] Several studies have shown that such first-generation biodiesels are not good fuel candidates for military tactical vessels since

FAMEs can be readily hydrolyzed and the microbial metabolism of the resulting intermediates linked with sulfide production can exacerbate the corrosion of carbon steel.[15, 20]

Therefore, the US Navy is now considering alternative biofuels [3, 21] including hydroprocessed camelina-JP5 and Fischer-Tropsch (FT) diesel fuel FT-F76 from renewable sources.[3] Typically, these renewable fuels are used experimentally as 50/50 blends with petroleum fuel in tactical vehicles.[6, 22] Previous studies have shown that the range of hydrocarbons in naval biofuels is narrower than that in traditional petroleum fuels.[23, 24] Moreover, FT fuels contain more branched alkanes and fewer aromatic compounds compared to petroleum fuels.[9] Recent studies have shown that FAME biodiesel and hydroprocessed biofuels (camelina-JP5 and algae-F76) are amenable to biodegradation under transient oxygen conditions and can accelerate carbon steel corrosion.[20, 23, 24] The black corrosion products deposited on coupons were mostly mineral sulfides suggesting that majority of metal damage occurred when anaerobic conditions prevailed. Therefore, an experimental protocol to evaluate the biostability of fuels under anaerobic conditions was recently published.[10] We implemented this protocol to, i) determine if the findings on fuel/biofuel stability could be extrapolated to other coastal seawater/sediment systems, ii) extend the findings to fuels not previously evaluated (e.g.FT-F76), and iii) examine the relationship between the degree of corrosion and the utilization of seawater sulfate.

Our findings suggest that camelina-JP5 was more amenable to biodegradation, but FT-F76 was relatively stable compared to the petroleum-based counterparts. Most importantly, both general and pitting corrosion were positively correlated with the

degree of sulfate loss linked to the anaerobic metabolism of fuel components. Due to the relatively rapid biodegradation of camelina-JP5, caution should be exercised with the use and storage of this hydroprocessed biofuel.

Experimental Section

Seawaters and Fuels. Coastal seawaters, which are typically exposed to naval biofuels inside the ballast tanks, were used as both medium and inoculum sources. Three geographically distinct seawaters from Key West (KW, Florida, USA), the Gulf of Mexico (GoM, Alabama, USA) and San Diego Bay (SDB, California, USA) were collected as previously described and shipped to the University of Oklahoma [11]. Sediment from SDB was also used in some experiments since marine sediment might be introduced into the ship ballast systems.[25] The seawater and sediment samples were stored at 4^{o}C until use. The fuels used (petroleum-F76, FT-F76, petroleum-JP5, camelina-JP5) were obtained from Naval Air Systems Command(NAVAIR) as cited in[23]. The fuel blends (50/50 mixture of FT- and petroleum-F76 and 50/50 mixture of camelina- and petroleum-JP5) were also tested since alternative fuels are typically blended with petroleum derived fuels to ensure ideal performance properties.[22] In addition, a mixture of *n*-alkanes (C_6-C_{12}), whenever required, was introduced as previously described.[10]

Experimental Design. The biodegradation and biocorrosion assays were performed according to a previously published protocol [10] and are summarized in Table S1. The seawater was bubbled with N_2 for 60 min and then reduced with a sterile stock solution of Na_2S (0.05 M). Resazurin (0.001%) was added as redox indicator to ensure that obligate anaerobic conditions were maintained throughout the incubation. For KW and

GoM incubation, reduced anaerobic seawater (40 mL) was dispensed inside a well-working anaerobic glove bag into sterile 120 mL serum bottles containing pre-weighed coupons. Since *n*-alkanes are the common hydrocarbons in these fuels, a hydrocarbon-degrading bacterium, 5 ml of *D. alkanexedens* strain ALDC^{T} [26] grown into the stationary phase (6.04-8.48×10^7 cells/mL), was inoculated into 35 ml seawater as a positive control. Due to the hydrocarbon biodegradation potential in SDB sediment [27], 10 g of sediment was placed in 40 ml seawater for SDB incubations as an additional inoculum source. Carbon-steel coupons were suspended by PTFE (polytetrafluoroethylene) coated quartz thread according to previous published procedures [10] whenever sediment was included. The headspace of the bottles was exchanged three times with N_2/CO_2 (80:20). Fuels were added in excess (approximately 2 g/L) aseptically by sterile syringes. Fuel-unamended and sterile incubations served as negative controls (Table S1). Autoclaved inocula (20 min at 121^{o}C; 20 psi) served as sterile controls. The experiment was conducted in triplicate (Table S1) and all incubations were in the dark at ambient temperatures (21±2 ^{o}C).

Corrosion Assay. The carbon-steel coupons (type 1018) were fabricated into round disks (9.53 mm in diameter; thickness,1 mm)with the same specification and dimensions described previously.[10] Coupons were cleaned with deionized water and then washed with two successive acetone treatments as described elsewhere [20]. The pre-cleaned coupons were then flushed with N_2 and sealed in serum bottles under N_2 before autoclaving. At the end of experiment, coupons were harvested and cleaned according to described ASTM G1-03 (American Society for Testing and Materials) standard procedures.[28] The cleaned coupons were dried under a stream of N_2 and stored under N_2

prior to weight loss measurements and profilometry analyses. The corresponding general corrosion rate (milli-inch per year, 1 mpy = 0.0254 mm/year) was calculated from mass loss data according to ASTM Standard G1-03.[28]

Analytic Techniques. Dissolved sulfide in KW incubations was determined spectrophotometrically by the methylene blue method.[29] Samples (0.5 ml) were withdrawn every 30 days from the incubations by a sterile and gassed syringe to monitor sulfate loss by ion chromatography (Dionex model IC-3000, 122 Sunnyvale, CA) as previously described.[14]

Fuel Characterization and Metabolite Profiling. To characterize major fuel components, petroleum (JP5 and F76) and biomass-based (camelina-JP5 and FT-F76) fuels were mixed with ethyl acetate (1:20) and directly analyzed by gas chromatography-mass spectrometry (GC/MS) as previously described.[14] To identify the metabolites generated during the course of fuel biodegradation in KW incubations, approximately 20 ml aqueous sample from each incubation, was collected, acidified (~pH 2 with 6 N HCl) and subjected to liquid-liquid extraction with an equal volume (20 ml) of ethyl acetate according to the previously described procedures.[15] The solvent extract was concentrated to approximately 100 µL and derivatized with N,O-Bis(trimethylsilyl) trifluoroacetamide (BSTFA) prior to analysis by GC/MS.[15]

To assess the kinetics of metabolite flux, as little as 300 µL samples of the GoM incubations were sampled over time and stored at - 20 ^{o}C. The frozen samples were thawed and subsequently extracted (as above, but not derivatized) and concentrated to dryness, followed by reconstitution in 100 µL isopropanol prior to analysis by high performance liquid chromatography (HPLC, Agilent 1290) and quadrupole time-of-

flight (q-TOF) mass spectrometry (MS, Agilent 6538). A similar procedure was used for metabolite profiling in the SDB incubations, except that 5 ml of the aqueous phase was initially solvent extracted, concentrated to dryness, and re-dissolved in 0.5 ml isopropanol. Typically, 5 μL samples were analyzed using HPLC-q-TOF MS in negative ionization mode. The instrument was operated under conditions reported elsewhere [30] with some modifications. An acquity HSS C18 SB (2.1x100 mm, 1.8 μm) analytical column was used with a linear gradient from 23.5% to 95.5% HPLC- grade acetonitrile over 35 minutes followed by 23.5% acetonitrile for an additional 7 minutes. The flow rate was 400 μL/min and the column temperature was maintained at 40°C.Triplicate analyses were performed in sequence followed by a blank before the analysis of the next sample. The acquired data were processed using Agilent B.04.00 MassHunter Qualitative Analysis software. Signature metabolites, such as alkylsuccinates and alkylbenzylsuccinates, were identified based on and their retention times and the exact mass verified by authentic standards [30].

Biofilm Characterization and Profilometry. For KW incubations, coupons were harvested and immediately imaged using a Canon EOS Rebel T3 camera to visualize corrosion products deposited on metal surfaces. To characterize potential biofilms formed on corroded metal surfaces, the corroded coupons were further examined using high resolution Field-Emission Scanning Electron Microscopy (FE-SEM) (Zeiss NEON 40 EsB,Carl Zeiss, Oberkochen, Germany) as previously described.[31] Meanwhile, the elemental composition of corrosion products was characterized to confirm the likely deposition of iron sulfide using the coupled Energy Dispersive Spectroscopy (EDS) at 10 kV.

The cleaned coupons after exposure were scanned using a Nanovea non-contact optical profilometer PS50 (MicroPhotonics, Inc, Irvine, CA) with a 4 μm step size as described previously [10] to acquire 3-dimentional images. Ultra MountainsMap Topography XT6.2 software (MicroPhotonics, Inc, Irvine, CA) was employed to process the topography data. For KW and GoM incubations, pits were defined as the points that are 20 μm below the mean plane (average depth of all measured points) and with an equivalent (the diameter of an irregular region whose outer circumference equals a circular disk) greater than 50 μm. To better reveal the severe pitting corrosion in SDB incubations, pits were defined as having a vertical depth of 50 μm below the mean plane and an equivalent diameter greater than 25 μm.

Results

Fuel Characterization. A better understanding of the chemical composition of various bio- and petrofuels can shed some light on their susceptibility to anaerobic biodegradation and their propensity to exacerbate metal corrosion. To that end, gas chromatographic profiles of biofuels (FT-F76 and camelina-JP5) and their petroleum counterparts (F76 and JP5) are depicted in Figure S1. The hydrocarbon composition of the petroleum and biomass-derived fuels are distinguishable with respect to abundance and complexity of the resolvable peaks in in the total ion chromatograms (Figure S1). Of course, mass spectral response factors vary for dissimilar classes of hydrocarbons and direct comparisons are not intended. That point notwithstanding, the relative abundance of major resolvable hydrocarbons in the fuels can be compared (Figure S2) by integrating the peak areas associated with particular classes of hydrocarbons. Thus, short chain *n*-alkanes (C_8-C_{12}) are detectable in all fuels, but vary from 2.2% to 12%

total peak area in FT-F76 and JP5, respectively. Longer chain *n*-alkanes (≥ 13 carbons) are relatively more abundant in petroleum-F76 (19.9%) than in any of the other fuels (2.8-7.9%)). Similarly, the relative abundance of aromatic hydrocarbons in petroleum fuels (F76 and JP5) was much greater than the corresponding measure in the biofuels. It is also apparent that the branched alkanes (*iso*-alkanes) are far more pronounced in camelina-JP5 and FT-76 than in their petroleum counterparts. In particular, the branched alkane fraction in FT-F76 is 50.6% and might reasonably be expected to impact the biological stability of this fuel.

Sulfate Reduction in Fuel/Seawater Incubations. None of the test fuels or blends stimulated sulfate loss in KW (240 d) or GoM (300d) seawater incubations relative to the fuel-unamended or sterile controls (Figure S3). When *D. alkanexedens* strain ALDC^T was used as a positive control bacterium, increased sulfate loss rates (Figure S4) in KW (16.7±5.2-23.4±0.6 μM/day) and GoM incubations (4.9±1.1-11.5±3.5 μM/day) relative to the fuel-unamended controls (KW:11.5±3.3 μM/day; GoM:3.7±0.4 μM/day) was noted. We presumed that the sulfate loss (0.2-3.1 mM, substracted from fuel-unamended controls) in the incubations was ascribed to oxidation of certain fuel components catalyzed by sulfate reducing bacteria. In a consistent fashion, we also measured the dissolved sulfide (0.3±0.17 - 0.59±0.07 mM) content in KW incubations and found that it was 2-6 times higher than in the sterile controls (Figure S5A). However, the amounts of dissolved sulfide were far less than the stoichiometrically expected quantities (2.1-4.8 mM) based on the degree of sulfate loss. The precipitation of iron sulfide minerals and the escaping H_2S in the headspace might explain the unbalance sulfur in the systems.

The highest rate of sulfate removal was observed in KW (45.8±3.5 - 80.8±8.1 μM/day) and GoM (23.3±3.4 - 76.7±2.4 μM/day) incubations when both *D. alkanexedens* strain ALDC^T and a mixture of C_6-C_{12} *n*-alkanes were used as experimental amendments (Figure 1A and B). Despite the precipitation of dissolved sulfide through reaction with released iron in the systems, sulfide accumulation in the aqueous phase was from 1.31±0.26 mM to 5.09±1.74 mM (Figure S5B) in KW incubations, or 3 - 15 times more than the fuel-unamended incubations. The sulfate loss associated with the fuel amendments in KW seawater was higher than that measured in the fuel-unamended controls (3.7±0.4 - 11.5±3.3 μM/day) or the *n*-alkane-amended incubation (16.6±0.7 - 39.4±0.2 μM/day). The higher rates of sulfate depletion might be attributed to the biodegradation of particular fuel components regardless of the fuel type. In both KW and GoM incubations, camelina-JP5 or its blend with its petroleum counterpart tended to stimulate the highest sulfate depletion rates relative to other fuels (Figure 1A and B).

The SDB incubations (without a *D. alkanexedens* amendment) presented a different scenario where seawater and sediment were chronically exposed to hydrocarbons [27]. Previous studies have demonstrated that enrichments from SDB sediment can metabolize *n*-alkanes and polycyclic aromatic hydrocarbons under sulfate-reducing conditions [27, 32]. In this regard, SDB sediment can represent a promising inoculum to accelerate the inherently slow sulfate reduction rates observed in seawater only incubations, most likely due to the lack of suitable hydrocarbon-degrading, sulfate reducing bacteria. Despite these differences, a very similar pattern of sulfate reduction (Figure 1C) was observed in the SDB incubations relative to the other seawater

incubations amended with the positive control bacterium and alkanes. The SDB sulfate depletion rates associated with fuel amendment (29.8±4.8 - 57.2±2.2 μM/day) were generally higher than the fuel-unamended control (26.7±0.8 μM/day). However, incubations amended with FT-F76 or its blend exhibited only baseline rates of sulfate loss (25.8±4.5 - 26.2±1.6 μM/day). Like the other incubations, the highest sulfate depletion rate was associated with camelina-JP5 in the SDB incubations. Such consistent observations in three marine incubations suggested that this hydroprocessed biofuel might harbor constituents that are more amenable to anaerobic biodegradable than other fuel options. No significant sulfate loss could be measured in any of the sterile controls with the three seawaters (Figure 1, S3 and 4).

Metabolite Profiling. When *D. alkanexedens* and a mixture of C_6-C_{12} *n*-alkanes were used as experimental variables, a series of new peaks were detected during the GC/MS analysis of the KW incubations containing either petroleum-JP5 or camelina-JP5 relative to sterile controls (Figure S6). The retention time of the peaks and their mass spectral profile allowed them to be identified as the alkylsuccinate metabolites that would be expected from the anaerobic metabolism of C_6-C_{12} *n*-alkanes in the incubation mixture (Figure S6). Other alkylsuccinates, beyond the range associated with the C_6-C_{12} *n*-alkanes or even different classes of hydrocarbon substrates (e.g. alkylbenzylsuccinates from alkylbenzenes) were below detection limits. Such a destructive sampling and limited profiling effort provides only a single snapshot of the metabolites detectable at the conclusion of the experiment.

However, the analyses of subsamples by q-TOF allowed for a better assessment of metabolite formation and utilization with higher resolution and greater sensitivity.

The kinetics of alkylsuccinate production and consumption was obtained from frozen samples (300 μL) that were periodically obtained from the GoM incubations (Figure S7 and S8) amended with *D. alkanexedens* and a mixture of C_6-C_{12} *n*-alkanes. For instance, a suite of alkylsuccinates containing 10 to 16 carbon atoms were detected after 150 d of incubation and increased with time in most cases (Figure S7). The detection of these particular alkylsuccinates in the GoM incubations confirmed that the C6 to C12 *n*-alkanes were at least being metabolized via fumarate addition reactions. Similarly, in incubations amended with both petroleum- and camelina-JP5, the same series of alkylsuccinates were accumulated up to 90 d of incubation and then were consumed to undetectable levels by the end of the incubation (Figure S8). The transitory nature of these signature metabolites suggested that sampling time is critical for the interpretatin of metabolite profiles.

In contrast to the KW and GoM incubations, a different series of metabolites were detected in the SDB experiments without an exogenous amendment of *n*-alkanes. In this case, alkylbenzylsuccinates with carbon atoms ranging from C13 to C16 were identified in incubations amended with petroleum fuels (Figure 2 and S10). However, only C_{13} alkylbenzylsuccinate (Figure 2 and S9) was identified in the incubation containing camelina-JP5 and none was detected in incubations amended with FT-F76 or its blend. As is typical for mass spectral analysis, the precise isomeric form of the alkylbenzylsuccinates produced during the course of these incubations cannot reliably be deduced. Nonetheless, the production of alkylbenzylsuccinates attests to the anaerobic metabolism of fuel components (i.e., alkylbenzenes) by fumarate addition reactions.

Biofilm and Corrosion Product Deposition. Carbon-steel coupons exposed to the fuel/seawater mixtures turned black with time due to the deposition of a precipitate (Figure S11). Coupons in non-sterile incubations containing fuel had a visually thicker layer of corrosion product deposition (Figure S4) relative to the corresponding sterile- or fuel-unamended controls (Figure S11). Energy dispersive spectroscopy revealed that the major elements in the corrosion product deposits were iron and sulfur (Figure S12,. S13). Numerous morphologically distinct bacterial cells were observed to be deeply embedded in the corrosion product (Figure S13B) that was deposited on the metal coupon surface.

Characterization of Corrosion. The general corrosion rate, calculated based on the degree of coupon weight loss over the course of the KW and GoM incubations, are shown in Figure 3. Relatively modest corrosion rates were measured in KW (0.53±0.03 - 1.14±0.08 mpy) and GoM (0.33±0.01 - 0.72±0.03 mpy) incubations containing only seawater and fuel (Figure 3A). These rates were only marginally higher than the corresponding sterile and fuel-unamended controls (Figure 3A). The profilometry analyses of these coupons revealed that no substantive localized or pitting corrosion was evident in the non-sterile or the sterile incubations (Figure S14 and S15). The number of pits in coupons exposed to various fuels was slightly higher than the corresponding sterile controls but comparable to the fuel-unamended incubations (Figure 6A).

The amendment of *D. alkanexedens* to the fuel/seawater incubations stimulated corrosion rates in KW and GoM incubations (Figure 3B) relative to comparable incubations containing only seawater as the inoculum (Figure 3A). Generally, the rates of corrosion were between 0.98±0.2 and 1.34±0.01 mpy in incubations amended with

different fuels (Figure 3B), which were slightly higher than the sterile (<0.37±0.14 mpy) and fuel-unamended (<0.81±0.08 mpy) controls (Figure 3B). Given the elevated sulfate depletion rates (Figure 1B), obvious pitting corrosion could be measured in all coupons irrespective of fuel type (Figure 6B, S16&17). Generally, pitting corrosion in KW incubations was much larger and deeper than that found in GoM incubations (Figure 6B, S16-17).

The amendment of both *D. alkanexedens* and alkanes to the incubations resulted in the highest general corrosion rates in KW (1.26±0.04 - 1.48±0.07 mpy) and GoM (0.61±0.07-1.19±0.01 mpy) incubations, relative to the fuel-unamended and the sterile controls (Figure 3C). However, general corrosion rates in SDB incubations with additional sediments as inocula were around 2 - 4.5 times higher than KW and GoM incubations (Figure 3C). The severest pitting corrosion was evident on the metal coupon surfaces (Figure 4 and 5) exposed to KW and SDB incubations irrespective of fuels type. The lesser degree of pitting in GoM incubations (Figures 4, 5 and 6) is likely due to the lower starting amount of sulfate in these incubations and correspondingly lesser amount of sulfide produced (Figure 1B). Certain coupons in SDB incubations were penetrated completely and thus maximum pitting depth could not be precisely determined, but must be in excess of 1 mm (Figure 6). In contrast, the surfaces of coupons exposed to sterile incubations showed no obvious signs of corrosion (Figure S18 and S19).

When the general corrosion rates and number of pits from all seawater incubations were plotted against sulfate loss, a positive linear correlation was obtained (Figure 7). This analysis revealed a large degree of variability in the experiments, but

similar linear correlations were obtained for both general (r^2=0.73) and pitting (r^2=0.69) corrosion (Figure 7A and 7B, respectively). Therefore, higher corrosion rates and severe pitting is a consequence of anaerobic fuel biodegradation linked to sulfate loss and sulfide deposition. In contrast, if no or minimum sulfate reduction occurs in anaerobic marine environments, general corrosion rates and localized corrosion impacts are effectively negligible, even in long-term incubations (300 days).

Discussion

Assessing the biological stability of alternative fuels and their potential impact on biocorrosion is of paramount importance due to concerns with the compatibility of emerging biofuels in the existing carbon-steel fueling infrastructure.[10] Biocorrosion of carbon steel in fuel-laden systems can be ascribed to complex interactions between microorganisms, fuels and metallic surfaces.[13] The selection of a proper inoculum for biodegradation and biocorrosion assays will depend on the fuel of interest and the particular environment under which biofuels are stored and transported. In this study, we evaluated two advanced biofuels (FT-F76 and camelina-JP5) and their conventional petroleum counterparts (F76 and JP5) which are primary fuels used by the US military [3]. These biofuels may be exposed to transient oxygen levels in seawater-compensated fuel ballast tanks that are onboard many naval vessels.[23, 24] Several studies have suggested that aerobic microorganisms might initiate the biodegradation of hydrocarbons to provide partially oxygenated chemical constituents to support the growth of SRBs.[20, 23, 24] It was also postulated that SRB would degrade fuel hydrocarbons directly when anaerobic conditions prevailed in the ballast systems [23, 24]. Such presumptions were supported by the detection of hydrocarbon-degrading SRB and

associated genes (alkylsuccinate synthase, *assA*) in naval ballast tank waters.[14] Due to the limited opportunity to obtain seawater-compensated fuel ballast tank samples, coastal seawaters used to initially fill such tanks were used as inocula in our experiments.

Since sulfate serves as the major electron acceptor in anaerobic marine environments, the depletion of this electron acceptor was monitored over time as initial evidence for fuel biodegradation.[14] No significant sulfate reduction was detected when fuels were exposed to KW and GoM seawaters over long incubation periods (240-300 days). Such findings are not surprising because the anaerobic SRB are typically at or below detectable levels in pristine aerobic seawaters.[20, 23] Given the difficulty in enriching for hydrocarbon-degrading sulfate reducers directly from such inocula, model microorganisms capable of metabolizing fuel components were incorporated into our experimental protocol to artificially mimic a ballast tank microbial community. Given the complexity of fuel constituents, it is advisable to target the most common hydrocarbons (i.e., *n*-alkanes) in the test fuels (Figure S1 and S2). To date, a number of SRB isolated from marine environments have been reported for their capacity to metabolize *n*-alkanes .[26, 33, 34] *D. alkanexedens* was chosen as a model organism since it was isolated from a naval wastewater facility handling shipboard oily wastes [26]. Additionally, *D. alkanexedens* is capable of activating *n*-alkanes (C_6-C_{12}) by the most frequently encountered fumarate addition mechanism [26, 35]. Most importantly, a previous study demonstrated that ballast tank water from a US Navy ship harbors various *assA* genotypes that are phylogenetically closely related to those found in *Desulfatibacillum alkenivorans* AK-01 and *D. alkanexedens* strain ALDC^T.[14] Therefore,

it is reasonable to use this organism to augment seawater in order to assess the biological stability of navy biofuels.

The addition of *D. alkanexedens* to the KW and GoM incubations slightly increased the sulfate depletion rate relative to fuel-unamended controls regardless of fuel type. It should be noted that both petroleum and biomass derived fuels contain C_8-C_{12} *n*-alkanes (Figure S2) that could serve as suitable substrates for the exogenous positive control inoculum.[26] The elevated sulfate loss in these incubations might reasonably be coupled with the oxidation of these short chain alkanes by *D. alkanexedens*. However, FT-F76 stimulated more sulfate reduction (2.1-2.6 mM) than the stoichiometrically required amount of sulfate (0.5 mM) needed to oxidize all available C_6-C_{12} *n*-alkanes in this fuel. Clearly, other fuel components in FT-F76 are also amenable to anaerobic decay. Not surprisingly, the amendment of additional C_6-C_{12} *n*-alkanes in the fuels stimulated the highest sulfate reduction rates probably due to the oxidation of these *n*-alkanes by *D. alkanexedens* strain ALDC^T. However, other fuel components were likely degraded as well because the presence of fuel (blended with *n*-alkanes) caused more sulfate loss relative to the incubations with alkanes only (Figure 1). Therefore, the amendment of readily degradable *n*-alkanes by *D. alkanexedens* strain ALDC^T might stimulate other indigenous microorganisms in seawater and thus enhance the biodegradation of both petroleum and biomass derived fuels. Nevertheless, these results suggested that *D. alkanexedens* strain ALDC^T could serve as an adequate positive control organism for the evaluation of the biological stability of alternate fuel formulations containing *n*-alkanes.[10]

Unlike the KW and GoM incubations, the SDB experiments represented a different scenario wherein seawater and sediment are clearly chronically exposed to hydrocarbon contamination from shipping and other anthropogenic activities.[27, 32] Resident microorganisms in SDB sediment were found to metabolize *n*-alkanes and polycyclic aromatic hydrocarbons under sulfate-reducing conditions.[27, 32] Therefore, sediment introduced into ballast tanks[25] might provide seed inocula to anaerobically biodegrade fuel components and thus exacerbate the rate of corrosion. When SDB sediment was incorporated into the experiments, the fuel amendment stimulated a similar sulfate loss pattern as that observed in the KW and GoM incubations with *D. alkanexedens*. However, the SDB incubations were not amended with the positive control bacterium. The elevated sulfate reduction rates in these incubations suggested that the indigenous microflora in the SDB seawater/sediment incubations were sufficient to initiate fuel biodegradation.

Notably, the highest sulfate depletion rates were always associated with camelina-JP5 or its blend in all three seawater incubations (Figure 1). Such consistent observations suggest that camelina-JP5 harbors fuel components that are more amenable to anaerobic biodegradation than any of the other test fuels. However, the chemical identity of the labile fuel components in this plant-based biofuel remains unknown. The presence of oxygenated fuel components in such hydroprocessed biofuels[36, 37] represents potential candidate substrates and should be investigated further if the Navy remains committed to the use of camelina-JP5. In contrast, the lowest sulfate reduction rate was associated with FT-F76 or its blend in KW and SDB incubations (Figure 3). The relative stability of FT-F76 was likely due to the

predominance of branched alkanes in this fuel (Figure S2). It has been documented that isoalkanes are less susceptible to anaerobic biodegradation than their straight chain counterparts[38]. The chemical composition of FT synthetic fuels can be somewhat tailored to meet desired physicochemical properties [18, 39]. It therefore seems reasonable to incorporate biostability characteristics in addition to combustion considerations in the design of next generation fuels.

While the elevated sulfate reduction rates indicated potential anaerobic metabolism of fuel components, the identification of signature metabolites such as alkysuccinates and benzylsuccinates are diagnostic of anaerobic metabolism of n-alkanes and alkylbenzenes, respectively.[40-42] Bench top GC/MS has been demonstrated to be effective in detecting such metabolites, but large sample volumes and high concentration factors are usually required for adequate detection. In this regard, HPLC-q-TOF offers the advantage of both higher resolution and sensitivity to identify targeted such metabolites.[30, 43, 44] We successfully employed this technique to obtain the kinetics of alkylsuccinate production and consumption in the GoM incubations. To our knowledge, this was the first time that rate information on the transitory nature of the anaerobic hydrocarbon metabolites could be coupled with their detection (Figure S7 and S8). The identification of alkylsuccinates in KW and GoM incubations (Figure S6-S8) attested to anaerobic metabolism of C_6-C_{12} *n*-alkanes via fumarate addition.[35] Presumably, *D. alkanexedens* strain ALDC^{T} [26] was primarily responsible for oxidizing these hydrocarbons. However, the prospect of indigenous microorganisms contributing to the overall metabolism of these substrates, via the same or by different mechanisms [11] cannot be ruled out. Since the exogenously added *n*-alkanes in the fuel were certainly

in excess, quantification of microbial metabolism by substrate utilization against the large background signal was not possible. However, the formation and consumption of alkylsuccinates confirms that at least the low molecular weight *n*-alkanes in both petroleum and biomass-derived fuels could be metabolized when the requisite microorganisms are available.

In this respect, the SDB incubations provide direct evidence of fuel biodegradation since exogenous *n*-alkanes were not added to these experiments. Alkylsuccinates was not detected at the end of the incubation, most likely due to transitory nature of such metabolites (Figure S8) or the biotransformation of the parent molecules by a different mechanism.[45] However, the identification of alkylbenzylsuccinates attested to the anaerobic metabolism of alkylbenzenes by the fumarate addition mechanism.[42] The production of alkylbenzylsuccinates was mostly associated with F76 and JP5 (Figure 2 and S10) as such petroleum-based fuels contain quantitatively more aromatic parent substrates than corresponding biofuels (Figure S9).[9] A qualitatively similar but quantitatively different suite of alkylbenzylsuccinates were also detected directly in seawater-compensated ballast tank water collected from onboard a naval destroyer (unpublished finding). It should be noted that the vessel used F76 as its primary fuel and that it was sampled when moored in San Diego Bay. Thus, it appears that SDB seawater/sediment is enriched in bacteria capable of metabolizing at least some of the F76 component hydrocarbons in both the laboratory and the field.

The sulfide production linked to anaerobic metabolism of the fuel components could conceivably contribute to shipboard corrosion problems.[14, 16, 20] Indeed, fuel amendment considerably increased corrosion rates when the requisite hydrocarbon-

degrading microbial communities were metabolically capable of catalyzing sulfate depletion and presumably sulfide production. In fact, the general corrosion rate was positively correlated with the degree of sulfate utilization (Figure 7A). While multiple mechanisms can be involved in catalyzing biocorrosion, these results quantitatively suggest that sulfide induced corrosion might largely (71%) account for the accelerated corrosion rates in fuel-amended systems. Since camelina-JP5 always stimulated more sulfate reduction than other fuels (Figure 1), one may speculate that this hydroprocessed biofuel is likely to be relatively more aggressive in accelerating carbon steel biocorrosion. However, the measured corrosion rates associated with camelina-JP5 were not significantly (*p*-value between 0.15-0.49) different from other fuels (Figure 3). A possible explanation would be that corrosion rates decreased over time because the corrosion crust (Figure S11) protected inner metal surfaces from corroding in the surrounding sulfidogenic environments. Since the corrosion rates were only determined at the conclusion of prolonged incubations (240-300 d), it is possible that camelina-JP5 may stimulate the highest corrosion rates during an earlier time of exposure.

Given the prolonged incubation time and limited metal surfaces of the coupon, the general corrosion rates fall into the moderate category according to NACE (National Association of Corrosion Engineers) standards.[46] However, this (Figure 3) does not imply that the risk to the integrity of the infrastructure is minimal. Typically, pitting is more of a detriment to the integrity of carbon-steel.[31] Profilometry is a powerful and versatile tool to evaluate pitting corrosion.[10, 16, 31, 47, 48] Quantitative analysis using this technique indicated that the severity of pitting also correlated well with sulfate loss (Figure 7B). Regardless of mechanism, the severity of pitting corrosion is also largely

(69%) associated with biogenic sulfide production in anaerobic fuel-degrading systems. Collectively, these findings suggest that the synergistic effects associated with corrosive sulfide formation, acidic metabolic production (e.g. organic acids) and biofilm formation accelerate the both general and pitting corrosion process on carbon steel surfaces.[16, 31, 44] Since the highest sulfate depletion rates were always associated with camelina-JP5, it can be reasonably speculated that such hydroprocessed biofuels might present more risk due to accelerated pitting corrosion under normal marine conditions relative to other fuels. Thus, particular attention should be paid to camelina-JP5 with respect to the biocrossoion of carbon-steel infrastructure particularly during long term storage. Lastly, these findings also verified the scientific basis of an existing protocol [10] and suggested that it could be used to evaluate the biological stability of other novel biofuels formulations. Such an assessment of the compatibility of fuel formulations with existing infrastructure components will ultimately facilitate societal decision-making with regard to biofuel options.

Acknowledgements

This study was financially supported by a grant (Award N000141010946) from the Office of Naval Research. We appreciated the help from Dr. Benjamin G. Harvey, Frank P. Harvey, Christopher R. Marks and Brian H. Harriman for collecting the seawater and sediment samples. We also want to thank the Naval Fuels and Lubes Cross Functional Team, NAVAIR for providing the biofuels tested in this study.

References

(1) Kaygusuz, K., Energy for sustainable development: A case of developing countries. *Renew. Sust. Energ. Rev.* **2012,** *16*, (2), 1116-1126.

(2) Ahmad, A.; Yasin, N. M.; Derek, C.; Lim, J., Microalgae as a sustainable energy source for biodiesel production: a review. *Renew. Sust. Energ. Rev.* **2011,** *15*, (1), 584-593.

(3) Bartis, J. T.; Van Bibber, L. Alternative fuels for military applications. http://www.rand.org/pubs/monographs/MG969.html (accessed September 25, 2014).

(4) Blakeley, K. DOD Alternative fuels: policy, initiatives and legislative activity. http://fpc.state.gov/documents/organization/202467.pdf (accessed October 4, 2015).

(5) Takeshita, T., Competitiveness, role, and impact of microalgal biodiesel in the global energy future. *Appl. Energ.* **2011,** *88*, (10), 3481-3491.

(6) Hamilton, L. J.; Williams, S. A.; Kamin, R. A.; Carr, M. A.; Caton, P. A.; Cowart, J. S. In *Renewable fuel performance in a legacy military diesel engine*, ASME Conference Procedings, 2011.

(7) Naik, C. V.; Puduppakkam, K. V.; Modak, A.; Meeks, E.; Wang, Y. L.; Feng, Q.; Tsotsis, T. T., Detailed chemical kinetic mechanism for surrogates of alternative jet fuels. *Combust. Flame.* **2011,** *158*, (3), 434-445.

(8) Bunting, B. G.; Bunce, M.; Barone, T. L.; Storey, J. M. Fungible and compatible biofuels: literature search, summary, and recommendations; Oak Ridge National Laboratory (ORNL). http://www.energy.gov/sites/prod/files/2014/03/f14/20110512135206-0.pdf (accessed October 4, 2015)

(9) Stamper, D. M.; Lee, G. F. The explicit and implicit qualities of alternative fuels: issues to consider for their use in marine diesel engines. http://oai.dtic.mil/oai/oai?verb=getRecord&metadataPrefix=html&identifier=ADA541584 (accessed October 4, 2015).

(10) Liang, R.; Suflita, J. M., Protocol for evaluating the biological stability of fuel formulations and their relationship to carbon steel biocorrosion. Handbook of hydrocarbon and lipid microbiology. Springer Berlin Heidelberg, 2015.

(11) Liang, R.; Harvey, B. G.; Quintana, R. L.; Suflita, J. M., Assessing the Biological Stability of a Terpene-Based Advanced Biofuel and Its Relationship to the Corrosion of Carbon Steel. *Energy Fuels* **2015**.

(12) Richard, T. L., Challenges in scaling up biofuels infrastructure. *Science(Washington)* **2010,** *329*, (5993), 793-796.

(13) Suflita, J.; Lyles, C.; Aktas, D.; Sunner, J., Biocorrosion issues associated with the use of ultra-low sulfur diesel and biofuel blends in the energy infrastructure. *Understanding Biocorrosion: Fundamentals and Applications* **2014,** *66*, 313.

(14) Lyles, C. N.; Aktas, D. F.; Duncan, K. E.; Callaghan, A. V.; Stevenson, B. S.; Suflita, J. M., Impact of Organosulfur Content on Diesel Fuel Stability and Implications for Carbon Steel Corrosion. *Environ. Sci. Technol.* **2013,** *47*, (11), 6052-6062.

(15) Aktas, D. F.; Lee, J. S.; Little, B. J.; Ray, R. I.; Davidova, I. A.; Lyles, C. N.; Suflita, J. M., Anaerobic metabolism of biodiesel and its impact on metal corrosion. *Energy Fuels* **2010,** *24*, (5), 2924-2928.

(16) Lyles, C. N.; Le, H. M.; Beasley, W. H.; McInerney, M. J.; Suflita, J. M., Anaerobic hydrocarbon and fatty acid metabolism by syntrophic bacteria and their impact on carbon steel corrosion. *Front. Microbiol.* **2014,** *5*.

(17) Ott, L. S.; Bruno, T. J., Variability of biodiesel fuel and comparison to petroleum-derived diesel fuel: application of a composition and enthalpy explicit distillation curve method. *Energy Fuels* **2008,** *22*, (4), 2861-2868.

(18) Schablitzky, H. W.; Lichtscheidl, J.; Hutter, K.; Hafner, C.; Rauch, R.; Hofbauer, H., Hydroprocessing of Fischer–Tropsch biowaxes to second-generation biofuels. *Biomass. Convers. Biorefin.* **2011,** *1*, (1), 29-37.

(19) Singh, S.; Singh, D., Biodiesel production through the use of different sources and characterization of oils and their esters as the substitute of diesel: a review. *Renew. Sust. Energ. Rev.* **2010,** *14*, (1), 200-216.

(20) Lee, J. S.; Ray, R. I.; Little, B. J.; Duncan, K. E.; Oldham, A. L.; Davidova, I. A.; Suflita, J. M., Sulphide production and corrosion in seawaters during exposure to FAME diesel. *Biofouling* **2012,** *28*, (5), 465-478.

(21) Mabus, R., *Department of the Navy's Energy Program for Security and Independence*.http://greenfleet.dodlive.mil/files/2010/04/Naval_Energy_Strategic_Roadmap_100710.pdf (accessed October 6, 2015).

(22) Rodriguez, B.; Bartsch, T. M. In The United States Air Force's process for alternative fuels certification, 26th AIAA Applied Aerodynamics Conference, 2008.

(23) Aktas, D. F.; Lee, J. S.; Little, B. J.; Duncan, K. E.; Perez-Ibarra, B. M.; Suflita, J. M., Effects of oxygen on biodegradation of fuels in a corroding environment. *Int. Biodeterior. Biodegr.***2013,** *81*, 114-126.

(24) Lee, J. S.; Ray, R. I.; Little, B. J.; Duncan, K. E.; Aktas, D. F.; Oldham, A. L.; Davidova, I. A.; Suflita, J. M., Issues for storing plant-based alternative fuels in marine environments. *Bioelectrochemistry* **2014,** *97*, 145-153.

(25) Burkholder, J. M.; Hallegraeff, G. M.; Melia, G.; Cohen, A.; Bowers, H. A.; Oldach, D. W.; Parrow, M. W.; Sullivan, M. J.; Zimba, P. V.; Allen, E. H., Phytoplankton and bacterial assemblages in ballast water of US military ships as a function of port of origin, voyage time, and ocean exchange practices. *Harmful Algae* **2007,** *6*, (4), 486-518.

(26) Davidova, I. A.; Duncan, K. E.; Choi, O. K.; Suflita, J. M., Desulfoglaeba alkanexedens gen. nov., sp. nov., an n-alkane-degrading, sulfate-reducing bacterium. *Int. J. Syst. Evol. Microbiol.* **2006,** *56*, (12), 2737-2742.

(27) Coates, J. D.; Woodward, J.; Allen, J.; Philp, P.; Lovley, D. R., Anaerobic degradation of polycyclic aromatic hydrocarbons and alkanes in petroleum-contaminated marine harbor sediments. *Appl. Environ. Microbiol.* **1997,** *63*, (9), 3589-3593.

(28) ASTM G1-03, A., Standard practice for preparing, cleaning, and evaluating corrosion test specimens. **2003**.

(29) Tanner, R. S., Monitoring sulfate-reducing bacteria: comparison of enumeration media. *J. Microbiol. Methods.* **1989,** *10*, (2), 83-90.

(30) Kimes, N. E.; Callaghan, A. V.; Aktas, D. F.; Smith, W. L.; Sunner, J.; Golding, B.; Drozdowska, M.; Hazen, T. C.; Suflita, J. M.; Morris, P. J., Metagenomic analysis and metabolite profiling of deep–sea sediments from the Gulf of Mexico following the Deepwater Horizon oil spill. Frontiers in microbiology 2013, 4.

(31) Liang, R.; Grizzle, R. S.; Duncan, K. E.; McInerney, M. J.; Suflita, J. M., Roles of thermophilic thiosulfate-reducing bacteria and methanogenic archaea in the biocorrosion of oil pipelines. *Front. Microbiol.* **2014,** *5*.

(32) Coates, J. D.; Anderson, R. T.; Lovley, D. R., Oxidation of polycyclic aromatic hydrocarbons under sulfate-reducing conditions. *Appl. Environ. Microbiol.* **1996,** *62*, (3), 1099-1101.

(33) So, C. M.; Young, L., Isolation and characterization of a sulfate-reducing bacterium that anaerobically degrades alkanes. *Appl. Environ. Microbiol.* **1999,** *65*, (7), 2969-2976.

(34) Cravo-Laureau, C.; Grossi, V.; Raphel, D.; Matheron, R.; Hirschler-Réa, A., Anaerobic n-alkane metabolism by a sulfate-reducing bacterium, *Desulfatibacillum aliphaticivorans* strain CV2803T. *Appl. Environ. Microbiol.* **2005,** *71*, (7), 3458-3467.

(35) Davidova, I. A.; Gieg, L. M.; Nanny, M.; Kropp, K. G.; Suflita, J. M., Stable isotopic studies of n-alkane metabolism by a sulfate-reducing bacterial enrichment culture. *Appl. Environ. Microbiol.* **2005,** *71*, (12), 8174-8182.

(36) McCormick, R. L.; Ratcliff, M. A.; Christensen, E.; Fouts, L.; Luecke, J.; Chupka, G. M.; Yanowitz, J.; Tian, M.; Boot, M., Properties of oxygenates found in upgraded biomass pyrolysis oil as components of spark and compression ignition engine fuels. *Energy Fuels* **2015,** *29*, (4), 2453-2461.

(37) Christensen, E. D.; Chupka, G. M.; Luecke, J.; Smurthwaite, T.; Alleman, T. L.; Iisa, K.; Franz, J. A.; Elliott, D. C.; McCormick, R. L., Analysis of oxygenated compounds in hydrotreated biomass fast pyrolysis oil distillate fractions. *Energy Fuels* **2011,** *25*, (11), 5462-5471.

(38) Prince, R. C.; Suflita, J. M., Anaerobic biodegradation of natural gas condensate can be stimulated by the addition of gasoline. *Biodegradation* **2007,** *18*, (4), 515-523.

(39) Liu, G.; Larson, E. D.; Williams, R. H.; Kreutz, T. G.; Guo, X., Making Fischer−Tropsch fuels and electricity from coal and biomass: performance and cost analysis. *Energy Fuels* **2010,** *25*, (1), 415-437.

(40) Parisi, V. A.; Brubaker, G. R.; Zenker, M. J.; Prince, R. C.; Gieg, L. M.; da Silva, M. L. B.; Alvarez, P. J. J.; Suflita, J. M., Field metabolomics and laboratory assessments of anaerobic intrinsic bioremediation of hydrocarbons at a petroleum-contaminated site. *Microb. Biotechnol.* **2009,** *2*, (2), 202-212.

(41) Agrawal, A.; Gieg, L. M., In situ detection of anaerobic alkane metabolites in subsurface environments. *Front. Microbiol.* **2013,** *4*.

(42) Gieg, L. M.; Suflita, J. M., Detection of anaerobic metabolites of saturated and aromatic hydrocarbons in petroleum-contaminated aquifers. *Environ. Sci. Technol.* **2002,** *36*, (17), 3755-3762.

(43) Brauer, J. I.; Makama, Z.; Bonifay, V.; Aydin, E.; Kaufman, E. D.; Beech, I. B.; Sunner, J., Mass spectrometric metabolomic imaging of biofilms on corroding steel surfaces using laser ablation and solvent capture by aspiration. *Biointerphases* **2015,** *10*, (1), 019003.

(44) Lenhart, T. R.; Duncan, K. E.; Beech, I. B.; Sunner, J. A.; Smith, W.; Bonifay, V.; Biri, B.; Suflita, J. M., Identification and characterization of microbial biofilm

communities associated with corroded oil pipeline surfaces. *Biofouling* **2014,** *30*, (7), 823-835.

(45) So, C. M.; Phelps, C. D.; Young, L., Anaerobic transformation of alkanes to fatty acids by a sulfate-reducing bacterium, strain Hxd3. *Appl. Environ. Microbiol.* **2003,** *69*, (7), 3892-3900.

(46) NACE Standard, Item No. 21017. *Preparation, installation, analysis, and interpretation of corrosion coupons in oilfield operations* **2005**.

(47) Lee, J. S.; McBeth, J. M.; Ray, R. I.; Little, B. J.; Emerson, D., Iron cycling at corroding carbon steel surfaces. *Biofouling* **2013**, 29(10), 1243-1252.

(48) Duncan, K. E.; Perez-Ibarra, B. M.; Jenneman, G.; Harris, J. B.; Webb, R.; Sublette, K., The effect of corrosion inhibitors on microbial communities associated with corrosion in a model flow cell system. *Appl. Microbiol. Biotechnol.* **2013**, 1-12.

Table S1 Summary for experimental design to assess the biological stability of petroleum and biomass-derived fuels with seawater from Key West (KW), Gulf of Mexico (GoM) and San Diego Bay (SDB). Note: Only experimental group 1 was included in SDB incubations since sediment was incorporated as additional source of inocula.

Test	Fuels	Treatment	Replicates
Experimental group 1	petroleum-F76	Seawater alone	3
	petroleum-JP5		3
	FT-F76		3
	camelina-JP5		3
	50/50 petroleum/FT-F76		3
	50/50 petroleum/camelina-JP5		3
Unamended	No fuel		3
Sterile	petroleum-F76	Heat killed Seawater alone	2
	petroleum-JP5		2
	FT-F76		2
	camelina-JP5		2
	50/50 petroleum/FT-F76		2
	50/50 petroleum/camelina-JP5		2
Experimental group 2	petroleum-F76	Seawater + *Desulfoglaeba alkanexedens*	3
	petroleum-JP5		3
	FT-F76		3
	camelina-JP5		3
	50/50 petroleum/FT-F76		3
	50/50 petroleum/camelina-JP5		3
Sterile	petroleum-F76	Heat-killed Seawater + Heat killed *Desulfoglaeba alkanexedens*	2
	petroleum-JP5		2
	FT-F76		2
	camelina-JP5		2
	50/50 petroleum/FT-F76		2
	50/50 petroleum/camelina-JP5		2
Experimental group 3	petroleum-F76	Seawater + *Desulfoglaeba alkanexedens* + C_6-C_{12} *n*-alkanes blend	3
	petroleum-JP5		3
	FT-F76		3
	camelina-JP5		3
	50/50 petroleum/FT-F76		3
	50/50 petroleum/camelina-JP5		3
Positive	C_6-C_{12} alkanes only		3
Unamended	No fuel or *n*-alkanes		3
Sterile	petroleum-F76	Heat-killed Seawater + Heat killed *Desulfoglaeba alkanexedens* + C_6-C_{12} *n*-alkanes blend	2
	petroleum-JP5		2
	FT-F76		2
	camelina-JP5		2
	50/50 petroleum/FT-F76		2
	50/50 petroleum/camelina-JP5		2
	petroleum-F76		2
	No fuel or *n*-alkanes		2

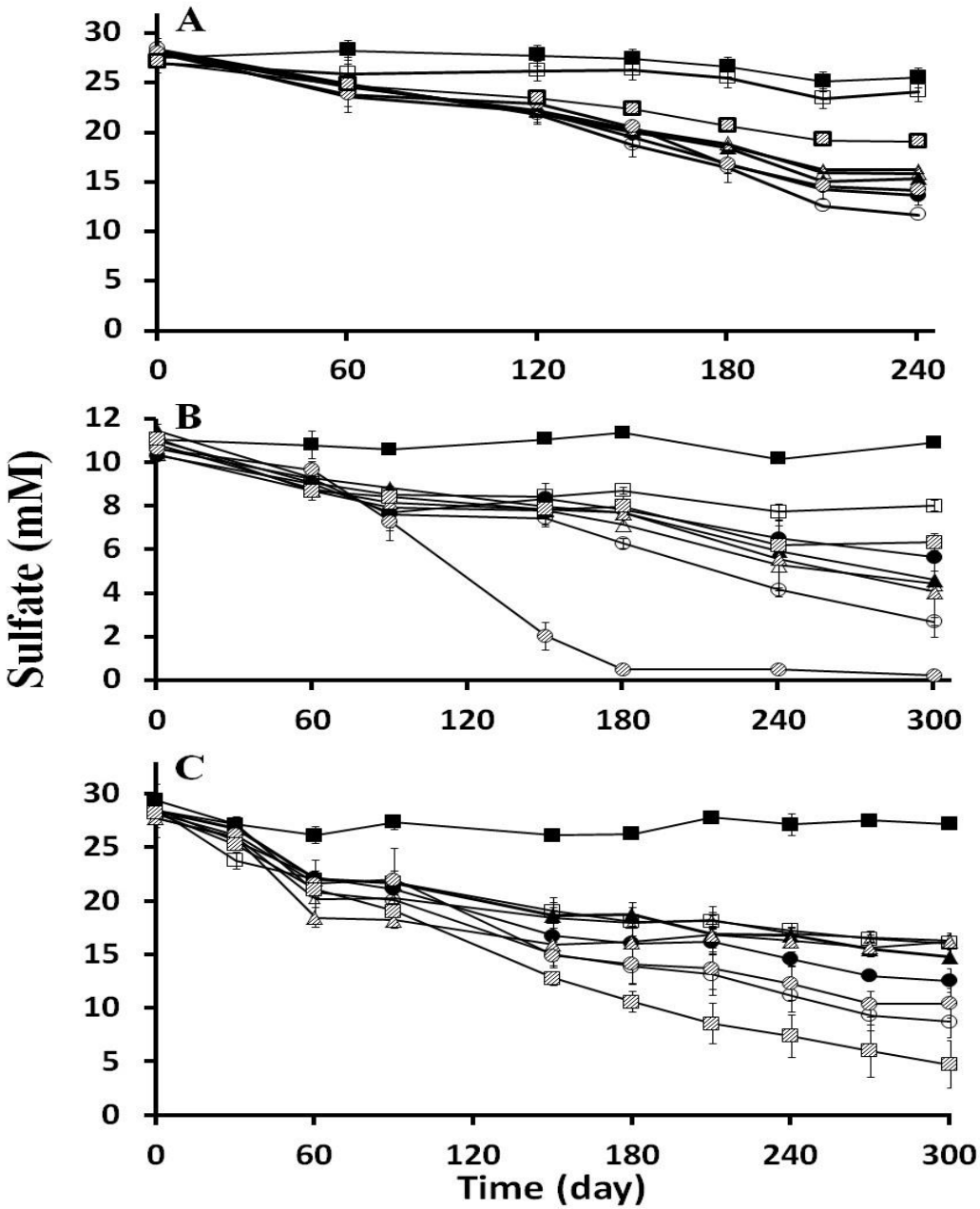

Figure 1 Sulfate reduction in seawater incubations from Key West (KW), Gulf of Mexico (GoM) and San Diego Bay (SDB). A. KW seawater + fuel + *D. alkanexedens* strain ALDC^T + alkanes; B. GoM seawater + fuel + *D. alkanexedens* strain ALDC^T +alkanes; C. SDB seawater + sediment + fuel. Legends: ■Sterile, inocula of seawater, sediment or *D. alkanexedens* strain ALDC^T was heat-killed by autoclaving; □Fuel-unamended; ▨ C_6-C_{12} *n*-alkanes; ▲petroleum-F76; Δ FT-F76; ◬ 50/50 blend of petroleum and FT-F76; ●petroleum JP5; ○ camelina-JP5; ⊘ 50/50 blend of petroleum and camelina-JP5.

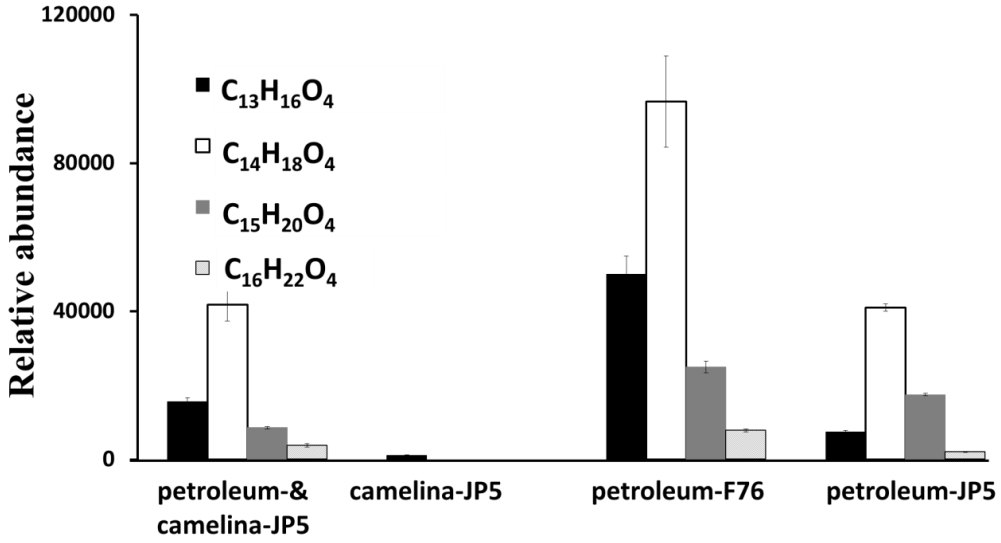

Figure 2 Relative abundance of putative C_{13}-C_{16} alkylbenzylsuccinates detected in SDB incubations.

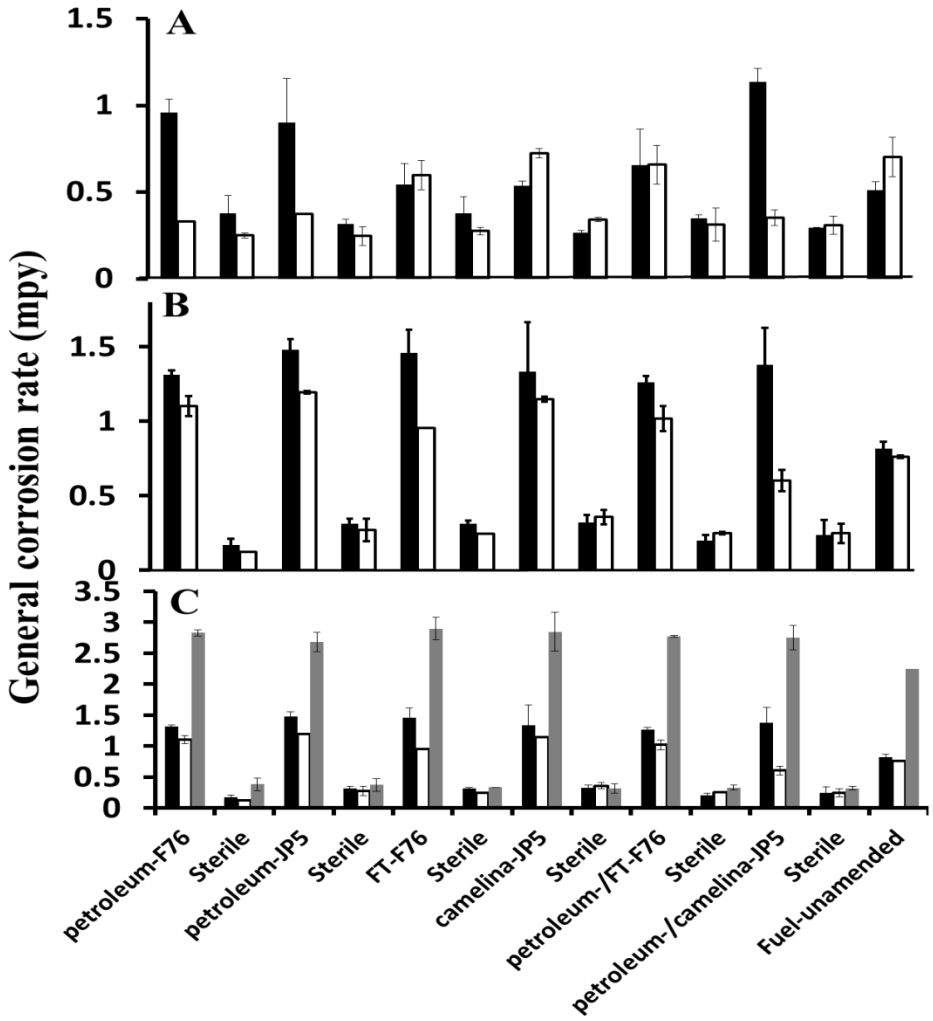

Figure 3 General corrosion rates observed in seawater incubations from KW (black bars), GoM (clear bars) and SDB (grey bars). A. seawater + fuel only; B. seawater + fuel + *D. alkanexedens* strain ALDC^T; C. seawater (KW and GoM) + fuel+ *D. alkanexedens* strain ALDC^T + C_6-C_{12} alkanes or SDB seawater + sediment + fuel. The fuel amendment under each condition and the corresponding sterile controls are indicated on the bottom of x-axis. (Sterile: any inocula of seawater, sediment or *D. alkanexedens* strain ALDC^T was heat-killed by autoclaving).

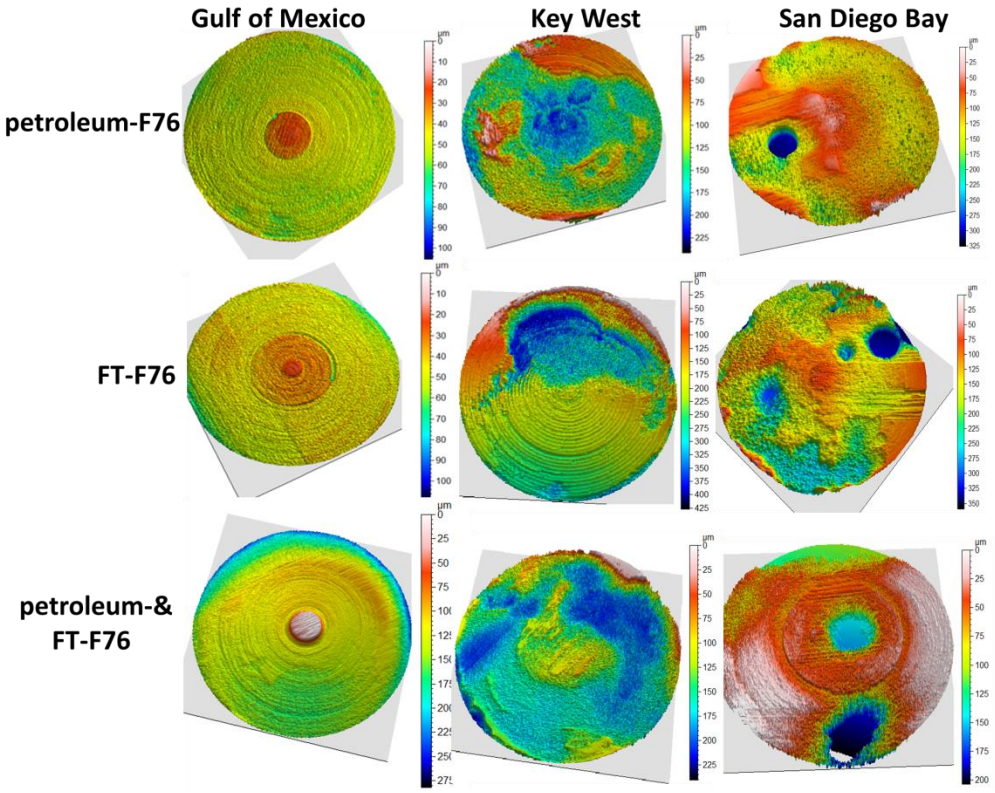

Figure 4 Profilometry profiles of carbon-steel coupons exposed to GoM, KW and SDB incubations amended with petroleum F76, FT-F76 and their blend. KW and GoM incubations: seawater + fuel + *D. alkanexedens* strain ALDC^{T} + C_6-C_{12} alkanes; SDB incubations: SDB seawater + sediment + fuel. The false colors on the scale correspond to the points of different depth (in μm, blue indicates deep points whereas red or yellow represent much shallower points) collected through the whole metal surfaces. Severe pitting corrosion was observed in KW and SDB incubations regardless of the fuel type.

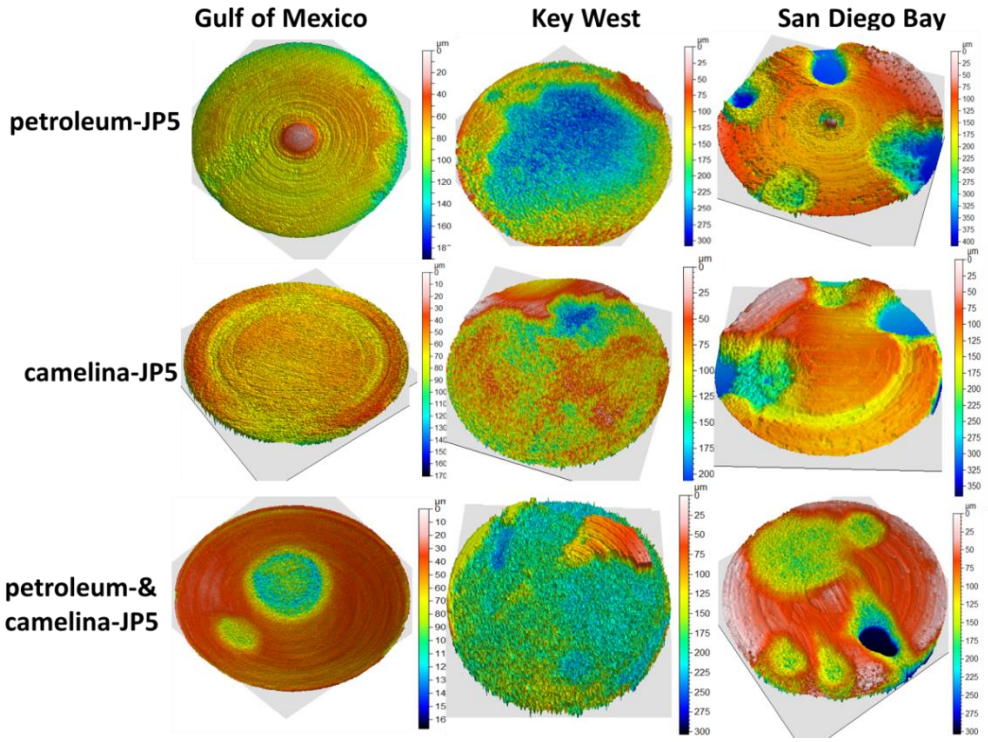

Figure 5 Profilometry profiles of carbons-steel coupons exposed to GoM, KW and SDB incubations amended with petroleum JP5, camelina-JP5 and their blend. KW and GoM incubations: seawater + fuel + *D. alkanexedens* strain ALDC^{T} + C_6-C_{12} alkanes; SDB incubations: SDB seawater + sediment + fuel. The false colors on the scale correspond to the points of different depth (in μm, blue indicates deep points whereas red or yellow represent much shallower points) collected through the whole metal surfaces. Severe pitting corrosion was observed in KW and SDB incubations regardless of the fuel type.

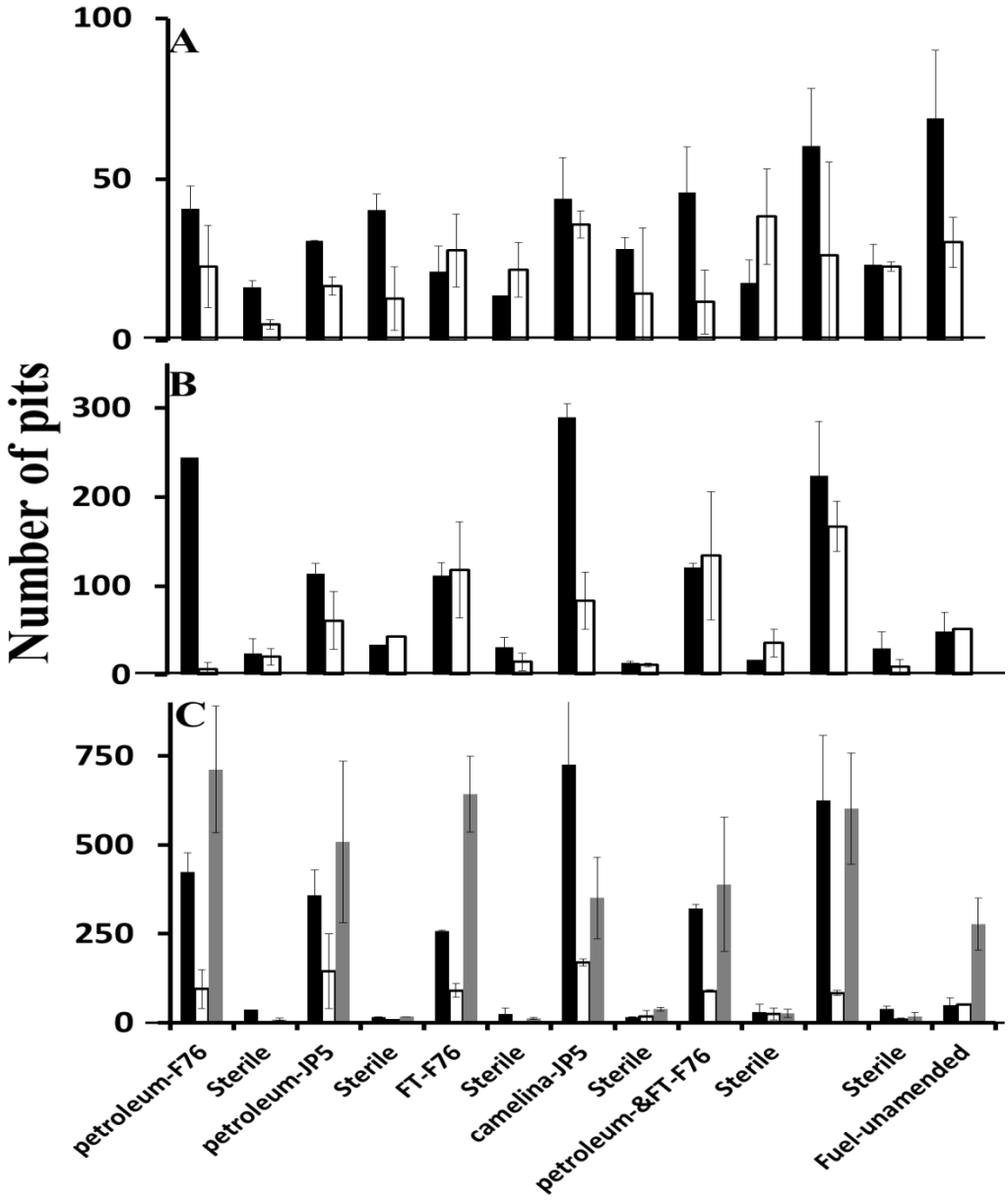

Figure 6 Number of pits counted on the post-cleaned coupons after exposure in seawater incubations from KW (black bars), GoM (clear bars) and SDB (grey bars). A. seawater + fuel only; B. seawater + fuel + *D. alkanexedens* strain ALDC^T; C. seawater (KW and GoM) + fue l+ *D. alkanexedens* strain ALDC^T + C_6-C_{12} alkanes or SDB seawater + sediment + fuel. The fuel amendment under each condition and the corresponding sterile controls are indicated on the bottom of x-axis. (Sterile: any inocula of seawater, sediment or *D. alkanexedens* strain ALDC^T was heat-killed by autoclaving).

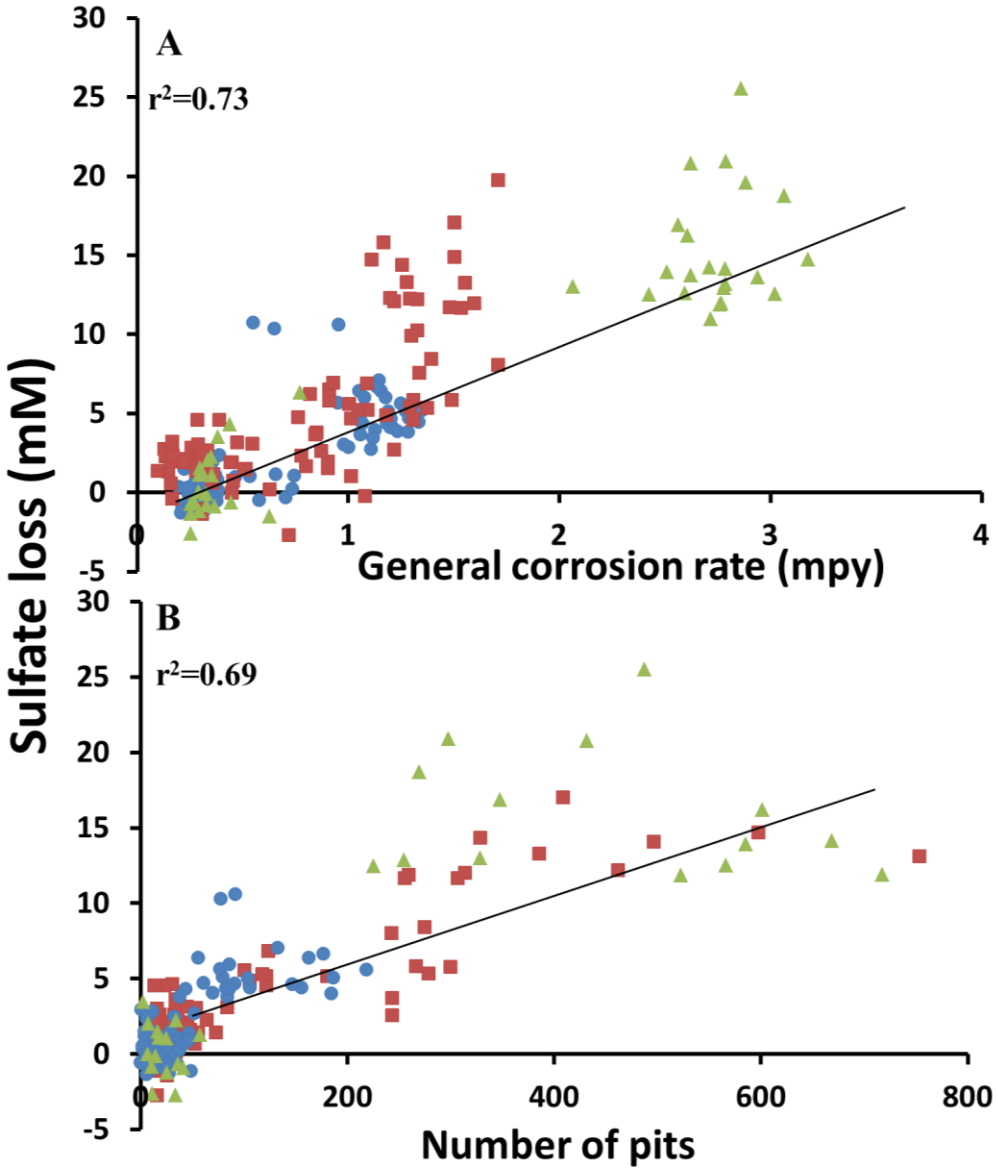

Figure 7 Plot of sulfate loss and general corrosion rate (A) and number of pits (B), respectively. The data points from KW (squares in red), GoM (round dots in blue) and SDB (triangles in green) are separated in A and B.

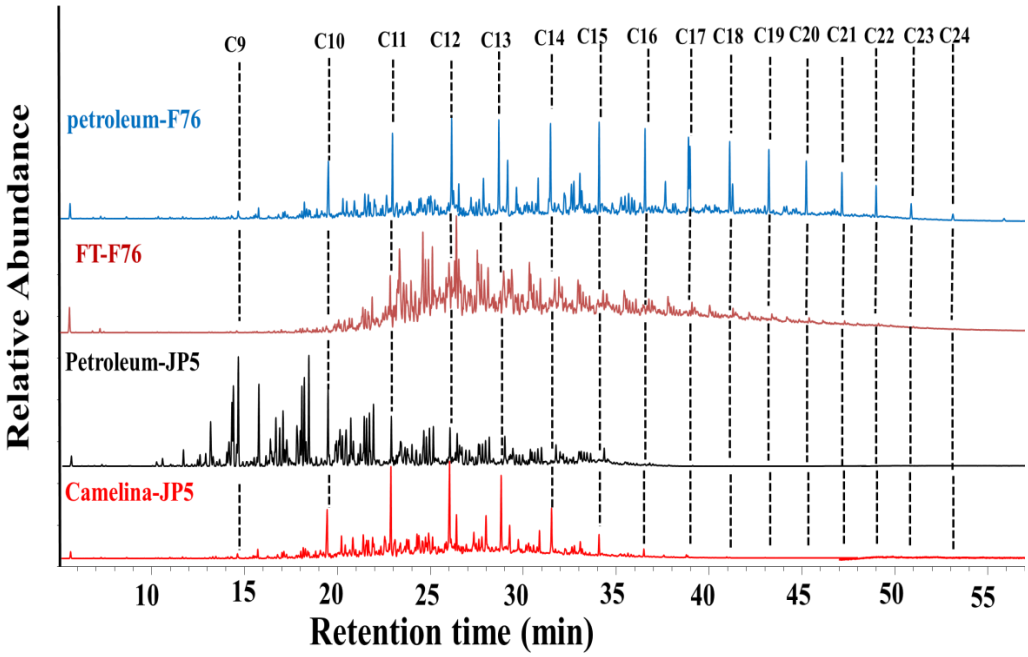

Figure S1 Gas chromatographic profiles of alternative fuels (FT-F76&camelina-JP5) and their petroleum-derived counterparts (F76&camelina JP5). The peaks (C9-C24) indicated with dashed lines refer to *n*-alkanes with varying carbon chain length.

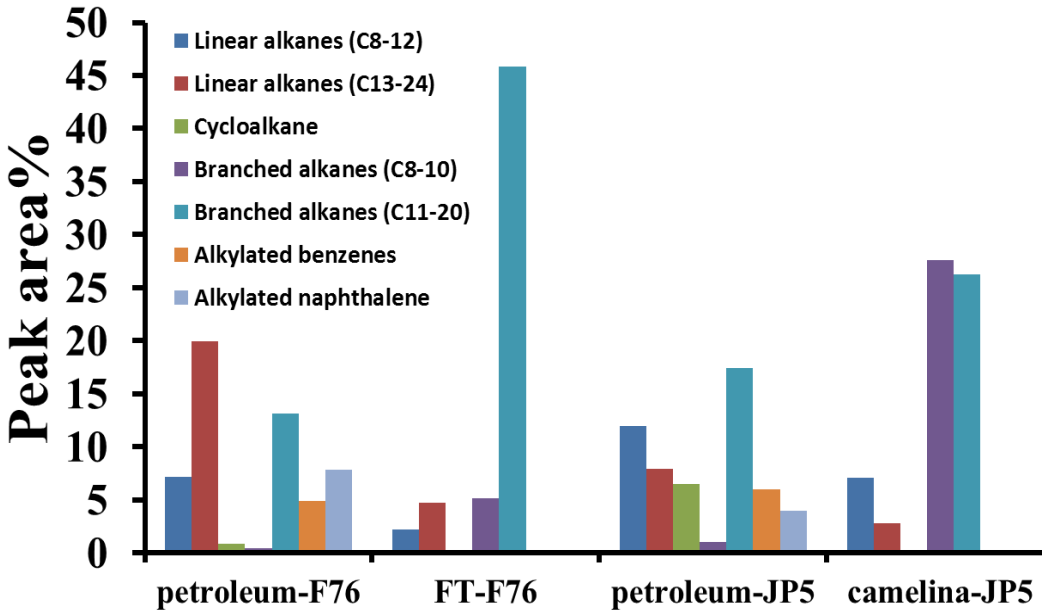

Figure S2 Relative abundance of major hydrocarbons in alternative fuels (FT-F76&camelina-JP5) and their petroleum-derived counterparts (F76&camelina JP5) according to the percentage of peak area of each compound. Strain chain and branched alkanes were grouped separately to better reflect the difference in chemical makeup in fuels.

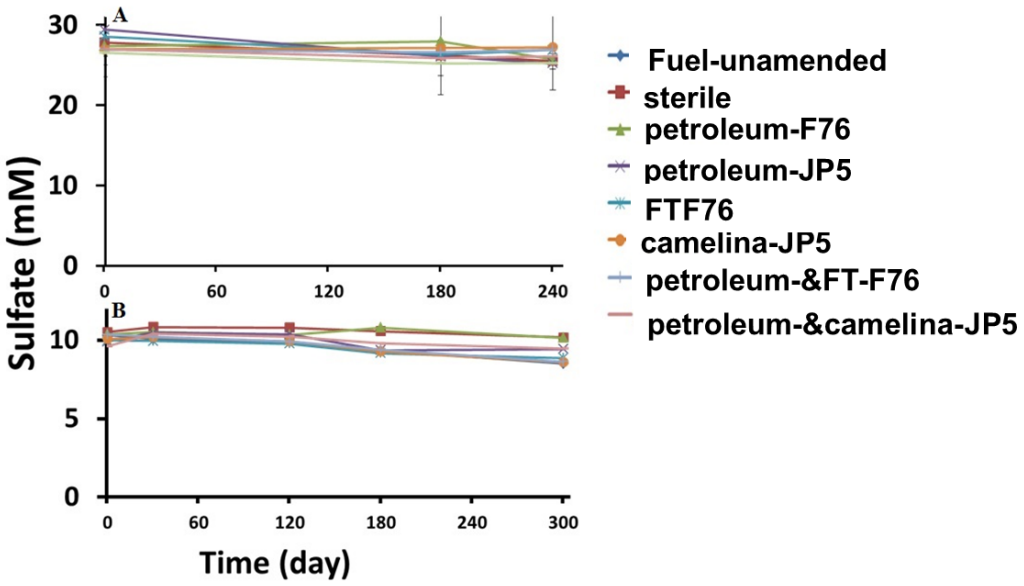

Figure S3 Sulfate reduction in KW (A) and GoM (B) incubations when only seawater and fuels were present. The legends on the left indicated the specific fuel amended in the system. Fuel-unamended: no fuel was added; sterile: seawater was sterilized by autoclaving.

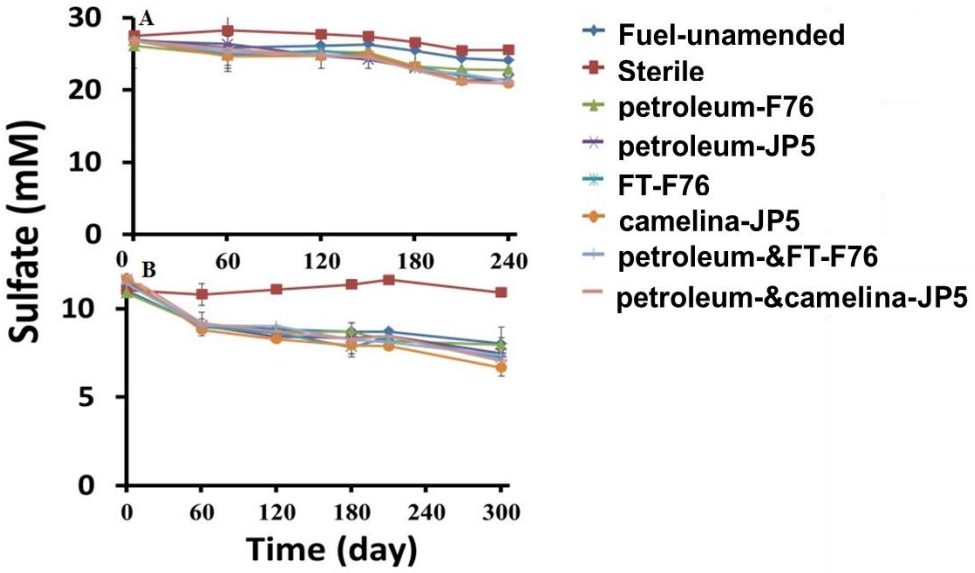

Figure S4 Sulfate reduction in KW (A) and GoM (B) incubations when *D. alkanexedens* strain ALDC^T was inoculated as a positive control. The legends on the right indicated the specific fuel amended in the system. Fuel-unamended: no fuel was added; sterile: seawater and *D. alkanexedens* strain ALDC^T were sterilized by autoclaving.

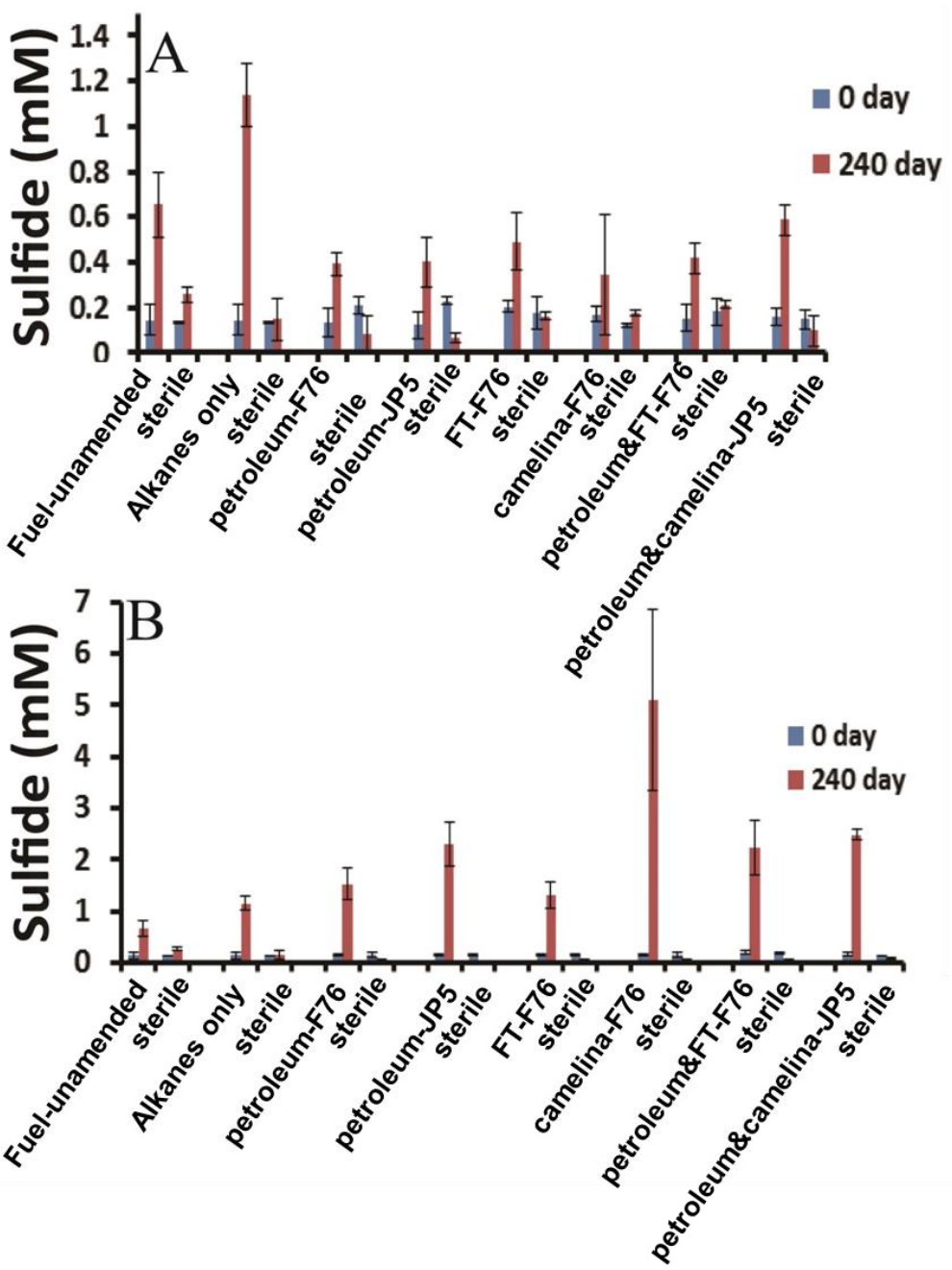

Figure S5 Dissolved sulfide in the aqueous phase at the beginning (blue bars) and conclusion (red bars) of the experiment in KW incubations. A, KW seawater+ *D. alkanexedens* strain ALDC^T +alkanes; B, KW seawater+fuel+ *D. alkanexedens* strain ALDC^T + C_6-C_{12} *n*-alkanes. Unamended control: no fuel was added; Sterile: seawater and *D. alkanexedens* strain ALDC^T were sterilized by autoclaving.

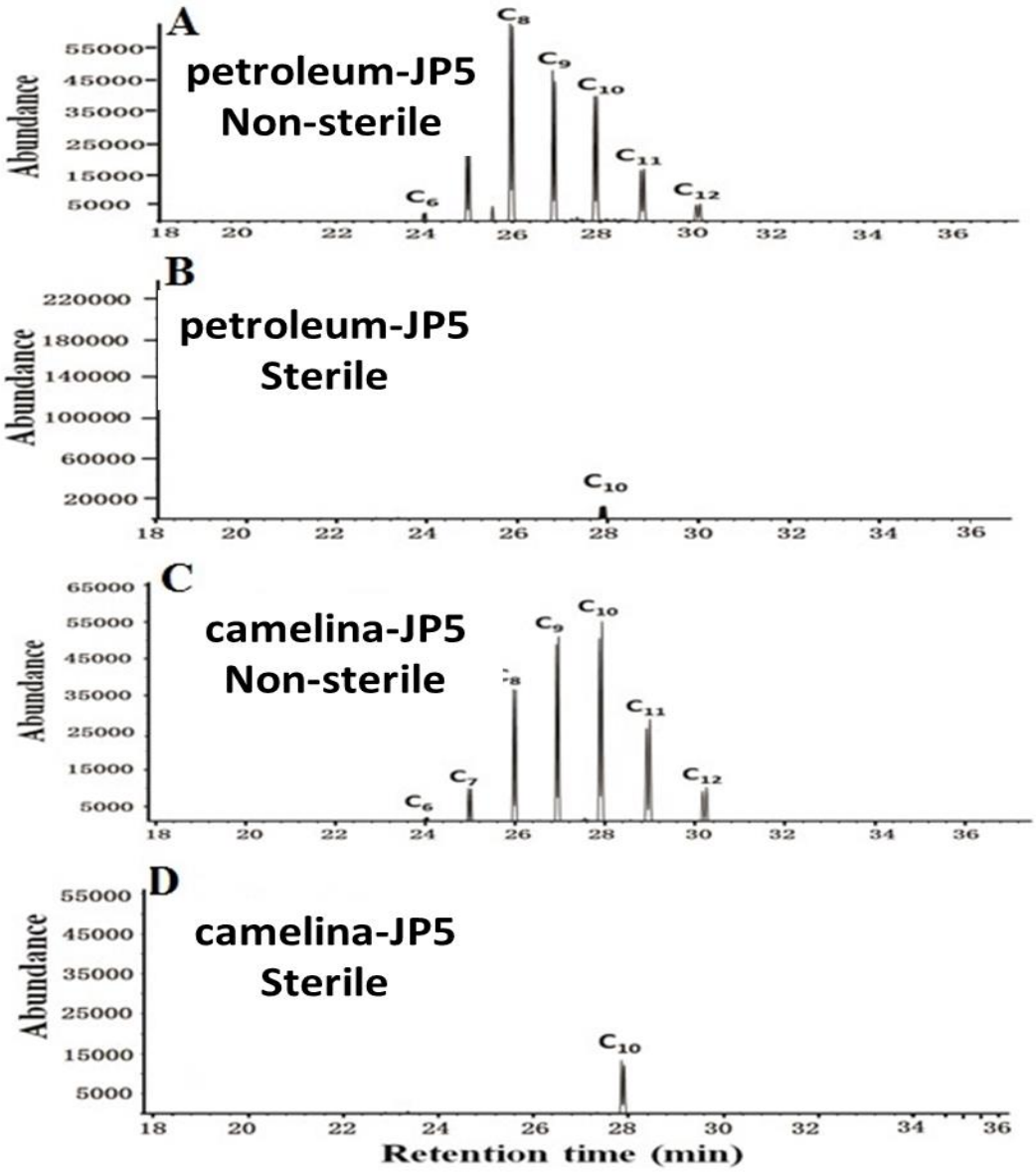

Figure S6 Gas chromatography profiles of extracted alkylsuccinates (m/z 262+) from KW incubations. A, KW seawater+petroleum JP5+ *D. alkanexedens* strain ALDC^T + C_6-C_{12} *n*-alkanes; B, the corresponding sterile control with petroleum JP5; (C) KW seawater+camelina JP5+ *D. alkanexedens* strain ALDC^T + C_6-C_{12} *n*-alkanes; (D) the corresponding sterile control with camelina JP5. Alkylsuccinates derived from C_6-C_{12} *n*-alkanes are designated on top of the peaks. C10 alkylsuccinates was also detected in sterile controls (C&D) due to the carrier over from the inocula of *D. alkanexedens* strain ALDC^T.

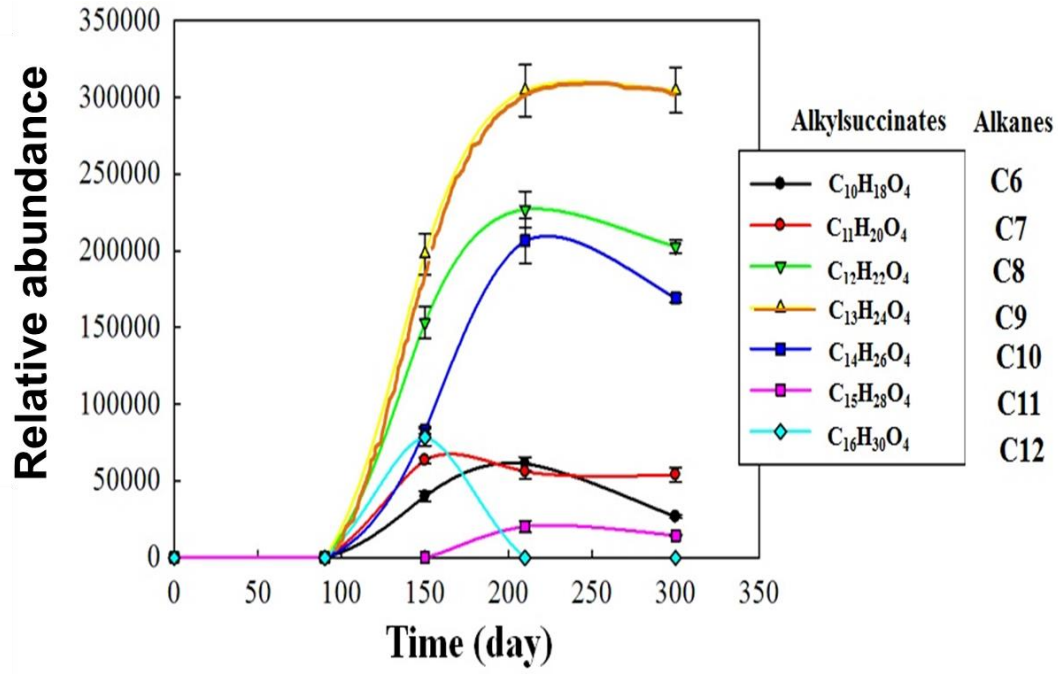

Figure S7 Kinetics of alkylsuccinates production and consumption in GoM incubations: seawater+petroleum-F76 +*D. alkanexedens* strain ALDC^T + C_6-C_{12} *n*-alkanes. Legends correspond to each type of alkylsuccinate (shown as molecular formula) derived from C_6-C_{12} *n*-alkanes as indicated on the right.

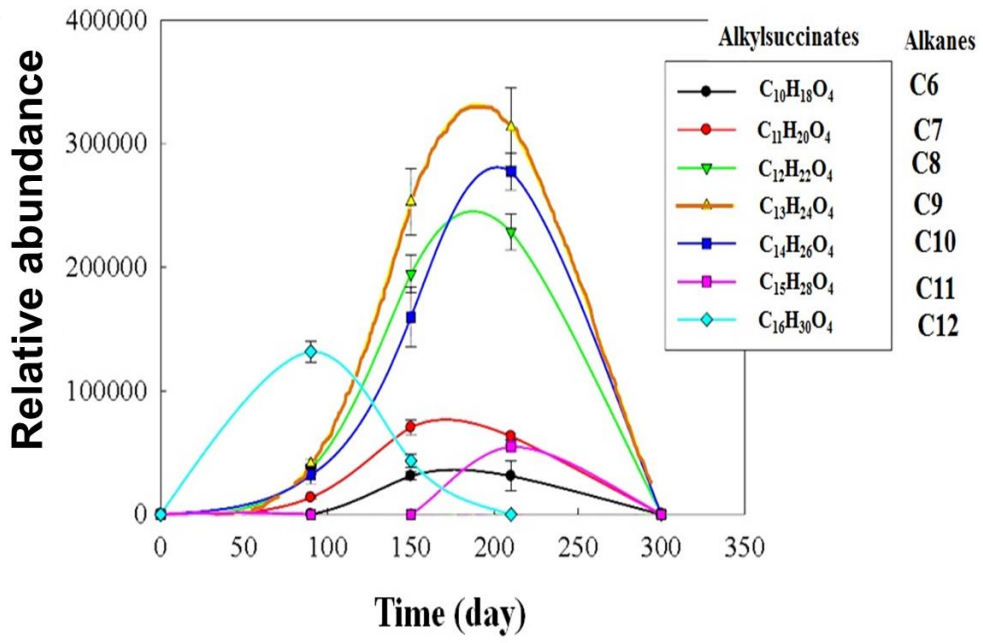

Figure S8 Kinetics of alkylsuccinates production and consumption in GoM incubations: seawater+petroleum-&camelina-JP5+*D. alkanexedens* strain ALDC^T + C_6-C_{12} *n*-alkanes. Legends correspond to each type of alkylsuccinate (shown as molecular formula) derived from C_6-C_{12} *n*-alkanes as indicated on the right.

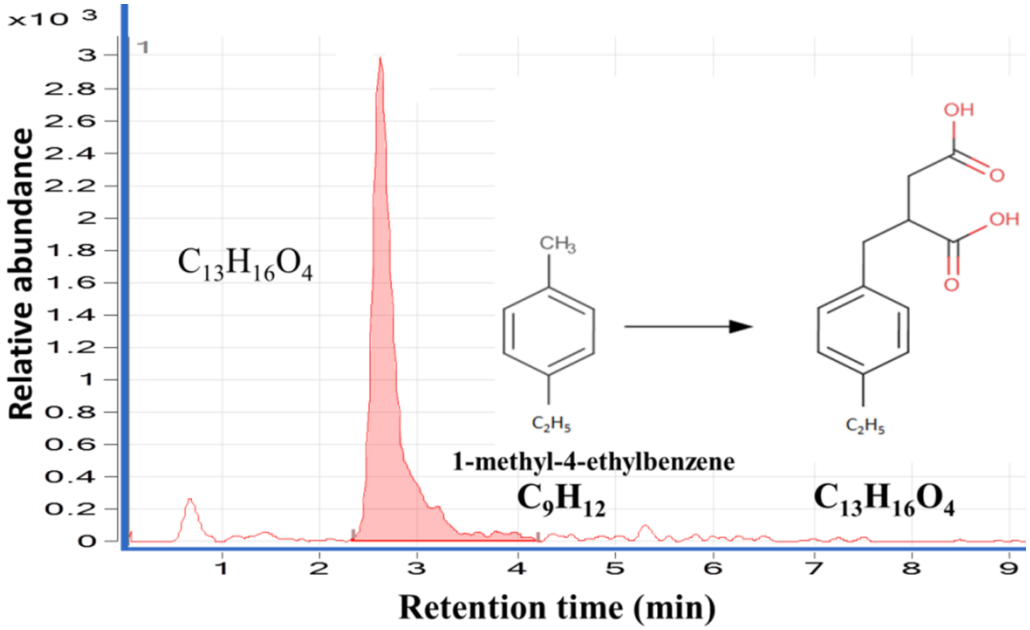

Figure S9 Extracted chromatography profile of an alkylbenzylsuccinate ($C_{13}H_{16}O_4$) in SDB incubations amended with camelina-JP5. The inserted chemical reaction represents an example that 1-methyl-4-ethylbenzene is activated via fumarate addition on the methyl group. The identified peak might represent any of the isomers of alkylbenzylsuccinate ($C_{13}H_{16}O_4$).

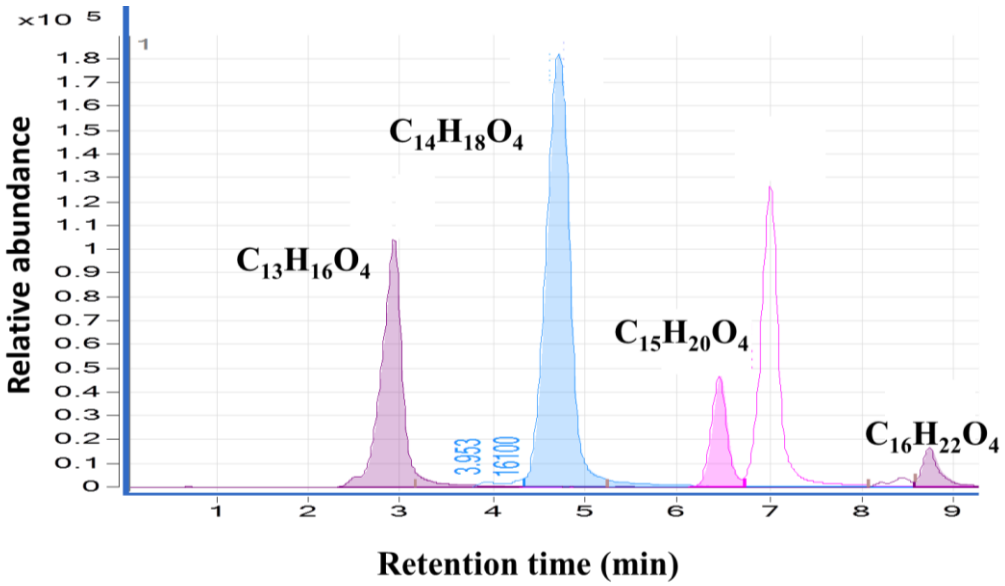

Figure S10 Extracted chromatography profile of alkylbenzylsuccinates ($C_{13}H_{16}O_4$-$C_{16}H_{22}O_4$) in SDB incubations amended with petroleum-JP5.

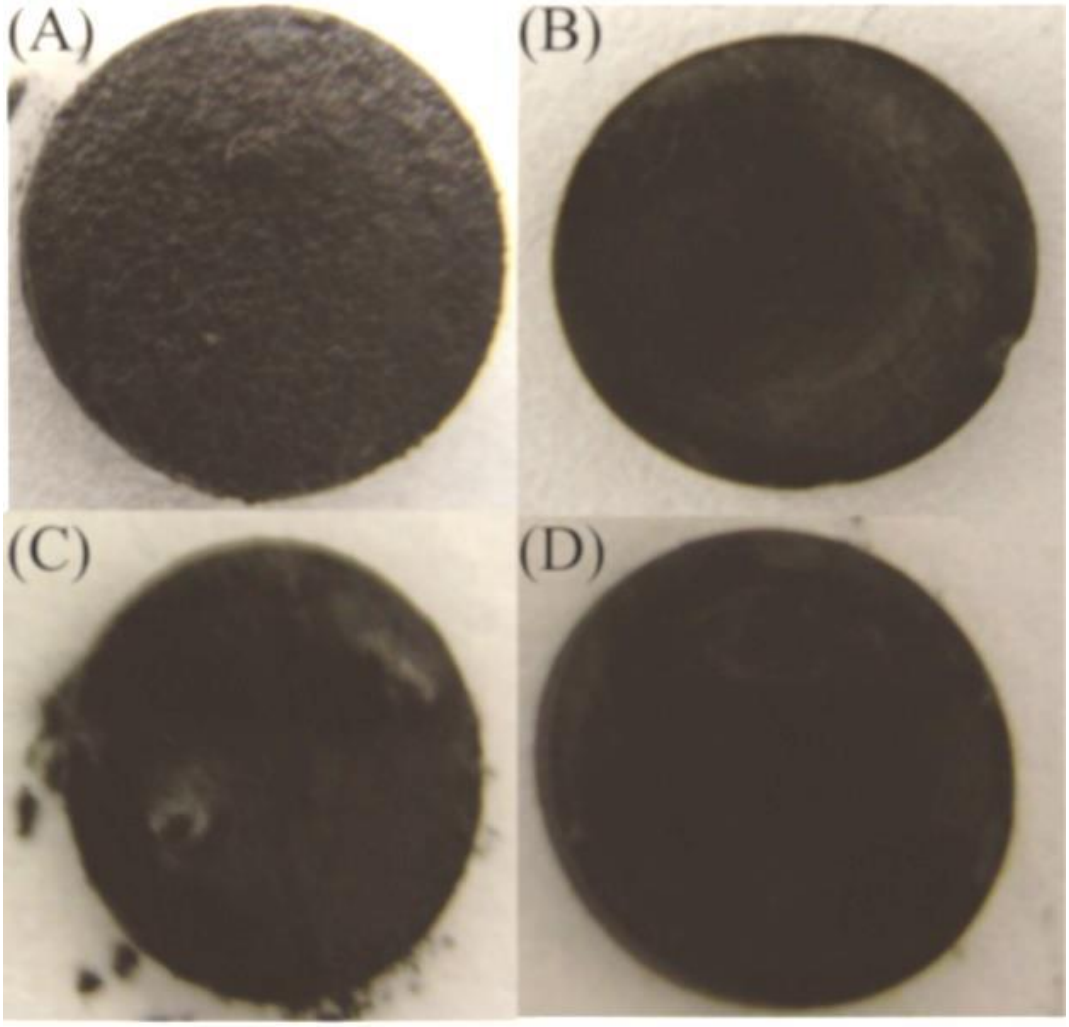

Figure S11 Images of corroded carbon steel coupons exposed to KW incubations after 240 days. A, KW seawater+ petroleum-JP5 *D. alkanexedens* strain ALDC^{T} + C_6-C_{12} *n*-alkanes; (B) Corresponding sterile control amended with petroleum-JP5; (C) KW seawater+ camelina-JP5 +*D. alkanexedens* strain ALDC^{T} + C_6-C_{12} *n*-alkanes; (D) Corresponding sterile control amended with camelina-JP5.

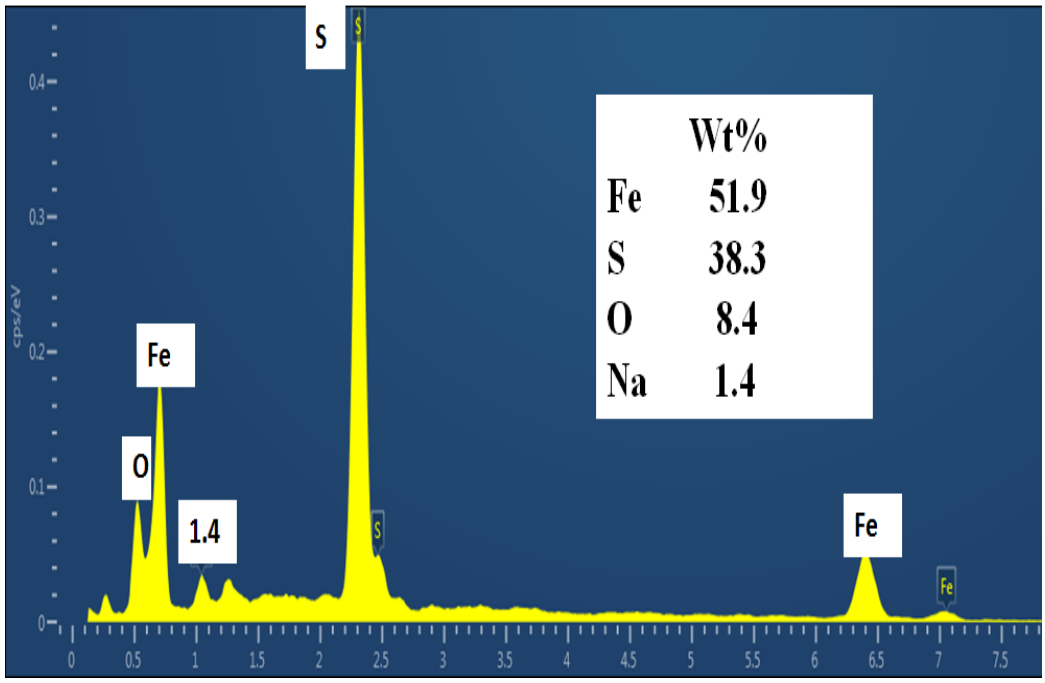

Figure 12 Elemental analysis of corrosion products deposited on carbon-steel coupons with coupled Energy dispersive spectroscopy (EDS). An example from KW incubations: KW seawater+ camelina-JP5 *D. alkanexedens* strain ALDC^{T} + C_6-C_{12} *n*-alkanes.

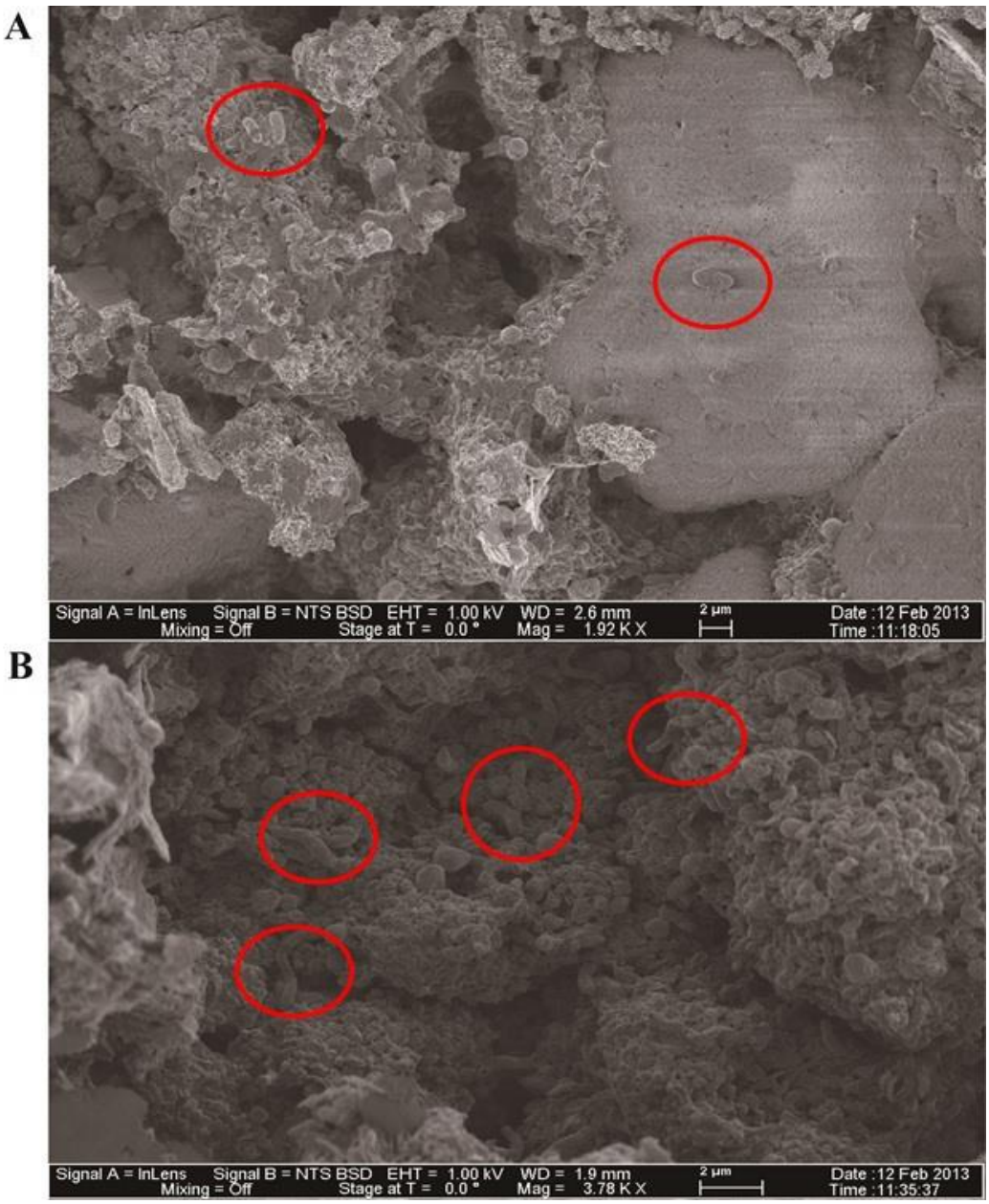

Figure S13 Biofilm characterization on corroded carbon-steel coupons exposed in KW incubations. A, KW seawater +petroleum-JP5+ C_6-C_{12} *n*-alkanes + *D. alkanexedens* strain ALDC^T; B, KW seawater+camelina-JP5+ *D. alkanexedens* strain ALDC^T + C_6-C_{12} *n*-alkanes. Red cycles indicate the regions where cells are embedded into the corrosion products. Note: images were captured after peeling off the top surface of corrosion products. Scale bars: 2 µm.

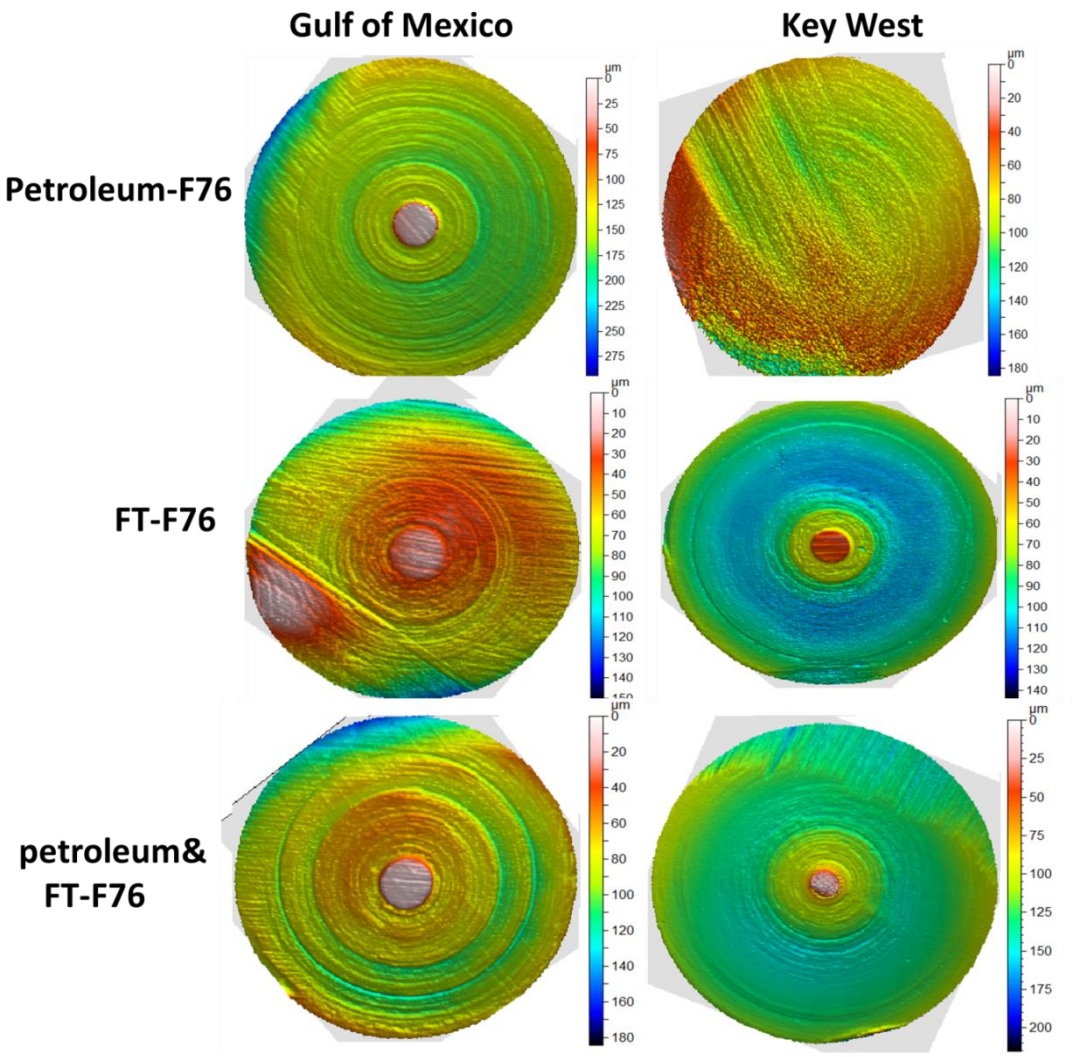

Figure S14 Profilometry profiles of carbons-steel coupons exposed to GoM and KW incubations when only seawater and fuels (amended with petroleum-F76, FT-F76 and their blend) were present. The false colors on the scale corresponding to the points of different depth (in µm, blue indicates deep points whereas red or yellow represent much shallower points) collected through the whole metal surfaces. No obvious pitting corrosion was observed in any of incubations regardless of the fuel type.

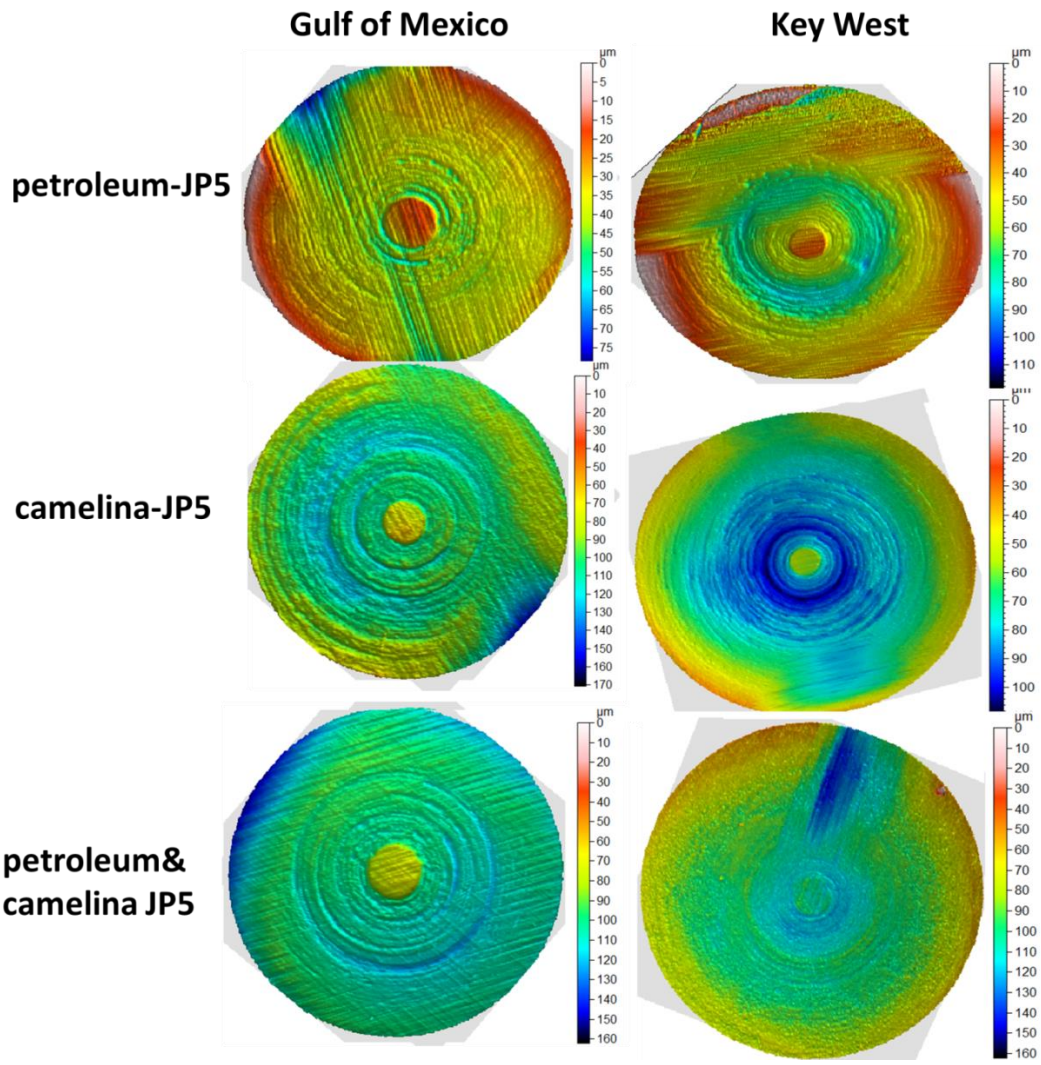

Figure S15 Profilometry profiles of carbons-steel coupons exposed to GoM and KW incubations when only seawater and fuels (amended with petroleum-JP5, camelina-JP5 and their blend) were present. The false colors on the scale corresponding to the points of different depth (in µm, blue indicates deep points whereas red or yellow represent much shallower points) collected through the whole metal surfaces. No obvious pitting corrosion was observed in any of incubations regardless of the fuel type.

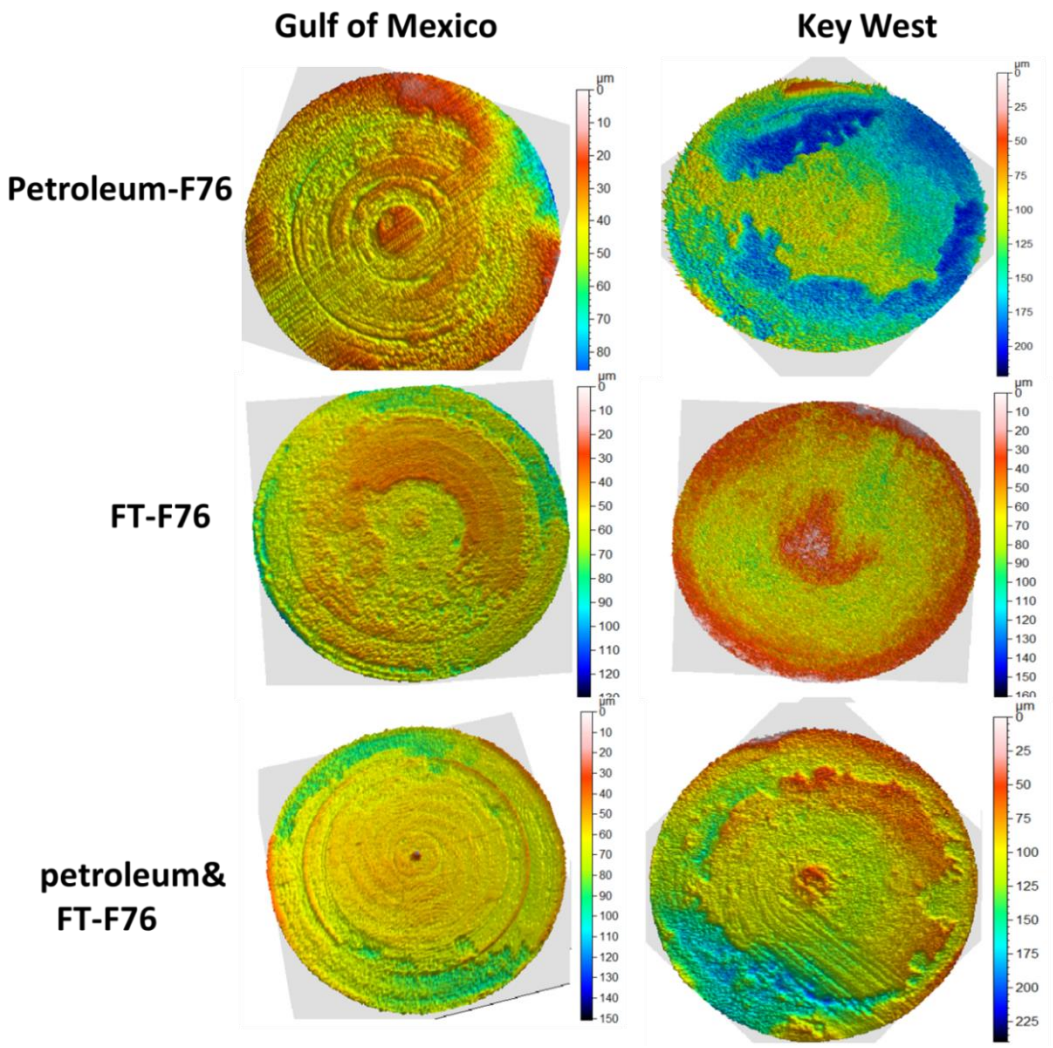

Figure S16 Profilometry profiles of carbons-steel coupons exposed to GoM and KW incubations when only seawater, *D. alkanexedens* strain ALDC^T and fuels (amended with petroleum-F76, FT-F76 and their blend) were present. The false colors on the scale corresponding to the points of different depth (in μm, blue indicates deep points whereas red or yellow represent much shallower points) collected through the whole metal surfaces. Moderate pitting corrosion was observed in both GoM and KW incubations regardless of the fuel type.

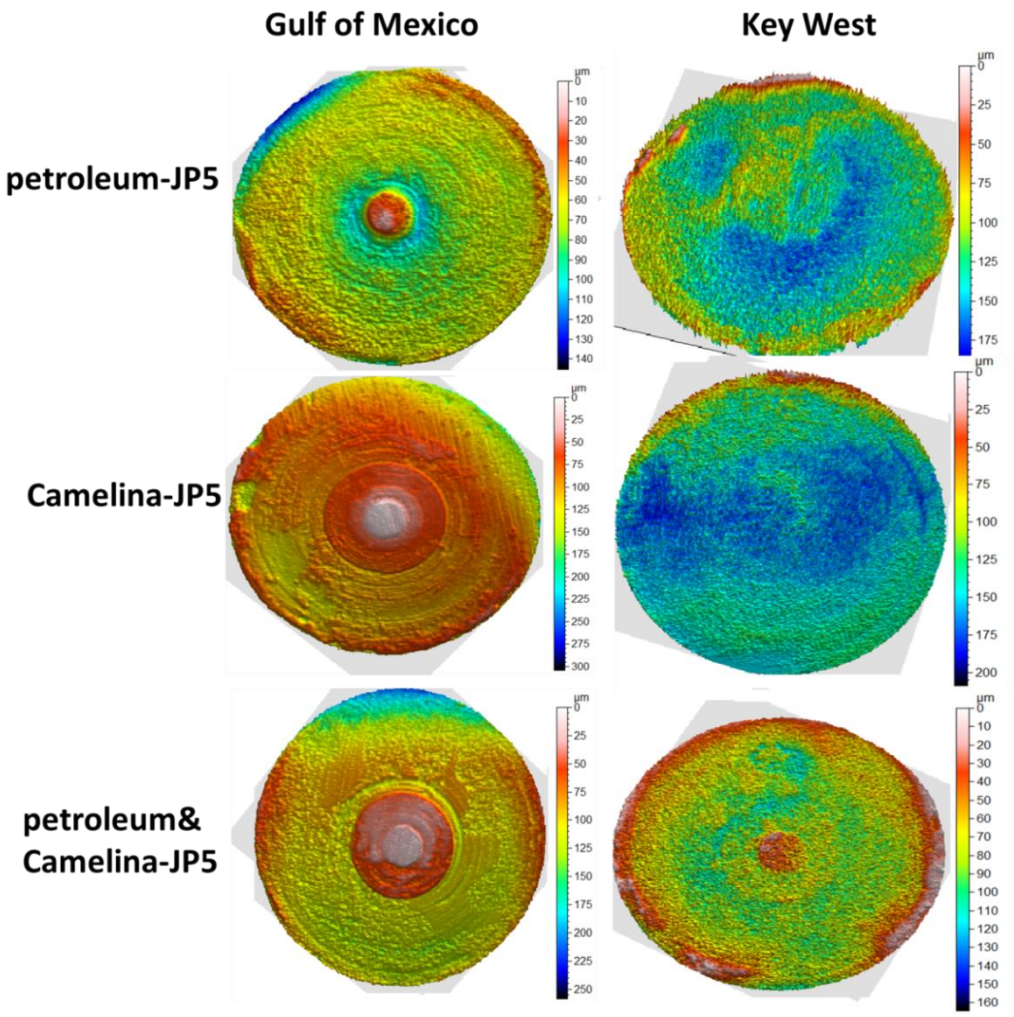

Figure S17 Profilometry profiles of carbons-steel coupons exposed to GoM and KW incubations when only seawater, *D. alkanexedens* strain ALDC^{T} and fuels (amended with petroleum-JP5, camelina-JP5 and their blend) were present. The false colors on the scale corresponding to the points of different depth (in µm, blue indicates deep points whereas red or yellow represent much shallower points) collected through the whole metal surfaces. Pitting corrosion in GoM was less pronounced in KW incubations regardless of the fuel type.

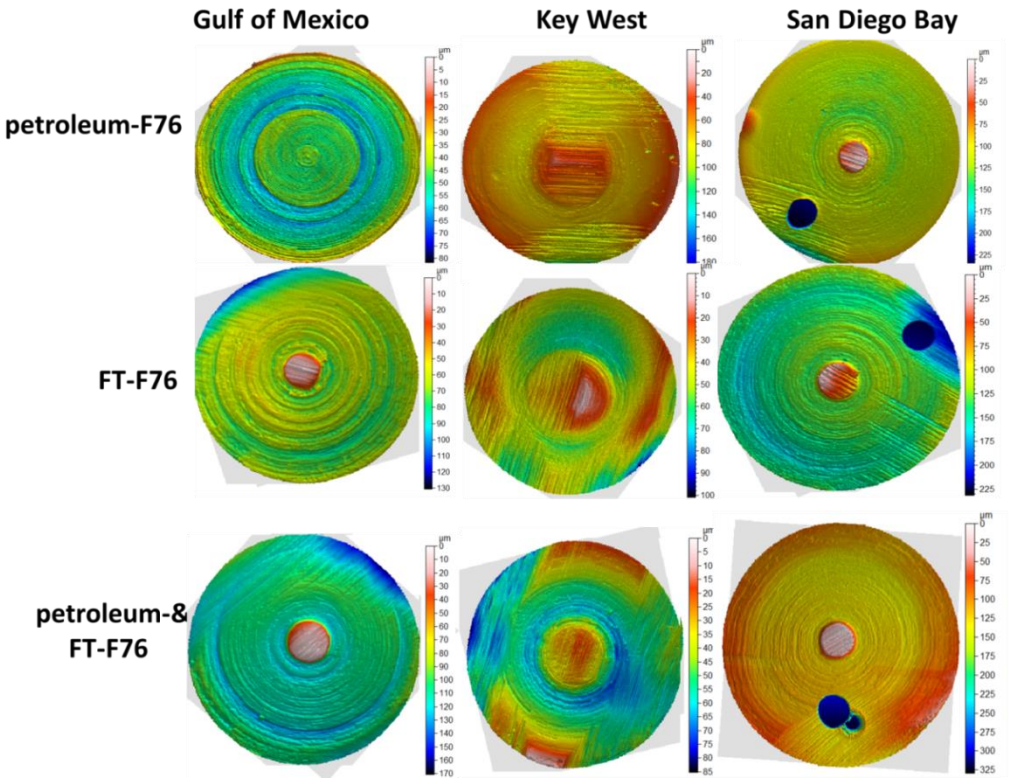

Figure S18 Profilometry profiles of carbons-steel coupons exposed to sterile GoM, KW and SDB incubations amended with petroleum-F76, FT-F76 and their blend. KW and GoM incubations: sterile seawater+fuel+ sterile *D. alkanexedens* strain ALDC^{T} + C_6-C_{12} *n*-alkanes; SDB incubations: sterile seawater+ sterile sediment+fuel. The false colors on the scale corresponding to the points of different depth (in μm, blue indicates deep points whereas red or yellow represent much shallower points) collected through the whole metal surfaces. No obvious pitting corrosion was observed in any of the three seawater incubations regardless of the fuel type.

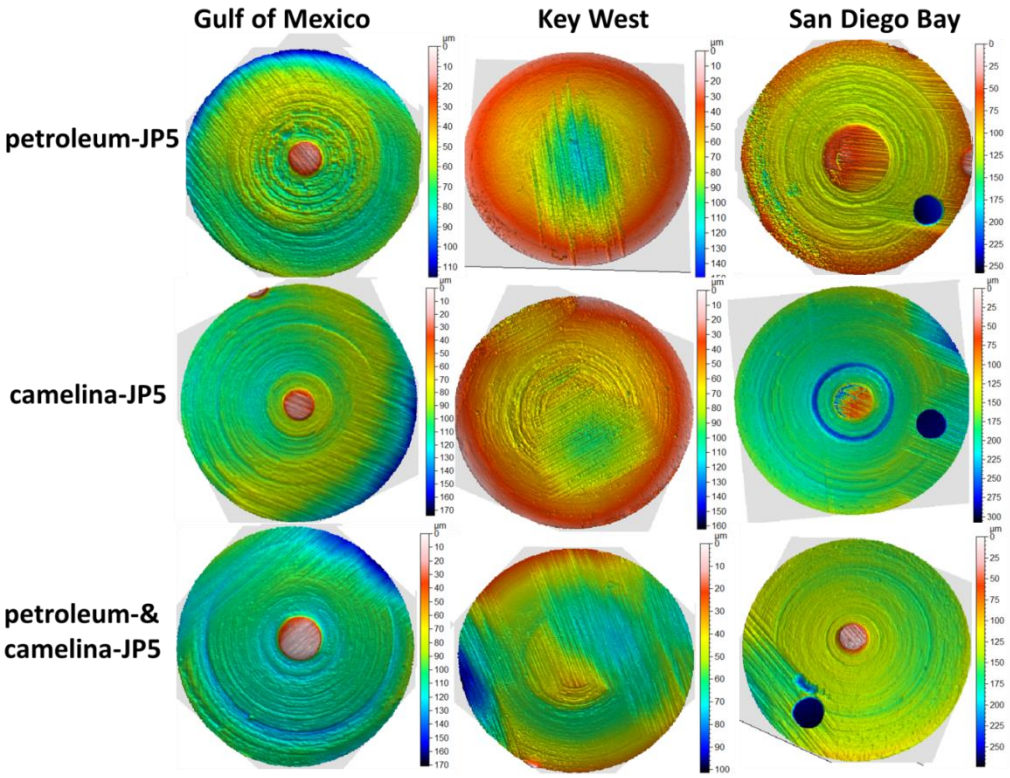

Figure S19 Profilometry profiles of carbons-steel coupons exposed to sterile GoM, KW and SDB incubations amended with petroleum-JP5, camelina -P5 and their blend. KW and GoM incubations: sterile seawater+fuel+ sterile *D. alkanexedens* strain ALDC^{T} +C6-C12 alkanes; SDB incubations: sterile seawater+sediment+fuel. The false colors on the scale corresponding to the points of different depth (in µm, blue indicates deep points whereas red or yellow represent much shallower points) collected through the whole metal surfaces. No obvious pitting corrosion was observed in any of the three seawater incubations regardless of the fuel type.

Chapter 4: Assessing the biological stability of a terpene-based advanced biofuel and its relationship to the corrosion of carbon steel

Abstract

Energy dense terpene biofuels have recently been recognized as renewable alternatives for high energy densiy petroleum-derived fuels. While the physicochemical properties of terpene dimer fuel (TDF) have been well documented, the propensity of these mixtures to undergo biodegradation and exacerbate the corrosion of the fuel infrastructure remains unknown. Coastal seawater/sediment incubations were amended with TDF or a blend of petroleum-derived hydrocarbons and incubated under strict anaerobic conditions. In some incubations, a model hydrocarbon-degrading sulfate reducing bacterium (*Desulfoglaeba alkanexedens,* strain ALDC^T) was inoculated as a positive control. No increase in sulfate reduction or corrosion was observed in long-term experiments (300 d) relative to TDF-free controls when only seawater/sediment served as the inoculum. However, inoculation with the positive control organism and a mixture of C_6-C_{12} *n*-alkanes increased both the sulfate reduction rate (95.2 ±5.2 μM/day) and general corrosion as determined by both coupon weight loss (27.9 ± 1.6 mg) and the number of pits (495 ± 62). The ratio of Mn/weight loss (0.34) in incubations exhibiting coupon pitting was lower than those (0.53-0.68) showing only generalized corrosion. Despite no indication for TDF biodegradation under all test conditions, the detection of a suite of alkylsuccinate metabolites attested to the anaerobic metabolism of the suite of *n*-alkanes when strain ALDC^T and the hydrocarbons served as amendments. These findings suggest that TDF is resistant to biodegradation and will not exacerbate the corrosion of carbon steel. If used in

combination with petroleum hydrocarbons the degree of metal corrosion would be that expected due to the presence of labile fuel components. However, the relatively recalcitrant nature of TDF might pose other risks if released to the environment and thus warrant further study.

Introduction

During the last few decades, sustainable production of advanced biofuels from a variety of renewable sources has attracted considerable attention due to depleting petroleum reserves[1], emissions of greenhouse gases[2] and long term energy security.[3] Although substantive progress has been made towards the production of first and second generation biofuels[4, 5], next generation biofuels that can replace petroleum-based military fuels remain a challenge. Military fuels must meet demanding specifications on energy content, viscosity, and density characteristics.[6, 7] Recent studies have demonstrated the successful synthesis of high-density biofuels through the selective dimerization of α-pinene, β-pinene, and camphene[6, 8], which can be produced from plants and even engineered microbes.[9, 10] Given the high gravimetric energy density and other superior characteristics, the terpene dimer fuels (TDF) represent promising surrogates for jet diesel and other tactical fuels.[6, 8, 11, 12]

Carbon steel is commonly used in components of the fueling infrastructure including ballast tanks, pipelines and storage tanks. It is well recognized that petroleum-based fuels are subjected to biodeterioration and thus lead to carbon steel corrosion.[13-16] Recently, a number of studies have shown that first generation biodiesels (mixtures of fatty acid methyl esters, FAME) were relatively rapidly biodegraded and exacerbated carbon steel biocorrosion.[17, 18] Furthermore, second-generation biofuels (defined here as

algae-derived F-76 and camelina-derived JP-5) were also found to be metabolized and stimulated corrosion under typical storage conditions with transient oxygen exposure.[19, 20] However, even though TDF is a promising high performance fuel, the susceptibility of this fuel to biodegradation and its propensity to accelerate carbon-steel corrosion processes remain unknown.

The precursors of TDF such as pinene, limonene and camphene are versatile compounds widely used in medical and cosmetic products.[21] Numerous studies have demonstrated that such monoterpene compounds can be degraded either aerobically or anaerobically by diverse microorganisms.[21-25] In contrast, the high-density TDFs are synthesized through selective dimerization of monomeric terpenes, that are then further hydrogenated before distillation.[6] It should be noted that unsaturated diterpenoids are naturally formed compounds that have been reported to be biodegradable under aerobic conditions.[26-28] Therefore, the biological stability of TDFs and its potential to accelerate corrosion should be critically evaluated before incorporating this fuel into the existing storage and transportation infrastructure.[29]

Typically, renewable biofuels are used as blends with petroleum-based fuels to ensure ideal compatibility and performance characteristics.[30, 31] For instance, the high viscosity of neat TDF precludes it from being used as a standalone high-density fuel.[7] To address this key drawback, a recent study demonstrated that blending terpene dimer fuels with conventional jet fuel (JP-8) could significantly reduce the low-temperature viscosity and while maintaining other required properties.[7] It should be noted that hydrocarbon components, like *n*-alkanes in petroleum-based fuels, can be subject to microbial metabolism under sulfate reducing conditions[32, 33] and hence cause

biocorrosion problems.[13, 34] In this regard, the impact of TDF on the biodegradation of common hydrocarbon components in conventional petroleum-derived fuels and its association with corrosion is also of importance.

Our findings suggest that TDF is relatively recalcitrant in marine environments under anaerobic conditions. There was also little discernable impact of TDF on the biodegradation of conventional hydrocarbons. While TDF might be potentially degraded by aerobic microorganisms, concerns over the environmental fate of TDF seem warranted due to its relative resistance to anaerobic biodegradation processes.

Experimental Section

Seawaters and Fuels. Three coastal seawaters from Key West (KW, Florida), Gulf of Mexico (GoM, Alabama) and San Diego Bay (SDB, California) were collected in 50 L carboys or 4 L Nalgene containers (Nalgene, Rochester, NY, USA) and shipped to the University of Oklahoma. In addition, SDB sediment was collected in 500 mL brown glass bottles that were filled to capacity with SDB seawater, and closed with screw cap lids. The seawater and sediment samples were stored at 4 ^{o}C prior to use. The terpene dimer fuel (TDF) was provided by the Naval Air Warfare Center, United States Navy, China Lake, California, USA. Figure S1 depicts the chemical structure of the particular TDF used in this study. In addition, an equimolar mixture of C_6-C_{12} *n*-alkanes (hexane, heptane, octane, nonane, decane, undecane and dodecane; Sigma-Aldrich, St. Louis, MO, USA) was prepared and blended with TDF to achieve a 50:50 (v/v) mixture for testing with conventional hydrocarbons.

Construction of Microcosms. The biodegradation and biocorrosion assays were conducted in accordance with a recently published protocol[35]. Seawater was flushed

with N_2 and reduced with Na_2S (0.0001%) in a sterile glass Schott bottle sealed with a closure to maintain anaerobic conditions. [35] The incubations were established in 120 ml serum bottles amended with seawater (40 ml) as inocula, the fuel combination of choice, and a preweighed carbon steel coupon. For SDB incubations, wet sediment (10 g) was also incorporated as an additional inoculum source to maximize the possibility of enriching TDF-degrading microorganisms. To assess the impact of TDF on the biodegradation of petroleum fuel components and associated corrosion, a 5 ml culture of *D. alkanexedens* strain ALDC^{T33} in stationary phase was inoculated into 35 ml seawater in KW incubations. The coupons were weighed and placed at the bottom of bottles for KW and GoM incubations. However, coupons were suspended in the aqueous phase with a PTFE coated quartz string when sediment was present in the SDB incubations. The TDF or TDF blend with alkanes (0.1 ml) was added aseptically by sterile syringe. Meanwhile, the TDF-unamended and sterile controls were also incorporated. The seawater and the *D. alkanexedens* strain ALDC^{T} cells were autoclaved for 20 min at 121 ^{o}C and 20 psi to serve as sterile controls. All the established mixtures were closed with a 1-cm-thick rubber stopper and incubated in the dark at room temperature (21±2 ^{o}C).

Corrosion Assay. The chemical composition of carbon steel (type 1018) used in this study is as follows (wt. %): 0.15–0.20% C, 0.6–0.9% Mn, 0.035% maximum S, 0.03% maximum P, and the remainder Fe. The carbon-steel coupons were fabricated with specifications as previously described.[36] The coupons were cleaned with deionized water and acetone according to the procedures published elsewhere.[36] To suspend the coupon, a PTFE string was used to tie the coupon and fixed with a needle partially

punctured through the stopper to avoid any gas leakage. Coupons at the conclusion of experiment were harvested and the corrosion products were removed with acid washing according to an ASTM standard G1-03 procedure.[37] The cleaned coupons were dried and stored under N_2 prior to analysis. The acid washing solutions were used for subsequent total Mn analysis. Individual coupons were weighed inside the anaerobic glove box to determine weight loss.

Analytic Techniques. Methylene blue method was employed to determine dissolved sulfide spectrophotometrically[38] at the onset and end of experiments. Sulfate consumption was monitored over time using ion chromatography (Dionex model IC-3000, 122 Sunnyvale, CA) as described previously[13] with the exception that the electrochemical suppressor was set at 27 mA. In addition, Manganese (Mn) dissolved from the metal surfaces was measured using atomic absorption spectrometer (Varian AA240FS/GTA120, Varian Inc., USA) at the conclusion of the experiment. The hollow cathode lamp for Mn was used and the wavelength was set at 279.5 nm. The calibrating standard (5-20 ppb) was prepared from commercial stock standard solutions of high-purity Mn and other metals. The samples were run in triplicate and the results represent the arithmeric average of the three determinations.

Profilometry. The topography of the cleaned metal coupons after exposure were scanned with a Nanovea non-contact optical profilometer PS50 (MicroPhotonics, Inc, Irvine, CA) with a 4 μm step size as described previously.[36] The acquired data was further analyzed with Ultra MountainsMap Topography XT6.2 software (MicroPhotonics, Inc, Irvine, CA). For the coupons exposed to KW and GoM incubations, pits were defined as having a vertical depth at 20 μm below the mean plane

and an equivalent diameter greater than 25 μm. Given the severity of pitting corrosion for SDB incubations, the criterion of 50 μm below the mean plane was used to define the pits and the number of pits with an equivalent diameter greater than 25 μm was counted.

Terpene Dimer Analysis and Metabolites Profiling. To assay for residual TDF, the entire content of the bottle was extracted three times with diethyl ether. The extracts were combined, dried over $MgSO_4$, and utilized directly for gas chromatography/mass spectrometry (GC/MS) analysis.[6] Gas chromatography was carried out on an Agilent 6890N GC using a Restek Rxi-5MS 20 m x 0.18 mm capillary column with a 0.18 μm coating of Crossbond 5% diphenyl / 95% dimethyl polysiloxane. The oven temperature was programmed from 40 to 100 °C at 5 °C/min and then 100 to 300 °C at 20 °C/min.

To identify the potential metabolites generated from the consumption of parent substrates, approximately 20 ml aqueous samples were withdrawn for extraction. The samples were acidified ($pH \leq 2$) with 6 N HCl and extracted three times with equal volume of ethyl acetate as described previously.[18] The pooled extracts were concentrated and derivatized for further analysis. The conditions for running GC/MS were the same as described previously.[18]

Results

Sulfate Reduction with Seawater/Sediment. The initial sulfate concentration in KW and SDB incubations was between 28-30 mM, whereas the GoM seawater contained only about 10 mM sulfate (Figure 1). After 300 days of incubation, the TDF-amended incubations from KW and GoM with seawater as inocula and medium showed marginal sulfate reduction (Figure 1), which was equivalent to the TDF-free incubation but

slightly higher than the sterile negative controls (Figure 1). By contrast, significant sulfate reduction rate (38.7 ±2.6 μM/day) was observed in the SDB incubations (Figure 1) when additional sediment was present. However, the TDF-unamended control also showed a comparable sulfate reduction rate (44.5 ±4.4 μM/day). No significant sulfate reduction was observed in the sterile controls in all three seawater incubations.

The highest sulfate reduction rate (95.2 ±5.2 μM/day) was observed when *D. alkanexedens* strain ALDC^T and a mixture of C_6-C_{12} *n*-alkanes were added to the incubation (Figure 4 A). The concomitant sulfide production (12.5±0.4 mM) was also detected in the aqueous phase but not in the TDF-free or sterile controls (Figure S2). It should be noted that the aqueous phase sulfide levels was less than that expected based on the theoretical stoichiometry most probably due to the precipitation of iron sulfide minerals and the escape of hydrogen sulfide to the headspace.

Terpene Dimer Analysis and Metabolites Profiling. The gas chromatographic profiles of TDF-amended incubations with KW and SDB seawaters were compared to the corresponding sterile controls after 300 days exposure. The gas chromatographic profile of neat TDF exhibited a complex mixture of peaks (Figure S3&S4) due to the presence of a number of different isomers and other minor compounds present in the synthetic fuel. No substantive disappearance of the peaks was observed in the final analysis of the seawaters in the incubations relative to the gas chromatographic profiles of the neat TDF (Figure S3&S4). In addition, the gas chromatographic profile of TDF in the non-sterile seawater incubations were nearly the same as the sterile controls (Figure S3&S4), indicating no substantive degradation of TDF after prolonged incubation, even when seawater/sediment served as the inoculum of interest.

Although significant sulfate reduction was evidenced with addition of *D. alkanexedens* strain ALDC^T and the low molecular weight *n*-alkane amendment, the gas chromatographic profiles of TDF also showed no difference relative to the sterile control (Figure 2A). However, a series of new peaks (absent in the sterile control) were detected when metabolites from the aqueous phase were profiled by GC/MS (Figure 2B). These new peaks were identified as alkylsuccinic acid metabolites derived from the C_6-C_{12} n-alkane amendment (Figure 2B). The detection of these intermediates confirmed anaerobic metabolism of parent substrates via a fumarate-addition mechanism known to be catalyzed by *D. alkanexedens*[39]. Meanwhile, only decylsuccinates (in much lower abundance) were detected in the sterile control (Figure 2B) that reflected carryover during the inoculum transfer. Unfortunately, no additional peaks pertaining to the potential metabolic products of TDF biodegradation could be detected in the TDF-amended incubations despite the highest sulfate reduction rate (95.2 ±5.2 μM/day).

Weight Loss and Pitting Corrosion under Different Conditions. For all the incubations with KW, GoM and SDB seawaters, the corrosion determined by weight loss was not significantly different (p value=0.088) between the TDF-amended and TDF-unamended incubations (Figure 3A). However, the weight loss in the non-sterile incubations was 1.5 to 4.2 times more than the corresponding sterile controls (Figure 3A). Notably, the corrosion in SDB incubations (84.5±7.9 mg) was much higher than the KW (8.5±0.5 mg) or GoM (23.7±1.5 mg) incubations probably due to the relatively high background rate of sulfate reduction (Figure 1). In addition, no obvious pitting corrosion was caused on the metal coupons for the KW (Figure S5) and GoM

incubations (Figure S6), which was similar to the TDF-unamended and sterile controls (Figure 3B). By contrast, severe pitting corrosion was caused on the metal surfaces (Figure S7) in SDB incubations. However, the TDF-unamended control also demonstrated the same degree of localized corrosion due to the high indigenous sulfate reduction rate (Figure 3B&S7).

In the KW incubations with addition of *D. alkanexedens* strain ALDC^T and alkanes, the weight loss increased markedly relative to the TDF-unamended and sterile controls (Figure 4B). Correspondingly, pitting corrosion was more pronounced than the sterile control with no sulfate reduction. It can be clearly seen that the milling grooves pattern in the sterile control (Figure 5B) remains intact after exposure whereas obvious localized corrosion (reduction in the appearance of the milling grooves) can be observed in the non-sterile incubations (Figure 5A). Specifically, the number of pits (475) was much higher than the TDF-unamended (61) and sterile controls (72) after 300 days incubation (Figure 4B). These results suggested that the biogenic sulfide production (Figure S2) at the expense of C_6-C_{12} *n*-alkanes contributed to the elevated corrosion in the presence of TDF.

Dissolved Manganese (Mn) and Corrosion. Mn in the original KW seawater was below detection level (5 ppb) as determined by atomic absorption spectrometry. However, significant amounts of Mn (1104±117 to 1772±332 ppb) were released from the metal coupons (Figure 6) after the 300 d incubation. Maximum Mn (1772±332 ppb) dissolution was noted in incubations that received the addition of *D. alkanexedens* and the *n*-alkane mixture (Figure 6). This is the same incubation that also exhibited the highest weight loss (27.9 ±1.6 mg, Figure 4B). Interestingly, the ratio of Mn/weight

loss (0.53%-0.67%) was close to the Mn content (0.6%-0.9%) in the matrix of the carbon steel when no obvious pitting was observed (Figure 6&S5). However, the ratio of Mn/weight loss decreased to 0.34% when pronounced pitting corrosion was observed (Figure 5&6). We suggest that the lower Mn/weight loss ratio might be indicative of the severity of pitting corrosion.

Discussion

Concerns about the stability and compatibility of emerging alternative fuels with the existing infrastructure are of importance due to the dual potential risks associated with fuel biodeterioration and metal biocorrosion.[13, 18] Several studies have shown that first-generation biodiesels are not good choices as fuels for military tactical vehicles since the fatty acid methyl esters are not stable, may undergo relatively rapid biodegradation and tend to exacerbate the corrosion of the carbon steel infrastructure.[17, 18] Moreover, recent studies also suggest that second generation naval biofuels, such as algae F-76 and camelina JP-5[19], were susceptible to biodegradation and stimulated corrosion under transient oxygen conditions.[19, 20] Although improvements in second-generation biofuels are under consideration, parallel efforts toward the development of next-generation terpene dimer fuels (TDF) have been made. The TDF are considered promising alternatives for high-density petroleum-derived military fuels.[6, 8] We assessed the biological stability of TDF and its potential impact on corrosion of carbon steel.

To mimic the environments where the next generation fuel might potentially be used, TDF was exposed to seawaters collected from locations near US Navy bases in Key West (KW), the Gulf of Mexico (GoM) and San Diego Bay (SDB). Typically, the abundance of sulfate reducing bacteria (SRB) is low or even below detection limits in

coastal seawaters.[17, 20] Moreover, the pristine, oxygenated seawaters were oligotrophic with low levels of dissolved organic matter.[19] Therefore, it is not surprising that only marginal sulfate reduction (Figure 1) was observed with and without addition of TDF after 300 d of incubation in KW and GoM incubations. In consistent fashion, the amendment of TDF caused only negligible coupon weight loss and pitting corrosion during the course of the incubation. These findings suggest that TDF is not a suitable source of electron donors to support anaerobic microbial sulfate respiration and sulfide formation. Thus, increases in biocorrosion of carbon steel were negligible and can essentially be ignored when only pristine coastal seawater is used as an inoculum source.

However, marine sediments typically harbor much greater numbers of SRB relative to overlying seawaters.[40, 41] When both sediment and seawater from SDB served as the inoculum source, the level of sulfate decreased at a rate of 38.7 ±2.6 μM/day (Figure 1). A similar trend in sulfate loss was also evidenced in TDF-free controls (44.5 ±4.4 μM/day). Of course, the comparable sulfate reduction rate cannot rule out the possibility that TDF might be decomposed by anaerobic microflora in the marine incubation. The increased sulfate reduction rate relative to the other samples can reasonably be ascribed to the larger amount of readily decomposable organic matter in the sediment[42], that was likely preferentially utilized (relative to TDF) as a source of electron donors for anaerobic heterotrophic respiration. Given the highest sulfate reduction rate in the SDB incubations (Figure 1), the weight loss of the coupon was 3.5-10 times larger than the comparable measure in the KW and GOM incubations (Figure 3). Moreover, pronounced pitting corrosion was detected on the metal surfaces (Figure S7) irrespective of the presence of TDF. Presumably, the biogenic sulfide production

contributed to the elevated weight loss and localized corrosion.[17, 34] These results also suggest that TDF itself did not inhibit sulfate reduction and corrosion if other labile forms of organic carbon were available in the incubations.

It should be noted that TDF is not qualified as a standalone fuel due to its high viscosity, but it can be blended with conventional petroleum-derived fuels to maintain desired physical properties.[7] Hence, the mixture of TDF and representative fuel components (e.g. the C_6-C_{12} *n*-alkane mixture) was also assessed with and without the addition of a known hydrocarbon-degrading sulfate reducing bacterium[33] in KW seawater incubations. The most sulfate was reduced (Figure 4A) when an alkane mixture was added, suggesting no substantive inhibitory effect on sulfate reduction by TDF. The presumption that the *n*-alkanes were indeed metabolized is bolstered by the detection of a suite of alkylsuccinate metabolites (Figure 2B) only in the *n*-alkane-amended incubations. These are exactly the metabolic intermediates that would be expected based on the known metabolic capabilities of *D. alkanexedens*.[39] Thus, we presume that the positive control organism was responsible for the observed biodegradation, but we cannot exclude the prospect that we might have also enriched for an *n*-alkane-utilizing microbe that was indigenous to seawater that employed the same or even other mechanisms for hydrocarbon metabolism linked to sulfate reduction[43, 44]. Most importantly, the coupon weight loss and pitting corrosion correlated well with the degree of sulfate reduction (Figure 4, 5). These results suggested that fuel constituents (e.g. *n*-alkanes) can be metabolized by SRB in the presence of TDF and contribute substantively to biogenic sulfide-induced corrosion of carbon-steel.

Given the high sulfate reduction rate in SDB incubations containing sediment (Figure 1) and KW incubations amended with *D. alkanexedens* strain ALDC^{T} (Figure 4), it can be reasonably speculated that TDF might be decomposed after 300 days. However, further GC/MS analysis revealed no indication of TDF metabolism under any of the testing conditions. No disappearance of parent substrates (Figure 2A, S3&4) or generation of metabolic intermediates was observed. Although the precursors of TDF have been demonstrated to be readily biodegradable[21, 24, 45], the recalcitrance of TDF is not surprising because the hydrogenation and dimerization processes considerably altered the chemical structure (Figure S1) compared to the unsaturated monoterpene compounds.[6, 8] While cycloalkanes such as cyclohexane can be biodegraded by SRB in marine sediments[46], steric hinderance of the requisite enzymes caused by branching and substrate dimerization (Figure S1) may preclude TDF from being metabolized by SRBs in seawater. However, aerobic microorganisms in marine and other environments might be capable of converting TDF to diterpenoids, which are naturally-occurring organic compounds and presumably more amenable to biodegradation.[27] In addition, none of the pristine seawaters were previously exposed to TDF, which could also decrease the probability of enriching TDF-degrading bacteria under laboratory conditions even with a long period of time (300 days). Regardless of the factors impeding the biodegradation, it should be pointed out that the recalcitrance of TDF might pose potential risks to the environments impacted by a spill of TDF. Although the toxicity of TDF is unknown, monomeric terpene compounds have been demonstrated to exert toxic effects against different organisms.[47-50] In this regard, the toxicity of TDF and its potential to impact the environmental ecosystems should be further investigated.

While more work is needed on the biological stability and toxicity of TDF, the measurement of released manganese (Mn) from metal surfaces and its correlation to pitting corrosion shed light on the mechanism of pit initiation and propagation in the TDF-laden systems. Typically, the combinations of elements vary in different types of carbon steel alloys to meet specific demanding properties. Among these elements, the added Mn can form manganese sulfide (MnS) inclusions to scavenge undesirable free sulfur in steel[51]. However, the MnS inclusions can provide sites for pits initiation and thus decreased corrosion resistance of steels.[51-53] Although measurement of Mn has been previously proposed to monitor corrosion rates in the field [54], the correlation between Mn dissolution from metal surfaces and pitting corrosion has not been fully understood. Not surprisingly, we found that the dissolved Mn from metal surfaces considerably increased after 300 days (Figure 6) probably due to the dissolution of MnS inclusions in the process of carbon steel corrosion.

It is interesting to note that the ratio of Mn/weight loss (0.53% and 0.67 %) was close to the Mn content (0.6%-0.9%) in the original matrix of steel when no obvious pitting corrosion was observed (Figure 6&S5). The comparable ratio of Mn/weight loss suggested that Mn and Fe dissolved at a similar rate from the metal surfaces when generalized corrosion was largely responsible for the weight loss. While elevated Mn was dissolved in incubations exhibiting more weight loss (Figure 6), the ratio of Mn/weight loss decreased to 0.34% when pronounced pitting corrosion was observed (Figure 5&6). The elevated Mn released from carbon steel provided evidence that the dissolution of MnS inclusions might be important in the early stage of pitting initiation.[51, 52] However, the lower ratio of Mn/weight loss implied that only certain

MnS inclusions eventually developed into macroscopic pits. The differential susceptibility to pitting propagation substantiated the theory that not all MnS inclusions are equally created and thus can be classified as active and inactive inclusions.[51, 53] Presumably, the biogenic sulfide production might facilitate the development of corroding microenvironments adjacent to the active MnS inclusions. The dissolution of immediate surroundings of the active MnS inclusions gradually enlarged and deepened the initiated pits to macroscopic scale. Apparently, more unknown factors are dictating the growth of pits and they should be sought in subsequent investigations. Despite the infeasibility of measuring total released Mn in the field due to precipitation, the low ratio of Mn/weight loss might be used as an additional indicator for evaluating pitting corrosion under controlled conditions.

Our findings suggest that TDF tends to be stable and resist biodegradation in anaerobic marine environments. The recalcitrance nature of TDF makes it unlikely to accelerate or inhibit baseline rates of sulfate reduction, sulfide formation and metal biocorrosion activity within the fuel infrastructure. However, the failure to observe any metabolic fate for TDF, even after prolonged incubation times, deserves at least a cautionary note. Like many other recalcitrant hydrophobic organic compounds, there may be unintended risks and consequences should this material get accidentally released to the environment. Therefore, it seems prudent to avoid contact of TDF with marine environmental compartments where anaerobic conditions may prevail. The possibility remains that TDF might be biodegraded by aerobic microorganisms and thus the environmental fate of this material in the presence of oxygen should be further explored if it is eventually used as a next generation biofuel.

Acknowledgements

The efforts of Joseph M. Suflita and Renxing Liang were financially supported by a grant (Award N000141010946) from the Office of Naval Research. Benjamin G. Harvey and Roxanne L. Quintana were supported from Office of Naval Research (ONR) Contract 000141-0W-X2-1-013 and NAWCWD. The authors appreciate the help from Dr. Mark A. Nanny, Dr. Robert W. Nairn, and Shuo Li for atomic absorption spectroscopy analysis. The authors also thank Frank P. Harvey, Christopher R. Marks, and Brian H. Harriman for collecting the seawater and sediment samples.

References

(1) Sharma, Y.; Singh, B.; Upadhyay, S. *Fuel* **2008,** 87, 2355-2373.

(2) Plevin, R. J.; Jones, A. D.; Torn, M. S.; Gibbs, H. K. *Environ. Sci. Technol.* **2010,** 44, 8015-8021.

(3) Bang, G. *Energy Policy.* **2010,** 38,1645-1653.

(4) Berndes, G.; Hansson, J.; Egeskog, A.; Johnsson, F. *Biomass and Bioenergy* **2010,** 34, 227-236.

(5) Harvey, B. G.; Meylemans, H. A.; Gough, R. V.; Quintana, R. L.; Garrison, M. D.; Bruno, T. J. *Phys. Chem. Chem. Phys.* **2014,** 16, 9448-9457.

(6) Harvey, B. G.; Wright, M. E.; Quintana, R. L. *Energy Fuels* **2010,** 24, 267-273.

(7) Meylemans, H. A.; Baldwin, L. C.; Harvey, B. G. *Energy Fuels* **2013,** 27, 883-888.

(8) Meylemans, H. A.; Quintana, R. L.; Harvey, B. G. *Fuel* **2012,** 97, 560-568.

(9) Zhang, F.; Rodriguez, S.; Keasling, J. D. *Curr. Opin. Biotechnol.* **2011,** 22, 775-783.

(10) Sarria, S.; Wong, B.; Martín, H. G.; Keasling, J. D.; Peralta-Yahya, P. *ACS Synth. Biol.* **2014,** 3, 466-475.

(11) Zhu, Y.; Li, S.; Davidson, D. F.; Hanson, R. K. *Proc. Combust. Inst.* **2015,** 35, 241-248.

(12) Harvey, B. G.; Merriman, W. W.; Koontz, T. A. *Energy Fuels* **2015**, 29, 2431−2436.

(13) Lyles, C. N.; Aktas, D. F.; Duncan, K. E.; Callaghan, A. V.; Stevenson, B. S.; Suflita, J. M. *Environ. Sci. Technol.***2013,** 47, 6052-6062.

(14) Suflita, J. M.; Aktas, D. F.; Oldham, A. L.; Perez-Ibarra, B. M.; Duncan, K. *Biofouling* **2012,** 28, 1003-1010.

(15) Rajasekar, A.; Babu, T. G.; Pandian, S. T. K.; Maruthamuthu, S.; Palaniswamy, N.; Rajendran, A. *J. Ind. Microbiol. Biotechnol.* **2007,** 34, 589-598.

(16) Muthukumar, N.; Mohanan, S.; Maruthamuthu, S.; Subramanian, P.; Palaniswamy, N.; Raghavan, M. *Electrochem. commun.* **2003,** 5, 421-425.

(17) Lee, J. S.; Ray, R. I.; Little, B. J.; Duncan, K. E.; Oldham, A. L.; Davidova, I. A.; Suflita, J. M. *Biofouling* **2012,** 28, 465-478.

(18) Aktas, D. F.; Lee, J. S.; Little, B. J.; Ray, R. I.; Davidova, I. A.; Lyles, C. N.; Suflita, J. M. *Energy Fuels* **2010,** 24, 2924-2928.

(19) Lee, J. S.; Ray, R. I.; Little, B. J.; Duncan, K. E.; Aktas, D. F.; Oldham, A. L.; Davidova, I. A.; Suflita, J. M. *Bioelectrochemistry* **2014,** 97, 145-153.

(20) Aktas, D. F.; Lee, J. S.; Little, B. J.; Duncan, K. E.; Perez-Ibarra, B. M.; Suflita, J. M. *Int. Biodeterior. Biodegr.* **2013,** 81, 114-126.

(21) Misra, G.; Pavlostathis, S.; Perdue, E.; Araujo, R. *Appl. Microbiol. Biotechnol.* **1996,** 45, 831-838.

(22) Yoo, S.; Day, D. *Process Biochem.* **2002,** 37, 739-745.

(23) Miller, M. J.; Allen, D. G. *Environ. Sci. Technol.* **2005,** 39, 5856-5863.

(24) Harder, J.; Probian, C. *Appl. Environ. Microbiol.* **1995,** 61, 3804-3808.

(25) Harder, J. Anaerobic degradation of isoprene-derived compounds. In *Handbook of Hydrocarbon and Lipid Microbiology*, Springer Berlin Heidelberg, 2010.

(26) Sun, H.-D.; Huang, S.-X.; Han, Q.-B. *Nat. Prod. Rep.* **2006,** 23, 673-698.

(27) Yu, Z.; Stewart, G. R.; Mohn, W. W. *Appl. Environ. Microbiol.* **2000,** 66, 5148-5154.

(28) Martin, V. J.; Mohn, W. W. *J. Bacteriol.* **2000,** 182, 3784-3793.

(29) Richard, T. L. *Science(Washington)* **2010,** 329, 793-796.

(30) Hamilton, L. J.; Williams, S. A.; Kamin, R. A.; Carr, M. A.; Caton, P. A.; Cowart, J. S. In *Renewable fuel performance in a legacy military diesel engine*, ASME Conference Proceedings 2011.

(31) Rodriguez, B.; Bartsch, T. M. In *The United States Air Force's process for alternative fuels certification*, 26th AIAA Applied Aerodynamics Conference, 2008.

(32) Caldwell, M. E.; Garrett, R. M.; Prince, R. C.; Suflita, J. M. *Environ. Sci. Technol.* **1998,** 32, 2191-2195.

(33) Davidova, I. A.; Duncan, K. E.; Choi, O. K.; Suflita, J. M. *Int. J. Syst. Evol. Microbiol.* **2006,** 56, 2737-2742.

(34) Lyles, C. N.; Le, H. M.; Beasley, W. H.; McInerney, M. J.; Suflita, J. M. *Front. Microbiol.* **2014,** 5.

(35) Liang, R.; Suflita, J. M. Protocol for Evaluating the Biological Stability of Fuel Formulations and their Relationship to Carbon Steel Biocorrosion. *Handbook of hydrocarbon and lipid microbiology*. Springer Berlin Heidelberg, **2015**.

(36) Liang, R.; Grizzle, R. S.; Duncan, K. E.; McInerney, M. J.; Suflita, J. M. *Front. Microbiol.* **2014,** 5.

(37) ASTM G1-03, A., Standard practice for preparing, cleaning, and evaluating corrosion test specimens. **2003**.

(38) Tanner, R. S. *J. Microbiol. Methods.* **1989,** 10, 83-90.

(39) Davidova, I. A.; Gieg, L. M.; Nanny, M.; Kropp, K. G.; Suflita, J. M. *Appl. Environ. Microbiol.* **2005,** 71, 8174-8182.

(40) Sahm, K.; MacGregor, B. J.; Jørgensen, B. B.; Stahl, D. A. *Environ. Microbiol.y* **1999,** 1, 65-74.

(41) Purdy, K.; Embley, T.; Nedwell, D. *Antonie van Leeuwenhoek* **2002,** 81, 181-187.

(42) Westrich, J. T.; Berner, R. A. *Limnol. Oceanogr.* **1984,** 29, 236-249.

(43) Callaghan, A. V. *Front. Microbiol.* **2013,** 4.

(44) Callaghan, A. V.; Gieg, L. M.; Kropp, K. G.; Suflita, J. M.; Young, L. Y. *Appl. Environ. Microbiol.* **2006,** 72, 4274-4282.

(45) Misra, G.; Pavlostathis, S. *Appl. Microbiol. Biotechnol.***1997,** 47, 572-577.

(46) Jaekel, U.; Zedelius, J.; Wilkes, H.; Musat, F. *Front. Microbiol.* **2015,** 6.

(47) Tsukamoto, S.; Kato, H.; Hirota, H.; Fusetani, N. *Biofouling* **1997**, 11, 283-291.

(48) Gallucci, M.; Oliva, M.; Casero, C.; Dambolena, J.; Luna, A.; Zygadlo, J.; Demo, M. *Flavour. Frag. J.* **2009,** 24, 348-354.

(49) Amaral, J.; Ekins, A.; Richards, S.; Knowles, R. *Appl. Environ. Microbiol.* **1998,** 64, 520-525.

(50) Andrews, R.; Parks, L.; Spence, K. *Appl. Environ. Microbiol.* **1980,** 40, 301-304.

(51) Avci, R.; Davis, B.; Wolfenden, M.; Beech, I.; Lucas, K.; Paul, D. *Corros. Sci.* **2013,** 76, 267-274.

(52) Shinozaki, J.; Muto, I.; Omura, T.; Numata, M.; Hara, N. *J. Electrochem. Soc.* **2011,** 158, C302-C309.

(53) Wranglen, G. *Corros. Sci.* **1974,** 14, 331-349.

(54) Bostic, D.; Burns, G.; Harvey, S. *J. Chromatogr. A* **1992,** 602, 163-171.

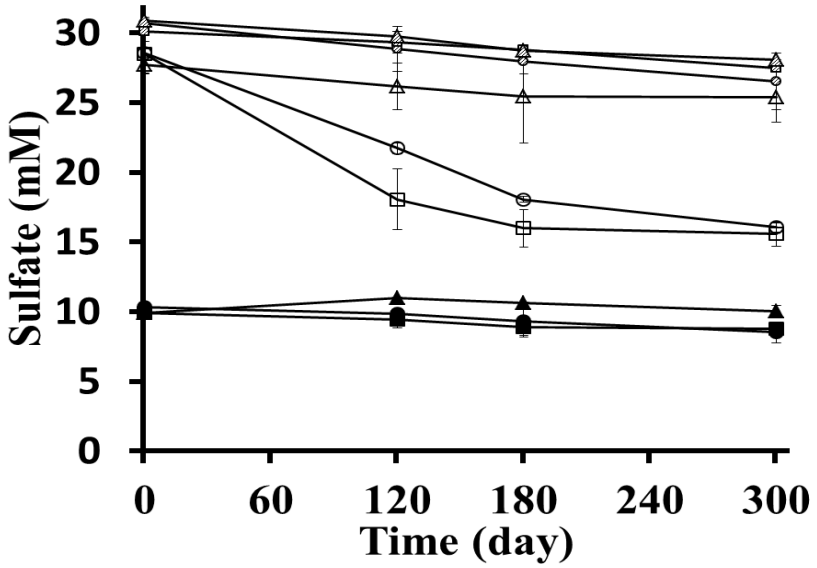

Figure 1 Sulfate reduction in seawater incubations containing terpene dimer fuel (TDF). Three seawaters from Key West (KW), Gulf of Mexico (GoM) and San Diego Bay (SDB) were tested. ⊘ KW seawater + No TDF; ▨ KW seawater + TDF; ◬ Sterile KW seawater + TDF; ○ SDB seawater + No TDF; □ SDB seawater + TDF; Δ Sterile SDB seawater + TDF; ● GoM seawater + No TDF; ■ GoM seawater + TDF; ▲ Sterile GoM seawater + TDF. Note: Sediment was included in SDB incubations.

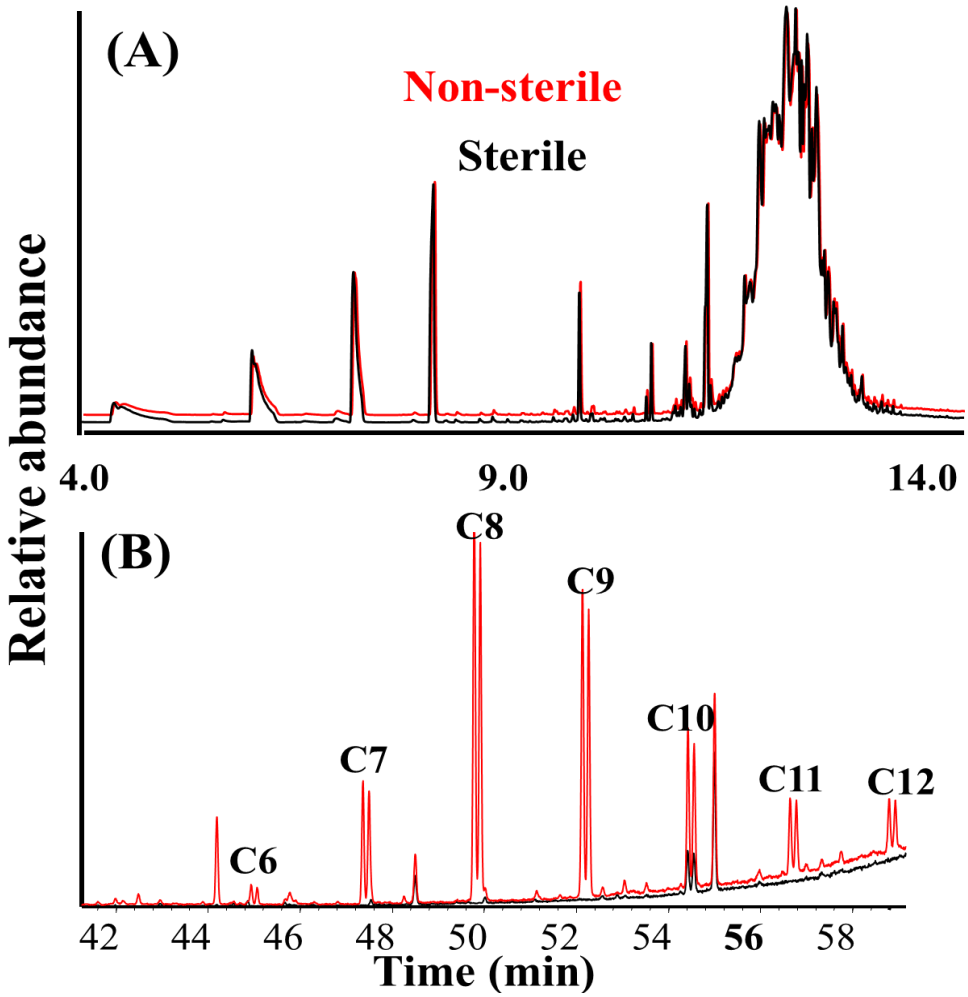

Figure 2 (A) Gas chromatography profile of TDF blend containing *n*-alkanes extracted from KW incubations with addition of *D. alkanexedens* strain ALDC^{T} and *n*-alkanes (C_6-C_{12}). Sterile (black): Sterile KW seawater + Sterile *D. alkanexedens* strain ALDC^{T} + TDF + *n*-alkanes; and Non-sterile (red): KW seawater + *D. alkanexedens* strain ALDC^{T} + TDF + *n*-alkanes. (B) Extracted profile of alkylsuccinates sharing the distinctive fragment ion at m/z 262[39]. C6-C12 on top of the peaks in Figure (B) represents the corresponding alkylsuccinates derived from *n*-alkanes with carbon chain length from 6 to 12.

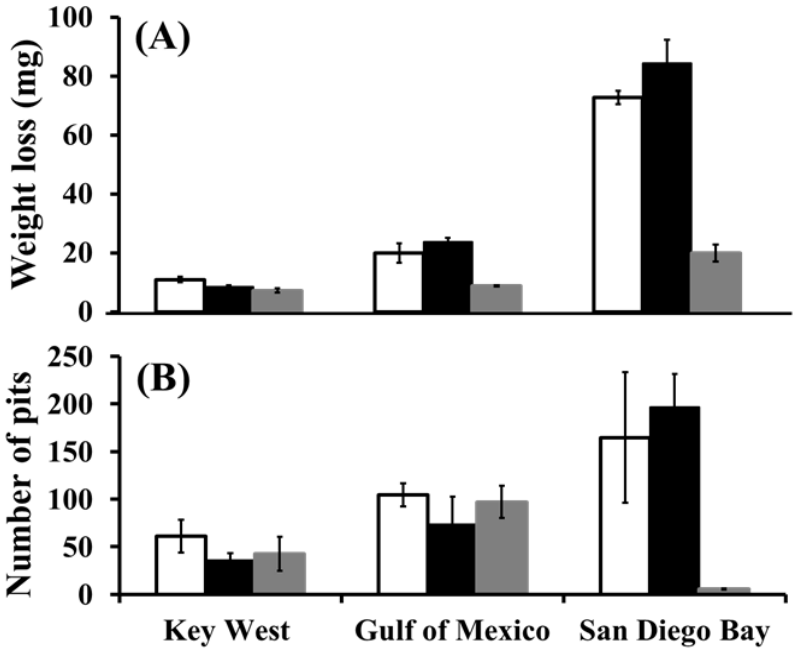

Figure 3 (A) Weight loss and (B) number of pits in incubations with KW, GoM and SDB seawaters. The clear bars in Figures (A) and (B) represent the fuel-unamended control with no addition of TDF; The black bars in Figures (A) and (B) are the experimental groups with amendment of TDF; and the grey bars in Figures (A) and (B) indicate the corresponding sterile control (autoclaved seawater/sediment) with amendment of TDF.

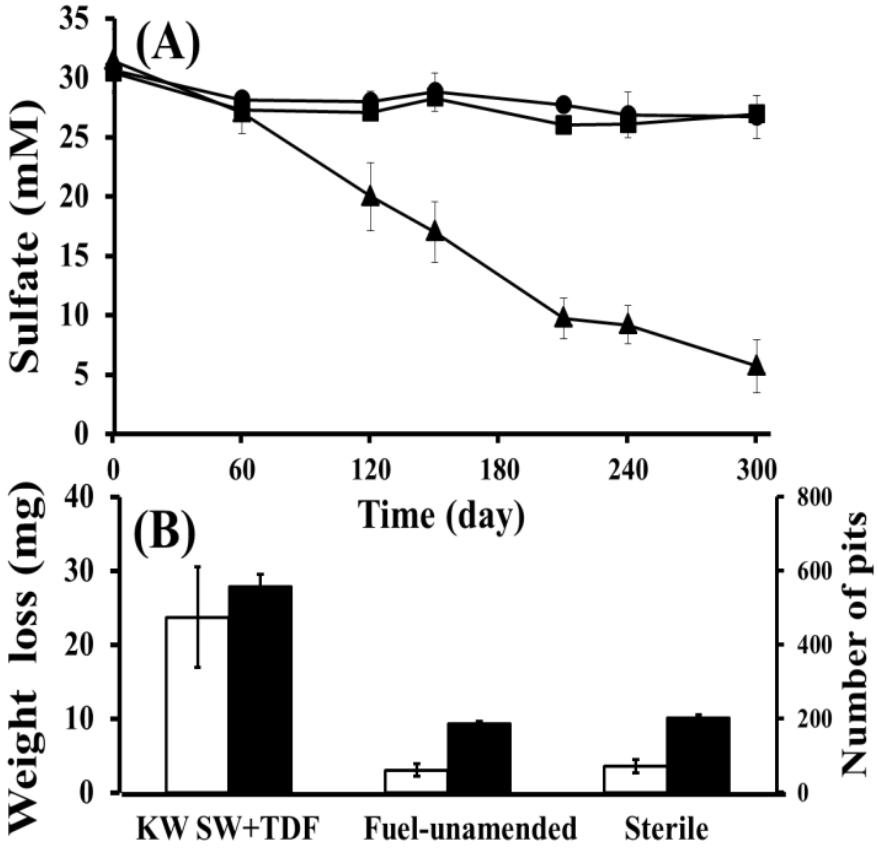

Figure 4 (A) Sulfate reduction in KW incubations with addition of *D. alkanexedens* strain ALDC^T and *n*-alkanes (C_6-C_{12}). ● (Fuel-unamended), KW seawater + *D. alkanexedens* strain ALDC^T + no TDF or alkanes; ■ (Sterile), Sterile KW seawater + Sterile *D. alkanexedens* strain ALDC^T + TDF + *n*-alkanes; and ▲(KW SW+TDF), KW seawater + *D. alkanexedens* strain ALDC^T + TDF + alkanes. (B) Weight loss and number of pits in the corresponding conditions with different degrees of sulfate reduction. The clear and black bars in Figure (B) represent the corrosion determined by weight loss and the number of pits quantified by profilometry, respectively.

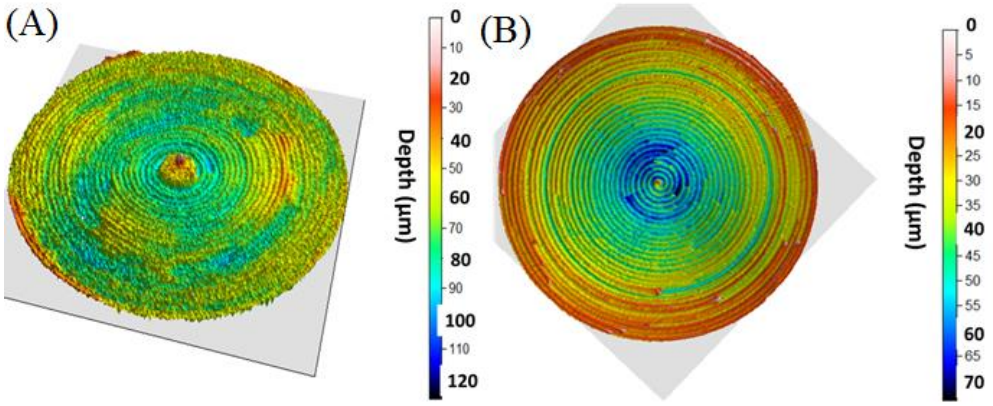

Figure 5 Profilometry analysis of coupons exposed to KW incubations with addition of *D. alkanexedens* strain ALDC^T and *n*-alkanes (C_6-C_{12}). (A) Non-sterile: KW seawater + *D. alkanexedens* strain ALDC^T + TDF + alkanes and (B) corresponding sterile control: Sterile KW seawater + Sterile *D. alkanexedens* strain ALDC^T + TDF + *n*-alkanes.

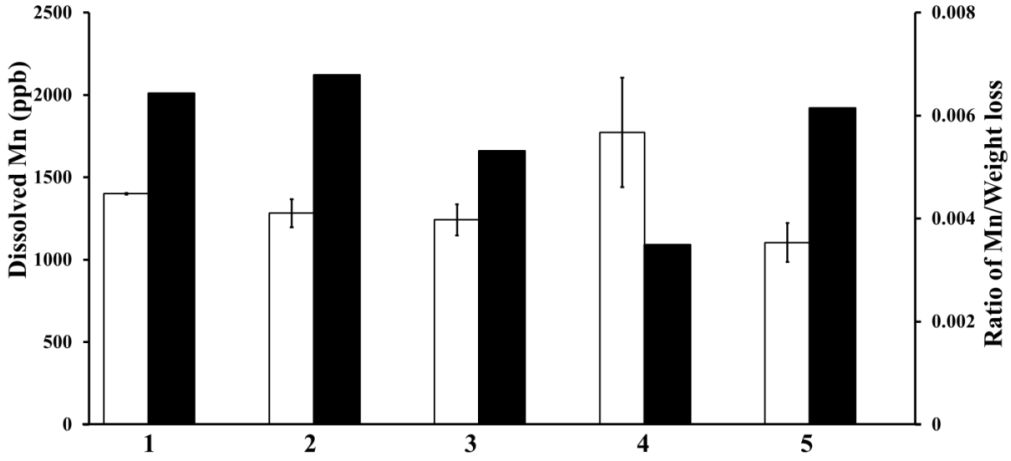

Figure 6 Dissolved Manganese (Mn) and calculated ratio of Mn/weight loss in KW incubations. The clear and black bars represent the dissolved Mn from the metal surfaces and the ratio of Mn/weight loss, respectively. 1, KW seawater + TDF; 2 Sterile KW seawater + TDF; 3, KW seawater + no TDF or *n*-alkanes + *D. alkanexedens* strain ALDC^T; 4, KW seawater + *D. alkanexedens* strain ALDC^T + TDF + *n*-alkanes; 5, Sterile KW seawater + Sterile *D. alkanexedens* strain ALDC^T + TDF + *n*-alkanes.

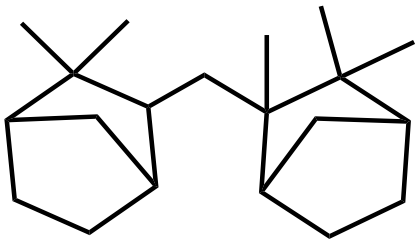

Figure S1 The chemical structure of terpene dimer fuel used in the present study: hydrogenated β-pinene dimers (Adapted from Harvey et al 2015).

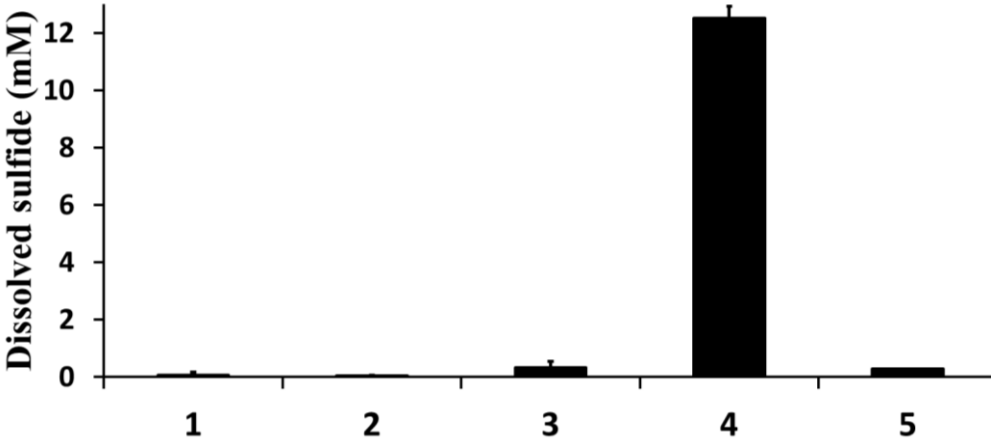

Figure S2 Sulfide production in KW incubations with addition of *D. alkanexedens* ALDC^T and *n*-alkanes (C_6-C_{12}). 1, KW seawater + Terpene dimer fuel (TDF); 2, Sterile KW seawater + TDF; 3, KW seawater + no TDF or alkanes+*D. alkanexedens* strain ALDC^T; 4, KW seawater + *D. alkanexedens* strain ALDC^T + TDF+ *n*-alkanes; 5, Sterile KW seawater +Sterile *D. alkanexedens* strain ALDC^T + TDF + *n*-alkanes.

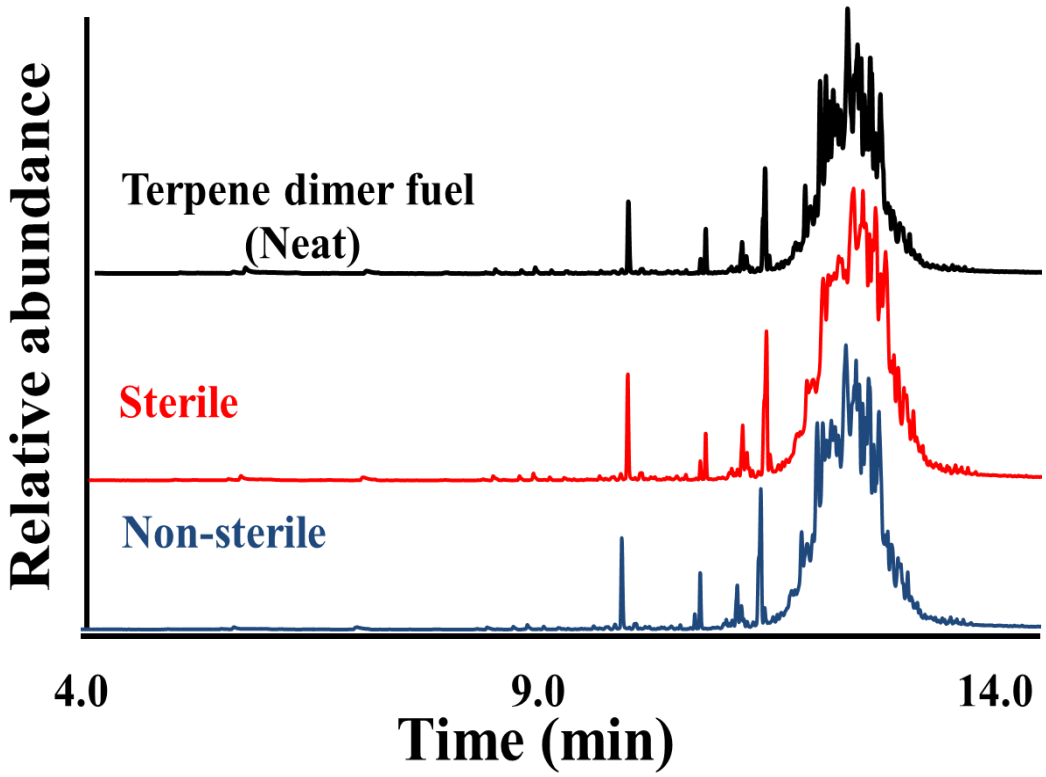

Figure S3 Gas chromatography profile of neat terpene dimer fuel (black) and those extracted from KW incubations. Non-sterile (blue), KW seawater + TDF; Sterile (red), Sterile KW seawater + TDF.

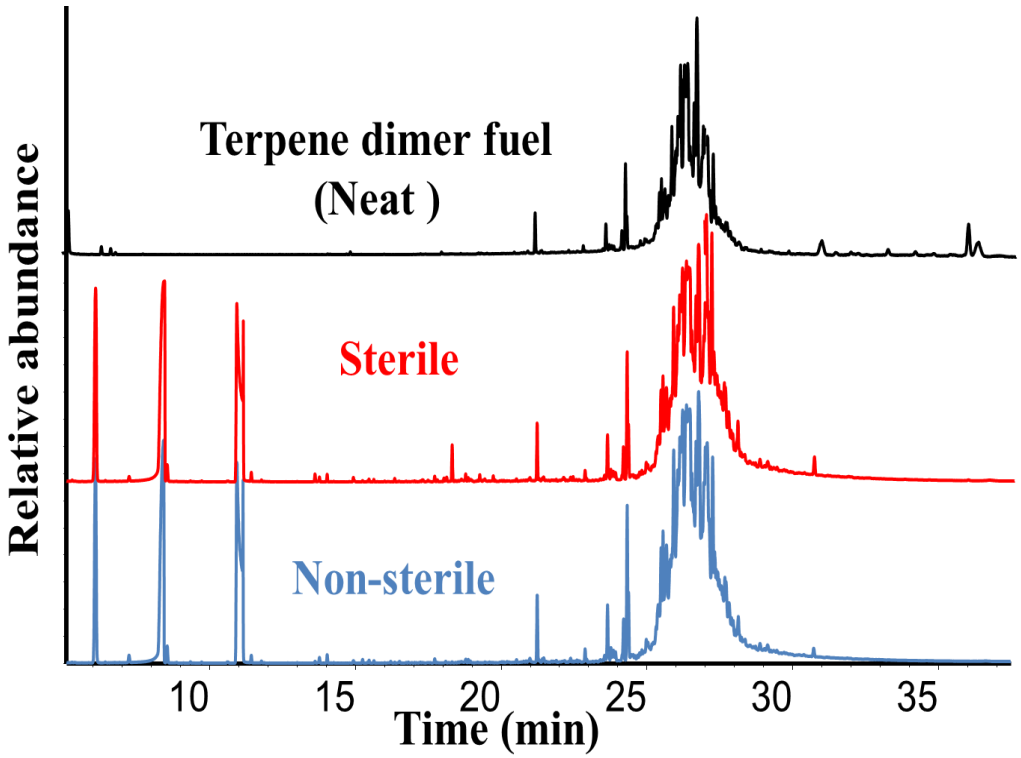

Figure S4 Gas chromatography profile of neat terpene dimer fuel (black) and samples extracted from SDB incubations. Non-sterile (blue), SDB seawater + TDF; Sterile (red), Sterile SDB seawater + TDF.

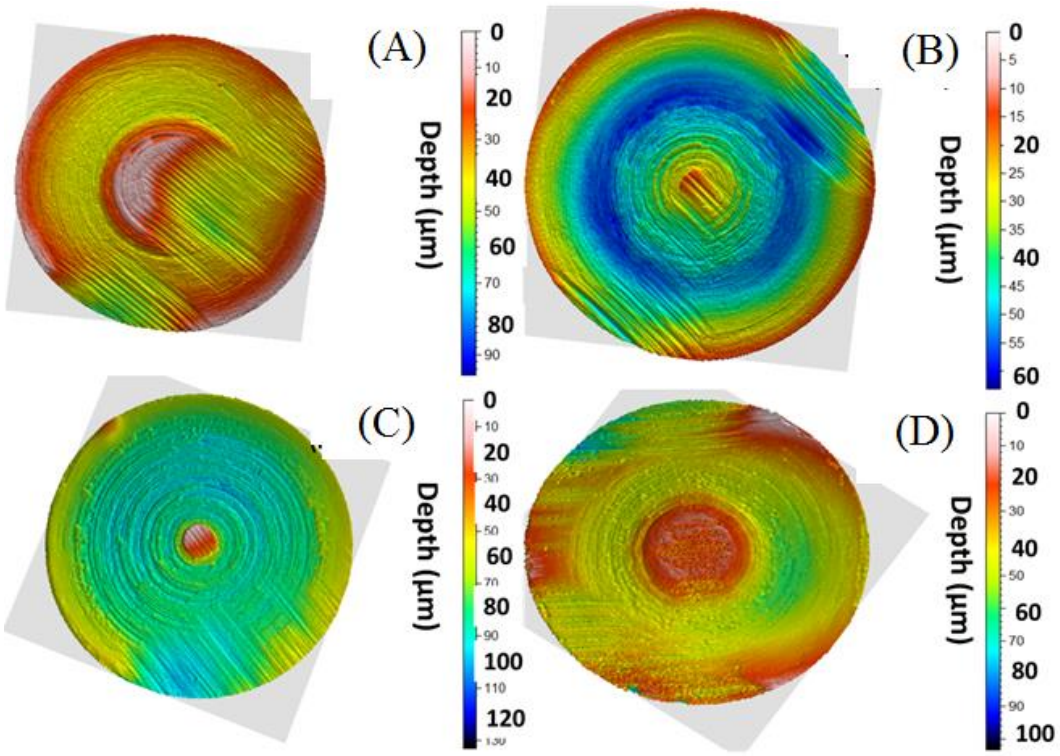

Figure S5 Profilometry profiles of metal coupons exposed to KW incubations: (A), KW seawater + TDF; (B) Sterile KW seawater + TDF; (C) KW seawater + no TDF; and (D) Sterile KW seawater + no TDF.

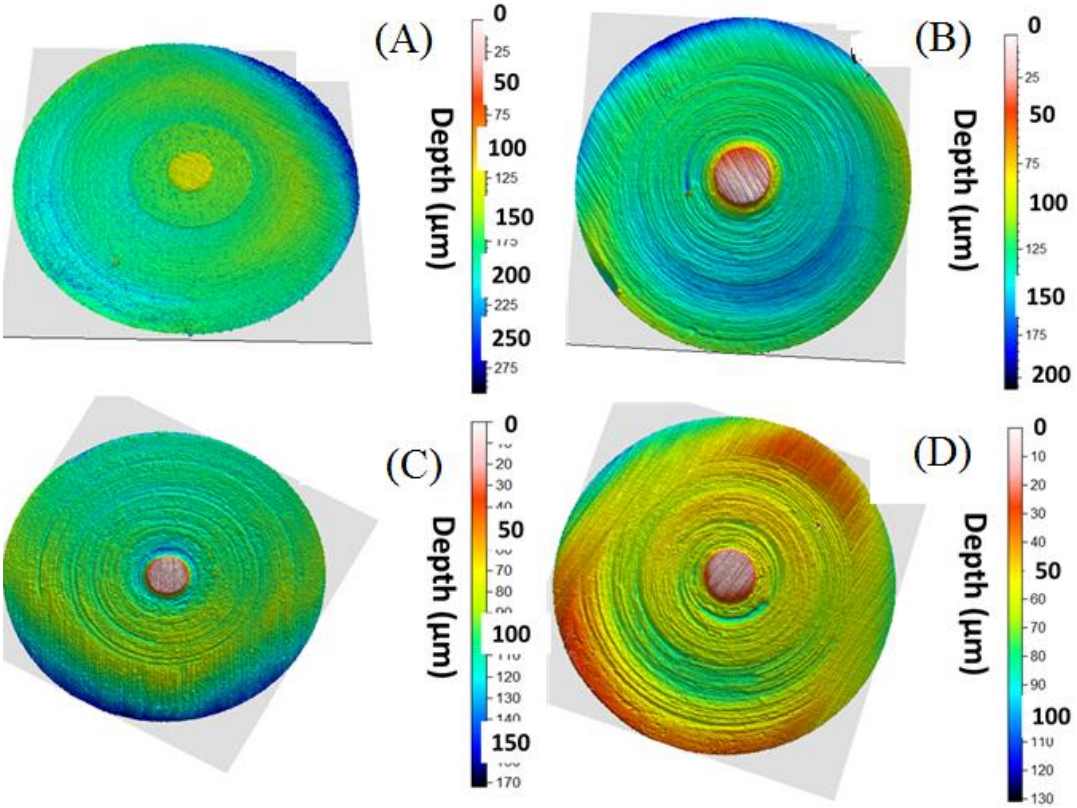

Figure S6 Profilometry profiles of metal coupons exposed to GoM incubations: (A), GoM seawater + TDF; (B) Sterile GoM seawater + TDF; (C) GoM seawater + no TDF; and (D) Sterile GoM seawater + no TDF.

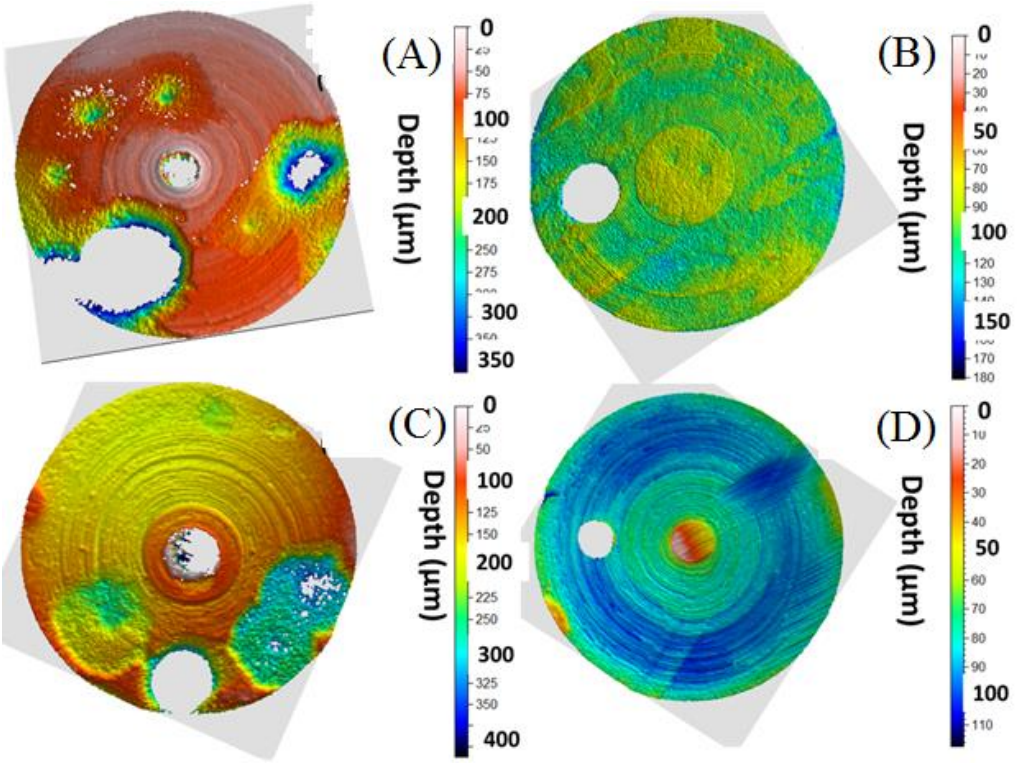

Figure S7 Profilometry profiles of metal coupons exposed to SDB incubations: (A), SDB seawater + TDF; (B) Sterile SDB seawater + TDF; (C) SDB seawater + no TDF; and (D) Sterile SDB seawater + no TDF.

Appendix A: Protocol for evaluating the biological stability of fuel formulations and their relationship to carbon steel biocorrosion

Abstract

The microbial metabolism of conventional and alternative fuels can be asscociated with the biocorrosion of the mostly carbon-steel energy infrastructure. This phenomenon is particularly acute in anaerobic sulfate-rich environments. It is therefore important to reliably assess the inherent susceptibility of fuels to anaerobic biodegradation in marine waters as well as provide a measure of the impact of this metabolism on the integrity of steel. Such an assessment of fuels is increasingly important since the exact chemical makeup of both traditional and biofuels can vary and even subtle changes have a profound impact on steel biocorrosion. Herein, we describe a simple protocol involving the incubation of carbon-steel coupons in seawater under anaerobic conditions. The increased depletion of sulfate in fuel-amended seawater incubations relative to both autoclaved and fuel-unamended negative controls is monitored as a function of time. We also recommend the incorporation a known hydrocarbon-degrading sulfate-reducing bacterium as a positive control in the assay to verify that the protocol is not predisposed to failure for unrecognized reasons. At the end of the incubation, corrosion is assessed by both coupon weight loss and a mass balance of the total iron released. Lastly, three-dimension non-contact profilometry is used to assess the degree of damage (e.g. pitting) to the coupons. The integration of the interdisciplinary approaches in this protocol allows for a critical assessment of the biological stability of both traditional and alternative fuel formulations and their potential in exacerbating biocorrosion.

Reference

Liang, R.; Suflita, J. M., Protocol for evaluating the biological stability of fuel formulations and their relationship to carbon steel biocorrosion. Handbook of Hydrocarbon and Lipid Microbiology; Springer: Berlin, Germany, **2015**.